C 51.17/12:989/8

Tech Notes

August 1989

PB89-925908

NTIS

U.S. DEPARTMENT OF COMMERCE
National Technical Information Service
Center for the Utilization of Federal Technology

U.S. DEPARTMENT OF COMMERCE
Robert A. Mosbacher, Secretary of Commerce

National Technical Information Service
Joseph F. Caponio, Director

ISSN 0889-8464

COPYRIGHT WARNING
International Copyright © National Technical Information Service, 1989. All portions of this publication are protected against copying or other reproduction outside of the United States under the provisions of Article II of the Universal Copyright Convention. United States copyright is not asserted under the United States Copyright Law, Title 17, United States Code.

The Secretary of Commerce has determined that the publication of this periodical is necessary in the transaction of the public business required by law of this department. Use of funds for printing this periodical has been approved by the Director of the Office of Management and Budget through 1989.

Tech Notes

Highlighting Selected U.S. Government Technology & Resources

August 1989

Contents

PENNSYLVANIA STATE
UNIVERSITY

AUG 27 1989

DOCUMENTS COLLECTION
U.S. Depository Copy

Agriculture & Food 618

Computers 620

Electrotechnology 622

Energy 639

Engineering 642

Environmental Science & Technology 660

Manufacturing, Machinery & Tools 663

Materials 671

Medicine & Biology 685

Natural Resources Technology & Engineering 693

Physical Sciences 695

Transportation & Components 704

Published monthly by the National Technical Information Service (NTIS), Tech Notes bring together individual one- to two-page fact sheets prepared by Federal agencies, their laboratories, or contractors. These fact sheets highlight current Federal technology determined to have commercial or practical application. Topics cover new processes, materials, techniques, software, instrumentation, and resources.

Some of the current sources are the Department of the Navy, Department of the Army, NASA, Department of Energy, Environmental Protection Agency, Department of the Interior, and the Department of Agriculture.

Special assistance is provided by the Federal Laboratory Consortium.

Change of address or questions concerning subscriptions should be sent to:
Subscriptions Department
National Technical Information Service
Springfield, VA 22161
(703) 487-4630

Suggestions, comments, or questions concerning Tech Notes should be directed to:
Tech Notes Editor
Room 300B F
National Technical Information Service
Springfield, VA 22161
(703) 487-4805

How to Use Tech Notes

Every Tech Notes fact sheet lists a source for additional information. The source of this information may be a special support package from the originating agency, a personal contact, a licensing opportunity, or a backup report available from NTIS.

Each fact sheet also is perforated to allow for easy removal for those subscribers who may wish to keep a special fact sheet file or route to others in their organization

Sources of Further Backup Information

Below are two representative examples of how each Tech Note fact sheet provides you with a source of further information. In most cases, this information is provided directly by the agency or its laboratory. However, there are cases where NTIS is the source for backup documentation. In these cases, use the order form at the end.

Examples:

significant distance from the endwalls. Therefore, a radial variation in efficiency should be used when designing small stators.
Project Officer Jeffrey E. Haas
(216) 433-4000.

FOR ADDITIONAL INFORMATION

You can learn more about this technology by ordering the NTIS report(s):
Cold-Air Performance of Compressor Drive Turbine
Order number: AD-A101066/NAA
Price code: A02
Order from:
National Technical Information Service
5285 Port Royal Road
Springfield, VA 22161
(703) 487-4650

158

Agency contact who can supplement the information contained in the backup report.

NTIS Order Number*

NTIS Price Code*

* See the order form and price code table at the end of the issue.

Suggested applications include other kinds of refrigerators, heat engines, thermal instrumentation, and heat switches.
This work was done by Emanuel Tward of Caltech for NASA's Jet Propulsion Laboratory.
NPO-15479/TN

FOR ADDITIONAL INFORMATION
Contact: Director, Technology Transfer Division, P.O. Box 8587, BWI Airport, MD 21240: (301) 621-0100 Ext.241.
REFER TO THE NUMBER LISTED AT THE END OF THE ARTICLE

178

Agency reference number

Source of more information about the technology described in the fact sheet

Page number

Tech Notes Title List for August 1989

Agriculture & Food

0618 Separation of Omega-3 Fatty Acids from Fish Oils
0619 Bacterium Produces a Sugar Never Before Found in Nature

Other Items of Interest

0671 Kenaf Paper: A Forest-Saving Alternative

Computers

0620 Improved Algorithm for Finite-Field Normal-Basis Multipliers—Self-dual normal bases reduce mathematical complexity.

Testing & Instrumentation

0621 Test Instrument Detects Computer Flaws (Licensing Opportunity)

Other Items of Interest

0635 Transferring Lens Prescriptions Between Lens-Design Programs—Most data are transferred automatically, and the user is notified of those that are not.
0643 Navy Personal Computers Challenge the High Sees
0664 PARDS to be Used in National Institute of Standards & Technology Research
0707 Software Helps Select Patrol Vehicles

Electrotechnology

0622 Electronic Analog Active Filters (Licensing Opportunity)
0623 Improving Shielding Effectiveness of Cables
0624 Acousto-optical/Magneto-optical Correlator or Convolver—Binary signals are processed optically in multiple channels. (Licensing Opportunity)
0625 Adaptive Force and Position Control for Robots—Precise knowledge of manipulator and environment is not required. (Licensing Opportunity)
0626 Advanced Components for Fiber-Optical Systems—This concise review emphasizes highly birefringent fibers, couplers, and polarizers.
0627 Closed-Loop Motor-Speed Control—Speed is sensed optoelectronically.
0628 Digital, Satellite-Based Aeronautical Communication—Advanced digital techniques will be needed eventually for greatest cost effectiveness.
0629 DMSK Receiver for Mobile/Satellite Service—A low-bit-rate demodulator operates in the presence of fading and Doppler shifts.
0630 Electrolytic Heat Switch—Thermal conduction is altered electrically.
0631 Jacobi-Bessel Analysis of Antennas with Elliptical Apertures—A coordinate transformation improves convergence in pattern analysis of elliptical-aperture antennas.
0632 Multiple-Beam Communications Antenna—This system has both fixed-spot and scanning coverage.
0633 Reflection-Zone-Plate Antenna—A microwave antenna is based on reflection holography.
0634 Photodiode-Coupled Light Modulator—The absorption of one light beam would control the transmission of another. (Licensing Opportunity)

Software

0635 Transferring Lens Prescriptions Between Lens-Design Programs—Most data are transferred automatically, and the user is notified of those that are not.

Testing & Instrumentation

0636 Optoelectronic Technique Eliminates Common-Mode Voltages—Small signals can be transmitted between circuits at large differences of potential. (Licensing Opportunity)
0637 Measuring Shapes of Reflectors by Microwave Holography—Theoretical and practical aspects of microwave holographic metrology are discussed. (Licensing Opportunity)
0638 Spectrograph Measures Contamination of Optical Elements—Reflective and transmittance are measured over a range of wavelengths. (Licensing Opportunity)

Other Items of Interest

0639 Axial-Gap Permanent Magnet Motor
0644 Crimping Wires in Cramped Spaces

Energy

0639 Axial-Gap Permanent Magnet Motor
0640 Bipolar Battery Using Conductive-Fiber Composite—Improved lead/acid battery features reduced weight and increased energy and power densities. (Licensing Opportunity)
0641 New Eyes for Wind Turbines Designers

Other Items of Interest

0679 Multiple-Purpose Rigid Foam Insulation—Properties can be adapted to a variety of demanding applications.

Engineering

0642 Coefferdams—Answer to Underwater Window Repair—Divers can control temperature and water quality during repair
0643 Navy Personal Computers Challenge the High Sees
0644 Crimping Wires in Cramped Spaces
0645 A Device that Rigidly Assembles Interlocking Parts
0646 Special Plug Lets Researchers 'See' Inside Auto Engines
0647 The Beam-Raising Vehicle

Engineering (Cont.)

0648 Beneficiation Technique Provides a Means for Capitalizing on Domestic Sources of Cobalt
0649 Novel Foam Application Lowers Longwall Dust
0650 High-Capacity Heat-Pipe Evaporator—The cylindrical configuration increases the contact conductance.
0651 High Temperature Gas-Gap Thermal Switch—The flow of heat is varied at will.
0652 Optimizing Locations of Nodes to Reduce Vibrations—The distribution of mass is modified to move the nodes to desired locations.
0653 Venting Gases with Minimum Loss of Heat—The design of a vent reduced radiative transfer of heat.
0654 Video Alignment System for Remote Manipulator—Crosshairs and a mirror provide angular references. (Licensing Opportunity)

Software

0655 Unified Engineering Software System—A collection of computer programs performs diverse functions in prototype engineering.

Testing & Instrumentation

0656 In Situ Measurement of Rock Stress with Hydraulic Borehold Pressure Cells
0657 Borescope Inspects with Visible or Ultraviolet Light—Quartz optical fibers improve performance at ultraviolet wavelengths.
0658 Densitometry by Acoustic Levitation—Detailed knowledge of the acoustic field is not necessary.
0659 Measuring Thermal Conductivities of Rough Specimens—Cost is reduced and accuracy and repeatability increased.

Other Items of Interest

0660 Emulsion-Phase Contactor
0661 New Inland Oil Skimmer
0665 Compliant Robot Wrist Senses Deflections and Forces—Precise parts can be assembled without damage.
0670 Strain-Gaged Bolt Process for the Direct Measurement of Valve-Stem Thrust
0700 Acoustical Measurement of Furnace Temperatures—Simple probes withstand severe conditions, yet give spatially-resolved temperature readings. (Licensing Opportunity)
0704 Injected Water Augments Cooling in Turboshaft Engine—Additional cooling enables operation at higher than usual power.

Environmental Science & Technology

0660 Emulsion-Phase Contactor
0661 New Inland Oil Skimmer

Testing & Instrumentation

0662 In Situ Groundwater Detection of Chloroform and Trichloroethylene

Other Items of Interest

0695 The Determination of pH by Flow Injection Analysis and by Fiber Optrode Analysis (Licensing Opportunity)
0698 Fourier Transform Infrared Spectrometry of Ambient Aerosols
0699 Investigation 2,4-Dinitrophenylhydrazine Impregnated Adsorbent Tubes for the Collection of Airborne Aldehydes

Manufacturing, Machinery & Tools

0663 Automated Chemical Analysis for Process Solutions
0664 PARDS to be Used in National Institute of Standards & Technology Research
0665 Compliant Robot Wrist Senses Deflections and Forces—Precise parts can be assembled without damage.
0666 Gray-Scale Processing for Tracking of Welds—Digital analysis of video images provides information for control of a welding robot. (Licensing Opportunity)
0667 Plating Repair of Nickel-Alloy Pressure Vessels—Localized plating builds up wall thickness.

Testing & Instrumentation

0668 Double-O-Ring Plug for Leak Tests—A verifiable redundant seal contributes to testing and assurance of safety.
0669 Identification of Anomalies in Welds—Advanced techniques are combined with conventional analytical methods.
0670 Strain-Gaged Bolt Process for the Direct Measurement of Valve-Stem Thrust

Other Items of Interest

0625 Adaptive Force and Position Control for Robots—Precise knowledge of manipulator and environment is not required. (Licensing Opportunity)
0654 Video Alignment System for Remote Manipulator—Crosshairs and a mirror provide angular references. (Licensing Opportunity)

Materials

0671 Kenaf Paper: A Forest-Saving Alternative
0672 Low Dislocation Density GaAs Crystals Grown Using Advanced Vertical Gradient Freeze Technique
0673 Eight New High-Temperature Superconductors Produced by Novel Process
0674 Method for Preparing Vanadium
0675 New Model Makes Glass-Fracture Predictions More Reliable
0676 Flexible, Polymer-Filled Metallic Conductors—Combined advantages of metals and polymers are exploited by advanced manufacturing techniques. (Licensing Opportunity)
0677 Fluoroepoxy Adhesives Bond Flouroplastics—Etching or other special preparation is unnecessary. (Licensing Opportunity)

0678 Low-Thermal-Expansion Filled Polytetrafluoroethylene—PTFE would be made thermally compatible with aluminum without changing its dielectric constant.

0679 Multiple-Purpose Rigid Foam Insulation—Properties can be adapted to a variety of demanding applications.

0680 Polymer Coatings Reduce Electro-osmosis—Poly(ethylene glycol) film controls the electrostatic potential across the surface. (Licensing Opportunity)

0681 Soluble Aromatic Polyimides for Film Coating—Films are nearly colorless and soluble and exhibit good mechanical properties.

0682 Polymer Lubricants for use in Vacuum—Both solid and film polyimides offer low friction and wear.

Testing & Instrumentation

0683 Measuring Fracture Times of Ceramics—Electrical measurements complement or replace fast cinematography.

0684 Ultrasonic Detection of Transply Cracks in Composites—The densities and propagation of cracks are measured nondestructively.

Other Items of Interest

0626 Advanced Components for Fiber-Optical Systems—This concise review emphasizes highly birefringent fibers, couplers, and polarizers.

0640 Bipolar Battery Using Conductive-Fiber Composite—Improved lead/acid battery features reduced weight and increased energy and power densities. (Licensing Opportunity)

0667 Plating Repair of Nickel-Alloy Pressure Vessels—Localized plating builds up wall thickness.

0669 Identification of Anomalies in Welds—Advanced techniques are combined with conventional analytical methods.

0702 Thermal-Wave Microscope—Images are produced by a modified computer-controlled scanning electron microscope.

Medicine & Biology

0685 Method Developed for Locating a Small Magnetic Object in the Human Body

0686 Clues Found to Infectivity of Herpes Simplex Virus

0687 Naval Dental Research Institute Studies Potential Etiologic Agents of Periodontitis

0688 Laboratory Animal Resource for Biomedical Research

0689 Navy Develops New Wound Dressing

0690 Mouse Model Resource for Human Inherited Diseases

0691 Mandrels for Microtextured Small-Vessel Implants—A surface-relief pattern should encourage growth of a healthy neointima. (Licensing Opportunity)

0692 Multimembrane Bioreactor—Metabolizing cells are well nourished while inhabiting products are removed.

Other Items of Interest

0619 Bacterium Produces a Sugar Never Before Found in Nature

Natural Resources Technology & Engineering

Software

0693 DAMBREAK Flood Forecasting Model

0694 A Computer Program for Detecting or Predicting Fracture Zones

Physical Sciences

0695 The Determination of pH by Flow Injection Analysis and by Fiber Optrode Analysis (Licensing Opportunity)

0696 Nonaggregating Microspheres Containing Aldehyde Groups—Aggregation is avoided by irradiating hydrophilic monomers in the presence of acrolein. (Licensing Opportunity)

Software

0697 Isothermal-Gas-Transfer Program—One or two tanks with or without venting or consumption can be simulated.

Testing & Instrumentation

0698 Fourier Transform Infrared Spectrometry of Ambient Aerosols

0699 Investigation 2,4-Dinitrophenylhydrazine Impregnated Adsorbent Tubes for the Collection of Airborne Aldehydes

0700 Acoustical Measurement of Furnace Temperatures—Simple probes withstand severe conditions, yet give spatially-resolved temperature readings. (Licensing Opportunity)

0701 Correlation Functions Aid Analyses of Spectra—Signals much weaker than noise are identified.

0702 Thermal-Wave Microscope—Images are produced by a modified computer-controlled scanning electron microscope.

0703 Phase-Modulation Gas-Correlation Spectroscopy—Features include high spectral discrimination and sensitivity.

Other Items of Interest

0646 Special Plug Lets Researchers 'See' Inside Auto Engines

0658 Densitometry by Acoustic Levitation—Detailed knowledge of the acoustic field is not necessary.

0663 Automated Chemical Analysis for Process Solutions

0672 Low Dislocation Density GaAs Crystals Grown Using Advanced Vertical Gradient Freeze Technique

0680 Polymer Coatings Reduce Electro-osmosis—Poly(ethylene glycol) film controls the electrostatic potential across the surface. (Licensing Opportunity)

Transportation & Components

0704 Injected Water Augments Cooling in Turboshaft Engine—Additional cooling enables operation at higher than usual power.

0705 Study of Flow About a Helicopter Rotor—A noninvasive instrument verifies a computer program that predicts velocities (Licensing Opportunity)

0706 Vibration-Testing Facility for Aircraft—Equipment, methods, and experience are described.

Software

0707 Software Helps Select Patrol Vehicles

Agriculture & Food

0618 Separation of Omega-3 Fatty Acids from Fish Oils

0619 Bacterium Produces a Sugar Never Before Found in Nature

Other Items of Interest

0671 Kenaf Paper: A Forest-Saving Alternative

NOAA Technology Brief

National Oceanic and Atmospheric Administration
National Marine Fisheries Service
Northeast Fisheries Center

Separation of Omega-3 Fatty Acids from Fish Oils

NOAA's National Marine Fisheries Service has successfully separated purified fractions of omega-3 fatty acids from refined menhaden oil using reverse phase high performance liquid chromatography. Fish oil is the richest dietary source of omega-3 fatty acids. Two of these fatty acids, eicosapentaenoic (EPA) and docosahexaenoic (DHA) acids, are the focus of concentrated research by the medical community for their purported beneficial effects in the prevention of cardiovascular diseases and inflammatory illnesses. This NOAA technology will make it possible to provide the research community with pure EPA and pure DHA for experimentation under a joint agreement with the National Institutes of Health.

Initial production scale runs have yielded about 98% purity EPA and 92% purity DHA from a starting material already concentrated by urea fractionation in EPA and DHA as the ethyl esters at 48% and 24%, respectively. Sixty grams of the starting material can be processed every three hours using ethanol and water to affect the separation. Amounts as low as 100 mg of fish oil fatty acid ethyl esters can be processed using scaled-down equipment.

A published report entitled "Purification of omega-3 fatty acids from fish oils using HPLC" appears in Proceedings of the 12th Annual Conference of the Tropical and Subtropical Fisheries Technological Society, June 1988, p. 74.

This work was performed by Judith Krzynowek of the Northeast Fisheries Center, Conservation and Utilization Division, National Marine Fisheries Service, Gloucester, MA.

Additional information is available from NOAA ORTA, Suitland Professional Center (SPC), Room 307, Suitland, Maryland 20233. Telephone (301) 763-4240.

Research Technology
Agricultural Research Service
U.S. Department of Agriculture

Bacterium Produces a Sugar Never Before Found in Nature

A bacterium in the digestive tract of cattle and other animals makes a sugar that until now was not known to occur in nature, a U.S. Department of Agriculture scientist has reported.

"Up to now, this sugar--L-altrose--has been known only as a chemical synthesized in laboratories," said Robert J. Stack, a biochemist with USDA's Agricultural Research Service here.

He found that a bacterium called Butyrivibrio fibrisolvens makes a polysaccharide that contains L-altrose. A polysaccharide is a long chain of sugar molecules linked together chemically.

"We don't yet know the significance of bacterial L-altrose or what commercial uses it might have," he said. "Industry has been investigating the use of L-altrose as a non-caloric sweetener, but chemically produced L-altrose is very expensive."

He doesn't know what the bacterially produced L-altrose would cost, but in any event, approval by the Food and Drug Administration would be necessary before the sugar could be added to foods.

"The bacterium that makes L-altrose is one of the most important of the hundreds of bacterial species that live in the rumen of animals such as cattle, sheep and goats," said Stack, a member of a team studying ruminal bacteria at the agency's Northern Regional Research Center. The rumen is the first of a series of four stomachs in these animals, and the bacteria digest the animals' feed for them.

The team's main goal is to find out how these bacteria break down the complex carbohydrates in the plant materials eaten by the animals.

"Some bacteria seem to be better at digesting grasses or other forages, while others do best with grains such as corn. Someday we hope to be able to match selected or genetically-engineered bacteria to specific animal diets. That could improve animal nutrition while making animal production more efficient," Stack said.

Stack points out that cattle generally digest only about 70 to 80 percent of the starch in corn. "If we can increase this just a few percentage points by manipulating the ruminal bacteria, we could lower costs for both the farmer and consumer."

FOR ADDITIONAL INFORMATION: To discuss this effort further, contact Dr. Robert J. Stack, biochemist, Fermentation Biochemistry Research, Northern Regional Research Center, Agricultural Research Service, USDA, Peoria, IL 61604; (309) 685-4011, ext. 339.

Computers

0620 Improved Algorithm for Finite-Field Normal-Basis Multipliers—Self-dual normal bases reduce mathematical complexity.

Testing & Instrumentation

0621 Test Instrument Detects Computer Flaws (Licensing Opportunity)

Other Items of Interest

0635 Transferring Lens Prescriptions Between Lens-Design Programs—Most data are transferred automatically, and the user is notified of those that are not.

0643 Navy Personal Computers Challenge the High Sees

0664 PARDS to be Used in National Institute of Standards & Technology Research

0707 Software Helps Select Patrol Vehicles

NASA Tech Brief
National Aeronautics and
Space Administration
NASA's Jet Propulsion Laboratory, Pasadena, California

Improved Algorithm for Finite-Field Normal-Basis Multipliers

Self-dual normal bases reduce mathematical complexity.

An improved algorithm reduces the complexity of the calculations that must precede the design of Massey-Omura finite-field normal-basis multipliers, which are used in error-correcting-code equipment and cryptographic devices. This algorithm represents an extension of the development reported in "Algorithm To Design Finite-Field Normal-Basis Multipliers" (NPO-17109), *NASA Tech Briefs*, Vol. 12, No. 5, page 82.

As described in the earlier article, the design of a multiplier requires a product function defined by a Boolean matrix. The product function is, in turn, found via an algorithm that generates a normal basis $\{\alpha\}$ and its dual basis $\{\beta\}$ in a Galois field $GF(2^m)$. It has been known for more than a decade that if m is odd, there exists a self-dual normal basis in $GF(2^m)$. Since the development of the previous algorithm, it was discovered that a self-dual normal basis yields a symmetrical Boolean matrix, and consequently, the construction of a product function for a self-dual normal basis is simpler than for an arbitrary normal basis.

The new algorithm (see figure) constructs the symmetrical Boolean matrix $\bar{\Omega}$ for odd m. It starts with the choice of any element θ in $GF(2^m)$. Using a new subalgorithm, it finds the vector $\boldsymbol{b}$ and the matrix $\bar{B}$, which are related to a basis $\{\beta\}$. It checks whether $\bar{B}$ is invertible: If so, then $\{\theta\}$ is a normal basis; if not, then another θ is chosen, and the process repeats until the resulting $\bar{B}$ is invertible. Then using a theorem that expresses the relationship between $\{\beta\}$, $\bar{B}$, and $\{\theta\}$, the algorithm calculates $\{\beta\}$, which has become a self-dual normal basis. Finally, using procedures similar to those of the previous algorithm, the new algorithm sets up $\bar{\Omega}$.

The complexity of a Massey-Omura multiplier depends on the number of ones in $\bar{\Omega}$: this number is smaller in a Boolean matrix generated from a self-dual normal basis than in a Boolean matrix generated from an arbitrary normal basis. In addition, the time required to construct $\bar{\Omega}$ can be reduced to one-third of that required for an arbitrary normal basis.

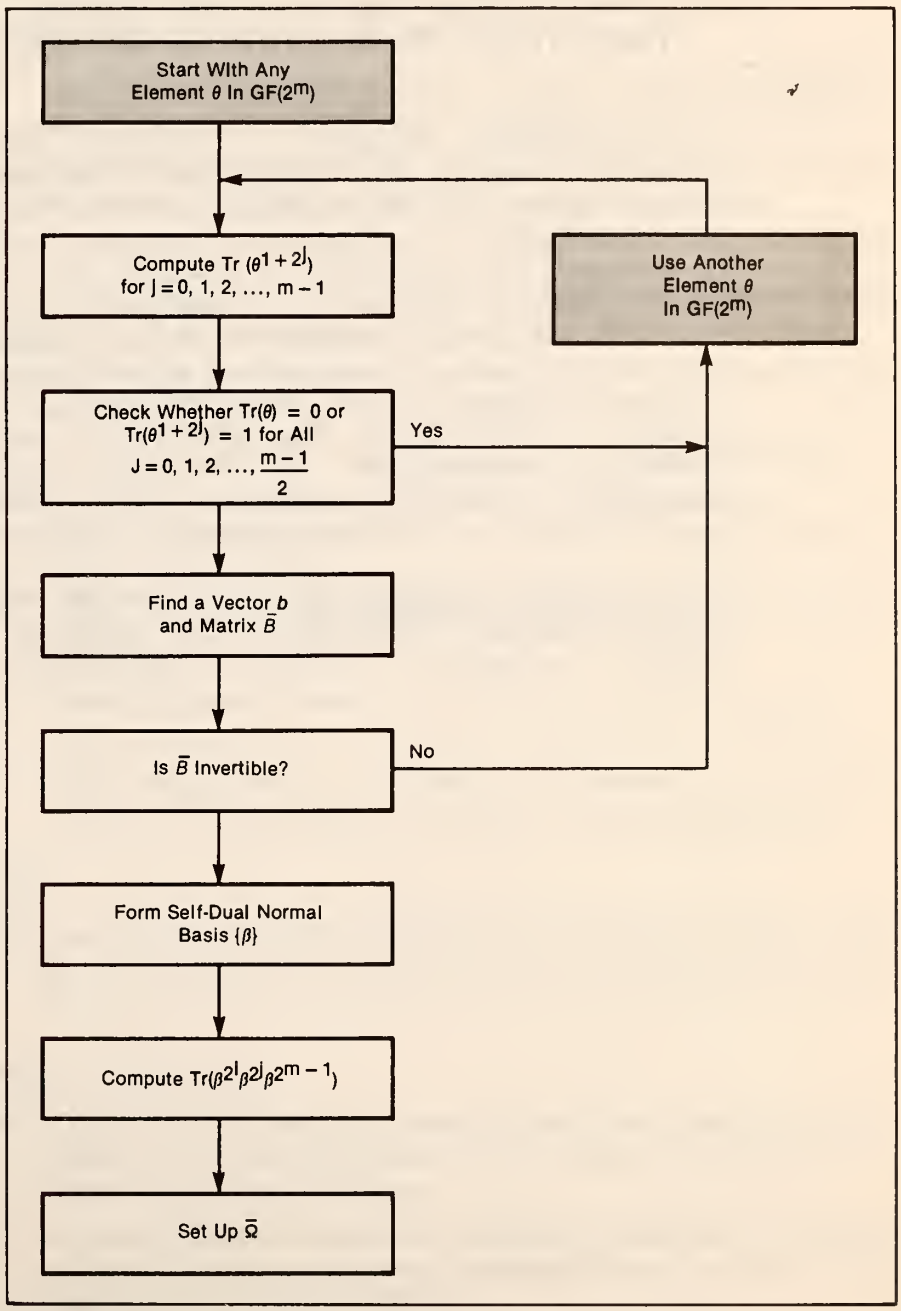

The **New Algorithm** generates a symmetrical Boolean matrix $\bar{\Omega}$, starting with the choice of any element θ in $GF(2^m)$.

This work was done by C. C. Wang of Caltech for **NASA's Jet Propulsion Laboratory**. *NPO-17225/TN*

FOR ADDITIONAL INFORMATION: *Contact: Director, Technology Transfer Division, P.O. Box 8757, BWI Airport, MD 21240; (301) 621-0100 Ext. 241*
REFER TO THE NUMBER LISTED AT THE END OF THIS ARTICLE

NIST Technology Update

Licensing Opportunity

National Institute of Standards & Technology
(Formerly the National Bureau of Standards)
U.S. Department of Commerce, Gaithersburg, MD 20899

Test Instrument Detects Computer Flaws

A test instrument designed by researchers from NIST and private industry to verify the correctness of information exchanges between large electronic devices recently was granted a patent (no. 4,764,863). It offers the designers, builders, and users of complex computer systems a powerful tool for tracking down subtle flaws in equipment in a way previously not possible. Most flaw-detecting instruments are programmed to "trigger" only when certain, predetermined events happen. This instrument can be programmed with an idealized model of a properly operating system; it then monitors the system until something out of the ordinary is encountered. At that point, recording circuits are triggered to memorize the anomaly. The instrument received an I-R 100 award in 1984 from Research & Development magazine.

FOR ADDITIONAL INFORMATION: For licensing information, contact Office of Federal Patent Licensing, National Technical Information Service, Springfield, VA 22161, (703)487-4732

Electrotechnology

0622 Electronic Analog Active Filters (Licensing Opportunity)

0623 Improving Shielding Effectiveness of Cables

0624 Acousto-optical/Magneto-optical Correlator or Convolver—Binary signals are processed optically in multiple channels. (Licensing Opportunity)

0625 Adaptive Force and Position Control for Robots—Precise knowledge of manipulator and environment is not required. (Licensing Opportunity)

0626 Advanced Components for Fiber-Optical Systems—This concise review emphasizes highly birefringent fibers, couplers, and polarizers.

0627 Closed-Loop Motor-Speed Control—Speed is sensed optoelectronically.

0628 Digital, Satellite-Based Aeronautical Communication—Advanced digital techniques will be needed eventually for greatest cost effectiveness.

0629 DMSK Receiver for Mobile/Satellite Service—A low-bit-rate demodulator operates in the presence of fading and Doppler shifts.

0630 Electrolytic Heat Switch—Thermal conduction is altered electrically.

0631 Jacobi-Bessel Analysis of Antennas with Elliptical Apertures—A coordinate transformation improves convergence in pattern analysis of elliptical-aperture antennas.

0632 Multiple-Beam Communications Antenna—This system has both fixed-spot and scanning coverage.

0633 Reflection-Zone-Plate Antenna—A microwave antenna is based on reflection holography.

0634 Photodiode-Coupled Light Modulator—The absorption of one light beam would control the transmission of another. (Licensing Opportunity)

Software

0635 Transferring Lens Prescriptions Between Lens-Design Programs—Most data are transferred automatically, and the user is notified of those that are not.

Testing & Instrumentation

0636 Optoelectronic Technique Eliminates Common-Mode Voltages—Small signals can be transmitted between circuits at large differences of potential. (Licensing Opportunity)

0637 Measuring Shapes of Reflectors by Microwave Holography—Theoretical and practical aspects of microwave holographic metrology are discussed. (Licensing Opportunity)

0638 Spectrograph Measures Contamination of Optical Elements—Reflective and transmittance are measured over a range of wavelengths. (Licensing Opportunity)

Other Items of Interest

0639 Axial-Gap Permanent Magnet Motor

0644 Crimping Wires in Cramped Spaces

U.S. Navy Fact Sheet

Electronic Analog Active Filters

Current active filters are normally made using operational amplifiers.(op-amps) which must have very high gain, but yet be stable with the output connected directly to the input. Op-amps have stability problems and do not work well at high frequency. A new active filter does not use the unstable, very high gain op-amps.

The high frequency action filter has an amplifier providing an open loop gain between one and three. The filter configuration consists of pole-zero pairs with no intentional connection between the negative input terminal of the amplifier and the output terminal of the amplifier. The active filter design provides active filters at high frequencies using low gain amplification stages.

In order to appreciate the advantages of the below discussed high frequency active filter design, a comparison between active and passive filters is presented:

a. Passive filters have virtually no high-frequency limit, but become bulky below 10 KHZ and are virtually unacceptable below 1 KHZ. Active filters suit the mid-range from 1 HZ to 1 KHZ, but also can be used with some care to 10 KHZ, and in limited applications can be used as high as 100 KHZ.

b. Passive filters usually must be impedance-matched on both input and output, while active filters normally have a high enough input impedance and a low enough output impedance that impedance is not a problem.

Active filters are normally made using operational amplifiers (op-amps). Op-amps must have very high (virtually infinite) gain, but yet be stable with the output connected directly to the (inverting) input (negative feedback). This is a difficult requirement and thus, op-amps have stability problems and do not work well at high frequency.

Therefore, it is desirable to provide a simple, concise, unified method for building any type of high frequency active filter without using unstable, very high gain op-amps. The herein presented design provides a high frequency active filter, without the use of high gain op-amps, which is stable at said high frequencies. This design premits the raising of the high frequency limit normally imposed on the use of active filters. Building active filters without op-amps can virtually eliminate stability problems and provide much larger bandwidths.

An amplifier having an open loop gain between one and three is provided with appropriate electrical components of appropriate values for generating the desired filter configuration of pole-zero pairs with no intentional connection between the negative input terminal of the amplifier and the output terminal of the amplifier.

The figure shows a general schematic of an exemplary embodiment of this design for generating pole-zero pairs.

FOR ADDITIONAL INFORMATION: Mr. Arthur D. Delagrange, NSWC/WO, CODE U25; 202-394-2475. Naval Surface Warfare Center, Silver Spring, MD 20903-5000. Refer to Patent 4,767,998.

NIST Technology Update

National Institute of Standards & Technology
(Formerly the National Bureau of Standards)
U.S. Department of Commerce, Gaithersburg, MD 20899

Improving Shielding Effectiveness of Cables

Aircraft, ships, missiles, and spacecraft each have miles of cable which, if not properly shielded, are susceptible to stray or intentional electromagnetic (EM) interference. This interference may affect vital systems, for example, causing helicopters to crash. The problem is becoming more challenging as metal structures are replaced with composite materials, leaving the cabling more vulnerable to EM threats including high-power microwave pulses, lightning, and EM pulses from nuclear detonation. NIST is working with the defense and aerospace industries to improve old and develop new standards for measuring the shielding effectiveness of cables connected to electronic equipment. NIST engineers are using special facilities--transverse electromagnetic (TEM) cells and reverberation chambers--to create EM fields in the laboratory to evaluate cables. Test frequencies range from 14 kHz to 18 GHz, with dynamic ranges up to 130 dB. NIST plans to develop guidelines for evaluating the shielding effectiveness of both coaxial and complex multiconductor cables/connection assemblies. Tests have already been done for Martin Marietta and ITT Cannon.

FOR ADDITIONAL INFORMATION: Myron L. Crawford, Division 723.03, NIST, Boulder, CO 80303; (303) 497-5497.

NASA Tech Brief
National Aeronautics and Space Administration
NASA's Jet Propulsion Laboratory, Pasadena, California

Licensing Opportunity

Acousto-optical /Magneto-optical Correlator or Convolver

Binary signals are processed optically in multiple channels.

An experimental system has been built to demonstrate the optical processing of multiple channels of binary signals. One of the input channels contains a signal that varies with time and is applied to a one-dimensional acousto-optical cell. The other input channel contains a two-dimensional pattern that can be stationary or that can vary with time and is applied to a magneto-optical spatial light modulator. The output is the time-varying correlation or convolution of the first input with one of the rows in the second input.

As shown in Figure 1, a laser beam is expanded in a horizontal plane by cylindrical lens L_1 and collimated by cylindrical lens L_2. The expanded beam passes through the acousto-optical cell, where it is intercepted by the moving diffraction grating created by the time-varying input signal. The transmitted, diffracted beam passes through Fourier-transform cylindrical lens L_3, which enables a spatial filter to select the portion of the signal refracted to the positive first order.

The beam is expanded vertically by cylindrical lens L_5, while a second Fourier-transform cylindrical lens, L_4, restores the filtered moving grating pattern. The fully expanded beam is imaged on the magneto-optical spatial light modulator. The pattern of light transmitted through this modulator contains the product of the one-dimensional, moving input pattern, with each of the patterns stored on each row of this modulator.

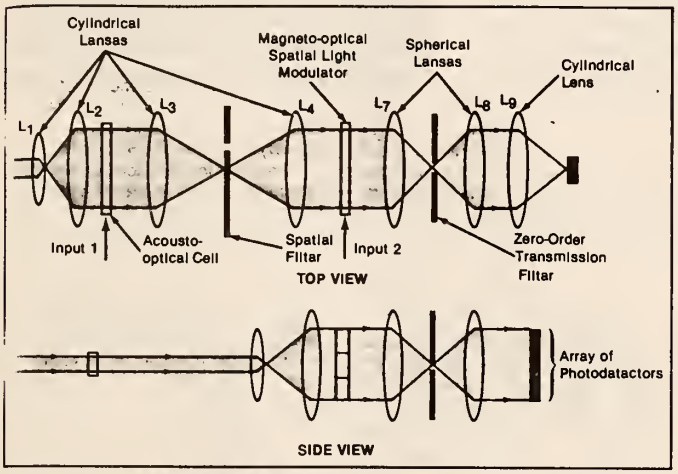

Figure 1. Using **Acousto- and Magneto-optical** spatial light modulators, this apparatus processes two streams of binary signals optically.

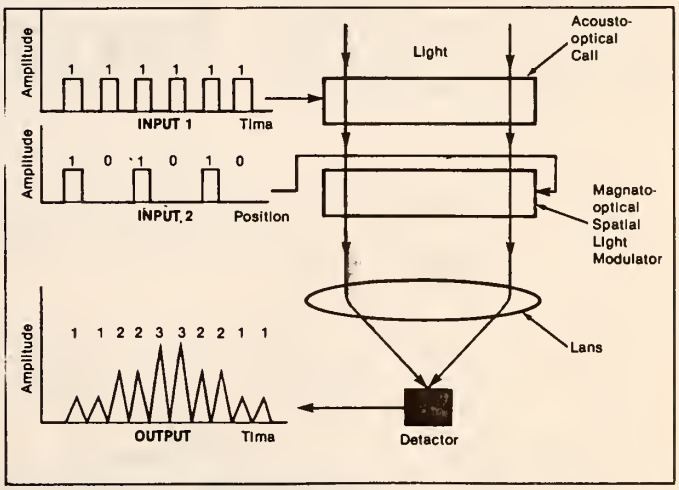

Figure 2. In this **Simplified Schematic Representation**, the convolution of the two inputs appears at the output of the photodetector as a signal that varies with time.

The convolution or correlation of the two patterns with each other is obtained via the Fourier transform of the product of the two input light-transmission patterns. (Whether the convolution or the correlation is obtained depends upon the order in which the information is stored in each row of the two-dimensional pattern.) Because the product of the two functions also contains the regular grid structure of the magneto-optical modulator, which would cause crosstalk between channels, the beam is Fourier-transformed by spherical lens L_7, passed through a zero-order transmission filter (which removes the grid), and retransformed by spherical lens L_8. The final cylindrical lens, L_9, focuses each convolution or correlation signal onto a series of photodetectors; the time-varying output of each photodetector is one of the designated correlation or convolution signals (see Figure 2).

This work was done by Hua-Kuang Liu of Caltech and Jeffrey A. Davis of San Diego State University for **NASA's Jet Propulsion Laboratory**.

This invention is owned by NASA, and a patent application has been filed. Inquiries concerning nonexclusive or exclusive license for its commercial development should be addressed to the Patent Counsel, NASA Resident Office-JPL Refer to NPO-17178/TN

Jet Propulsion Lab.
NASA Resident Office
Technology Utilization Officer: Gordon S. Chapman
Mail Stop 180-801
4800 Oak Grove Drive
Pasadena, CA 91109
(818) 354-4849
Patent Counsel: Paul F. McCaul
Mail Code 180-801
4800 Oak Grove Drive
Pasadena, CA 91109
(818) 354-2734
Technology Utilization Mgr. for JPL: Norman L. Chalfin
Mail Stop 156-211
4800 Oak Grove Drive
Pasadena, CA 91109
(818) 354-2240

FOR ADDITIONAL INFORMATION: *Contact: Director, Technology Transfer Division, P.O. Box 8757, BWI Airport, MD 21240; (301) 621-0100 Ext. 241*
REFER TO THE NUMBER LISTED AT THE END OF THIS ARTICLE

NASA Tech Brief
National Aeronautics and Space Administration
NASA's Jet Propulsion Laboratory, Pasadena, California

Licensing Opportunity

Adaptive Force and Position Control for Robots

Precise knowledge of manipulator and environment is not required.

A control system causes the end effector of a robot manipulator to follow a prescribed trajectory and apply the desired force or torque to an object that it is manipulating or with which it is in contact. The system is characterized by a hybrid control architecture, in which the positions and orientations along unconstrained coordinate axes are controlled by a position-control subsystem, while the forces and torques along the constrained coordinate axes are controlled by a force-control subsystem (see figure). The system compensates for the dynamic cross-coupling between the force- and position-control loops and does not require knowledge of the complicated model of the dynamics of the manipulator and its environment.

In the force-control subsystem, the feedforward force vector P_r (representing the desired effector contact forces) is processed along with the measured (feedback) force vector P, an auxiliary signal d, and the velocity feedback $\dot{Z}$ to produce the control vector F_z for the forces and torques applied to the end effector along the constrained axes by the manipulator-joint actuators. The control law includes proportional, integral, and derivative gain matrices K_p, K_I, and K_v, respectively, that vary with time according to the equations of the adaptation scheme, which strives to reduce the error vector, e_Z, between the feedforward and feedback force vectors.

The position-control subsystem enforces a linear adaptive control law that produces the manipulator force-and-torque control vector F_Y for the unconstrained axes from the feedforward position vector R and from the feedback position and velocity Y and $\dot{Y}$, respectively. An auxiliary vector f and the control-gain matrices K, C, A, B,

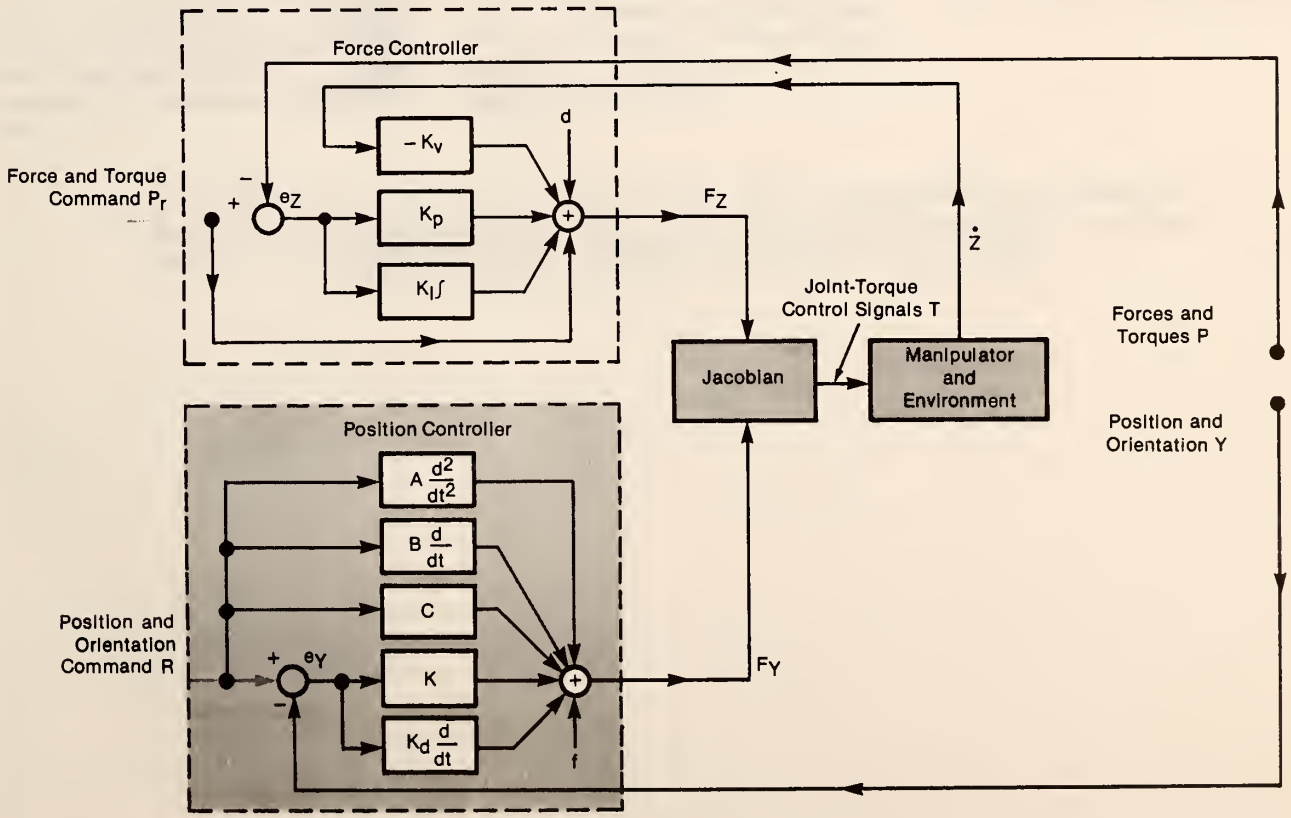

The **Control Gains** (represented by the small rectangles on the left) of this position- and force-control system are continually adapted according to prescribed adaptation laws to reduce the error signals e_Y and e_Z.

and K_d are calculated according to adaptation equations, the forms of which resemble those of the force controller, and which reduce the error vector e_Y.

The force- and position-control signals are in Cartesian coordinates of the workspace and are transformed to equivalent joint-torque-control signals in manipulator-joint space via the Jacobian matrix of the manipulator-joint coordinate system. The dynamic cross-coupling effects are mathematically modeled as disturbance terms in the force- and position-control loops.

The adaptive force and position controllers have, in effect, learning capabilities to cope with unpredictable changes in the manipulator or the environment; this is because the controller gains are adapted rapidly on the basis of manipulator performance by use of simple arithmetic operations. The control scheme is computationally fast enough for use at sampling rates as high as 1 kHz.

This work was done by Homayoun Seraji of Caltech for **NASA's Jet Propulsion Laboratory**.

In accordance with Public Law 96-517, the contractor has elected to retain title to this invention. Inquiries concerning rights for its commercial use should be addressed to

Edward Ansell,
Director of Patents and Licensing
Mail Stop 301-6
California Institute of Technology
1207 East California Boulevard
Pasadena, CA 91125

Refer to NPO-17127/TN

Jet Propulsion Lab.
NASA Resident Office
Technology Utilization Officer: Gordon S. Chapman
Mail Stop 180-801
4800 Oak Grove Drive
Pasadena, CA 91109
(818) 354-4849
Patent Counsel: Paul F. McCaul
Mail Code 180-801
4800 Oak Grove Drive
Pasadena, CA 91109
(818) 354-2734
Technology Utilization Mgr. for JPL: Norman L. Chalfin
Mail Stop 156-211
4800 Oak Grove Drive
Pasadena, CA 91109
(818) 354-2240

FOR ADDITIONAL INFORMATION: *Contact: Director, Technology Transfer Division, P.O. Box 8757, BWI Airport, MD 21240; (301) 621-0100 Ext. 241*

REFER TO THE NUMBER LISTED AT THE END OF THIS ARTICLE

NASA Tech Brief
National Aeronautics and
Space Administration

Advanced Components for Fiber-Optical Systems

This concise review emphasizes highly birefringent fibers, couplers, and polarizers.

A paper reviews the statuses of some advanced passive and active optical components for use with optical fibers. The emphasis is on highly birefringent components that control polarization, because the control of polarization is critical in such applications as fiber-optical gyroscopes, interferometric sensors, and coherent communications.

The classes of passive components reviewed include highly birefringent fibers, coupler-based devices, and polarizers. Birefringent fibers have elliptical, stressed, cut, or otherwise non-circularly-symmetrical cores that maintain polarization. Such fibers are expensive (>$10/m) but perform well in that cross-coupling to the undesired polarization is typically less than 5×10^{-3} $(km)^{-1}$.

The coupler-based components include polished and fused single-mode couplers, special items that perform at several wavelengths, arrays of high uniformity, and units made partly of highly birefringent fibers. Some of these devices couple both polarizations to the same degree, while others have been built to couple primarily one polarization, thus acting analogously to polarizing beam splitters.

Fiber polarizers are made by a polishing technique similar to that used to make some couplers. In this approach, a dielectric layer and then a metal layer are deposited on the polished face of a flat longitudinal cut that passes near the axis at a bend in the fiber. In an alternative version, only a metallic layer is deposited.

The active components of interest include piezoelectric transducers that indirectly produce optoelectronic or electro-optical effects to modulate phase, frequency, or polarization. Typically, a piezoelectric device surrounds a fiber and constricts it when an electrical signal is applied. The constriction gives rise to the birefringence that modulates the light traveling along the fiber.

This work was done by Ramon De Paula of Caltech and David W. Stowe of Aster Corp. for **NASA's Jet Propulsion Laboratory**. *"Overview of Advanced Components for Fiber Optic Systems," NPO-17080/TN*

FOR ADDITIONAL INFORMATION: *Contact: Director, Technology Transfer Division, P.O. Box 8757, BWI Airport, MD 21240; (301) 621-0100 Ext. 241*
REFER TO THE NUMBER LISTED AT THE END OF THIS ARTICLE

NASA Tech Brief
National Aeronautics and
Space Administration
Marshall Space Flight Center, Alabama

Closed-Loop Motor-Speed Control

Speed is sensed optoelectronically.

The electronic motor-speed control circuit shown in the figure is designed to operate in an electrically noisy environment. The circuit includes an optoelectronic pickup device, which is placed inside the motor housing to provide a speed feedback signal. The circuit automatically maintains the speed of the motor at a commanded value. The major advantage of the particular circuit design is low cost.

The pickup device contains an infrared light-emitting diode and a phototransistor. The radiation from the diode is chopped by the fan blades of the motor into pulses, which are detected by the phototransistor. The train of pulses from the phototransistor is fed to a frequency-to-voltage converter, the output of which is a voltage proportional to the speed of the motor. This voltage is low-pass filtered, amplified, and compared with a manually-adjustable control voltage that represents the commanded speed.

The difference between the speed-measurement and speed-command signals is amplified and fed as a control voltage to an external power amplifier that drives the motor. A selector switch at the output of the final amplifier of this circuit also enables the operator to bypass the circuit and manually set the control voltage for the external amplifier.

This work was done by Matthew A. Smith, Ray C. Delcher, and Steven W. Huston of Rockwell International Corp. for **Marshall Space Flight Center**. *No further documentation is available. MFS-29469/TN*

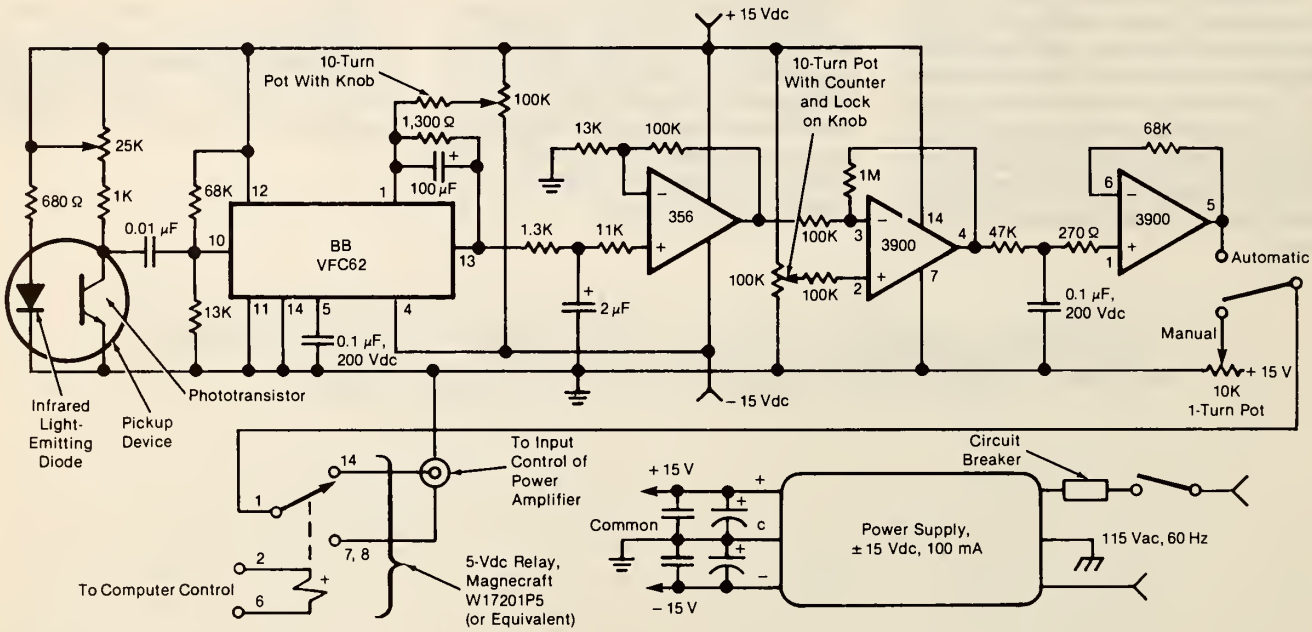

Notes: 1. Bypass supply pins with large and small capacitors
2. All resistors ¼ W, 5 percent tolerance
3 The unused inputs 3900 (8,11,12,13) to ground

The **Speed-Control Circuit** measures the speed of the motor in terms of the frequency of pulses of infrared light chopped by the fan blades of the motor. The difference between the measured and commanded speeds serves as a control signal for an external amplifier that drives the motor.

FOR ADDITIONAL INFORMATION: *Contact: Director, Technology Transfer Division, P.O. Box 8757, BWI Airport, MD 21240; (301) 621-0100 Ext. 241*
REFER TO THE NUMBER LISTED AT THE END OF THIS ARTICLE

NASA Tech Brief
National Aeronautics and
Space Administration
NASA's Jet Propulsion Laboratory, Pasadena, California

Digital, Satellite-Based Aeronautical Communication

Advanced digital techniques will be needed eventually for greatest cost effectiveness.

A proposed satellite system would relay communication between aircraft and stations on the ground. Such a system would offer better coverage than is now possible with direct communication between the air and the ground, would cost less, and would make possible new communication services.

The system would carry both voice and data. Because many of the data exchanged between an aircraft and the ground contain safety-related information, a low probability of bit errors will be essential.

An aeronautical-mobile/satellite system poses a special combination of conditions for designers. The channels will be subject to a mild form of multipath fading because of the motions of aircraft and satellites. The receivers will be burdened by bursty signals because of the short messages that will be transmitted. Moreover, both the spectrum and the available power will be limited.

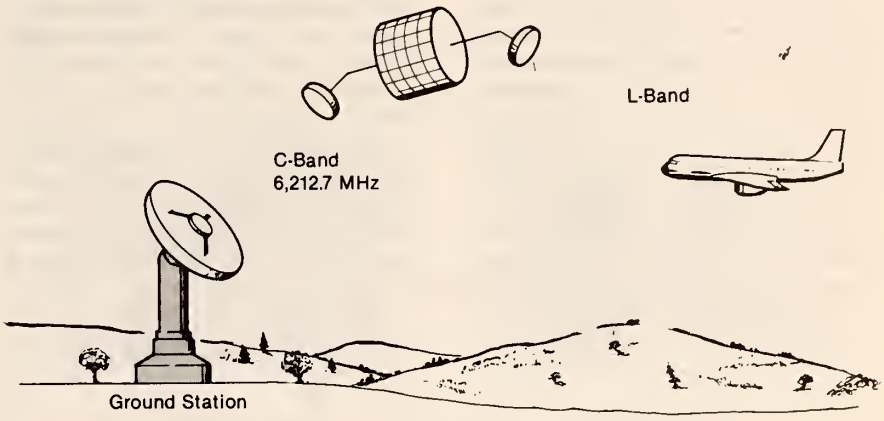

The **Proposed Satellite-Based Communication System** for aircraft was explored in an experiment. The dashed line represents a reflection that contributes to multipath signals—a problem that system designers must take into account.

An experiment was conducted to examine the characteristics of the aeronautical-mobile/satellite channel (see figure). Delay spreads, scattering coefficients, and other parameters were measured. The experimental data were used to evaluate the merits of wideband versus narrowband transmission and coherent versus noncoherent demodulation.

Given fixed resources of power and spectrum, new digital modulation technologies should be evaluated to bring services to the greatest number of users and thereby reduce costs and increase coverage. For the first-generation system, such proved modulation schemes as quaternary phase-shift keying are good candidates. More advanced techniques like trellis-coded M-ary modulation warrant consideration for later generations, but additional development and experimentation are needed.

Adequate power margin, guard band, and guard time will be needed to ensure reliable operation with semistationary channels. For the sake of safety, data messages will have to be transmitted with error-correcting and error-detecting codes. Voice messages will need little encoding, if any — users can simply request the repetition of unintelligible transmissions.

The proposed information rate per user is 4,800 bits per second. This rate will be adequate for data and for speech of fair quality. At 4,800 bits per second, the frequency interval between channels will be 10 kHz or less, depending on the modulation scheme.

This work was done by F. Davarian of Caltech for **NASA's Jet Propulsion Laboratory**. *NPO-17252 /TN*

FOR ADDITIONAL INFORMATION: *Contact: Director, Technology Transfer Division, P.O. Box 8757, BWI Airport, MD 21240; (301) 621-0100 Ext. 241*
REFER TO THE NUMBER LISTED AT THE END OF THIS ARTICLE

NASA Tech Brief
National Aeronautics and
Space Administration
NASA's Jet Propulsion Laboratory, Pasadena, California

DMSK Receiver for Mobile/Satellite Service

A low-bit-rate demodulator operates in the presence of fading and Doppler shifts.

A receiver for 2.4-kbit/s differential minimum-shift keying (DMSK) and Gaussian minimum-shift keying (GMSK) is suitable for communication between land-mobile stations via geostationary satellites. Operating on a phase-shifted signal in the 800-MHz band, in the presence of fading and Doppler frequency shifts, the receiver is compact, makes efficient use of the frequency spectrum, and wastes little power. The receiver design can be implemented in very-large-scale-integrated circuits.

The incoming signal is shifted to an intermediate frequency of 50 MHz, wide-bandpass filtered, amplitude limited, then mixed with in-phase and 90°-phase-shifted signals from a 50-MHz voltage-controlled oscillator (see figure). The in-phase and quadrature mixer products are low-pass filtered at baseband and sent to "two-bit" differential detectors — so called because each mixes its input signal with the same signal delayed by two bit periods — to produce an output indicative of the difference in phase between the signal values at those two times.

The problem in receiver design is to assure that the phase detector makes the correct decision ($\pm\pi$ or 0) concerning this phase difference. The phase-shift error is minimized by operating the two-bit detectors at baseband rather than at the intermediate frequency. The low-pass filters in the in-phase and quadrature signal paths have a Gaussian characteristic and a peak-to-peak delay differential of 17 μs within the passband. (A differential as small as this would be difficult to achieve at the intermediate frequency.) The maximum peak-to-peak differential delay of the delay line is only 5 μs. As a result, the maximum anticipated phase error at the frequency-shift-keying tone frequency of 600 Hz is only 4.7°.

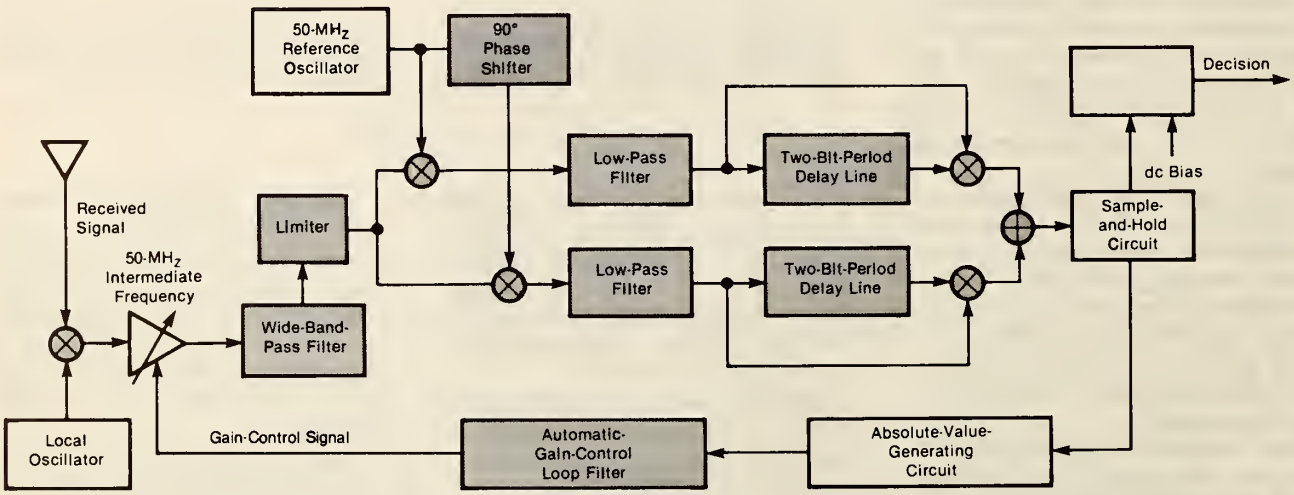

The **Basic DMSK Receiver Design** relies on baseband rather than intermediate-frequency processing of the in-phase and quadrature signal components because the phase errors due to differential delays are smaller at baseband. In the prototype receiver, the basic design shown here is augmented with automatic frequency control to correct frequency errors.

The performance of the receiver was measured in the presence of thermal noise. A plot of the measured error rate as a function of the ratio of bit energy to noise energy closely followed the prediction of previous authors for the ideal case.

The error performance was measured in the presence of Rayleigh fading with a Doppler frequency of 20 Hz and Rician fading with a Doppler frequency of 72 Hz and a line-of-sight-to-multipath ratio of 10. The irreducible-error rate was also measured and plotted for a Doppler frequency of 72 Hz and a range of line-of-sight-to-multipath ratios. At a ratio of 10, the irreducible-error rate is 10^{-6}, which is well below the network requirement of 10^{-3} for digital communications.

Receivers of this type are known to be sensitive to large frequency offsets, and tests confirmed that the performance of this receiver is degraded severely by frequency errors larger than 20 Hz. To overcome this deficiency, an automatic-frequency-control loop was added; this reduced the frequency error to a negligible level. The cost of the frequency-control loop to the static performance of the receiver is about 0.5 dB.

This work was done by Faramaz Davarian, Marvin K. Simon, and Joe T. Sumida of Caltech for **NASA's Jet Propulsion Laboratory**.
NPO-16659/TN

FOR ADDITIONAL INFORMATION: *Contact: Director, Technology Transfer Division, P.O. Box 8757, BWI Airport, MD 21240; (301) 621-0100 Ext. 241*
REFER TO THE NUMBER LISTED AT THE END OF THIS ARTICLE

NASA Tech Brief
National Aeronautics and Space Administration
Marshall Space Flight Center, Alabama

Electrolytic Heat Switch

Thermal conduction is altered electrically.

Experiments have demonstrated the feasibility of an electrolytic device of electrically-controllable thermal conductivity. The investigation continues in the effort to develop a thermal switch that will be lightweight, less than 1 cm thick, and easily integrable into existing heat-transfer systems, and that will consume minimal electric power while switching between the "off" state (low thermal conductance) and the "on" state (thermal conductance 10 times that of the "off" state).

The device includes an inner ionomeric layer of low thermal conductivity sandwiched between two metal-foil electrodes (see figure). When the device is fully developed, the ionomeric layer will likely be a conductive polymer — perhaps polyaniline. In effect, the device will be a metal/conductive-polymer secondary electrical cell.

The electrical charging of this cell causes metal dendrites to grow from the foils across the inner layer by the deposition of ions from the electrolyte. Because the thermal conductivity of the metal is much greater than that of the ionomer, the overall thermal conductance of the device decreases as the dendrites grow across the inner layer.

The useful lifetime and operating characteristics of the device depend on many factors that interact with each other. Of primary concern is that the metal deposits be dendritic rather than spongy or densely-packed, smooth layers of crystals. The properties of the metal deposits are affected by the temperature, current density, type and concentration of electrolyte, the type of ionomer, the type of filler material (if any) in the inner layer, and the sizes, shapes, and materials of the electrodes.

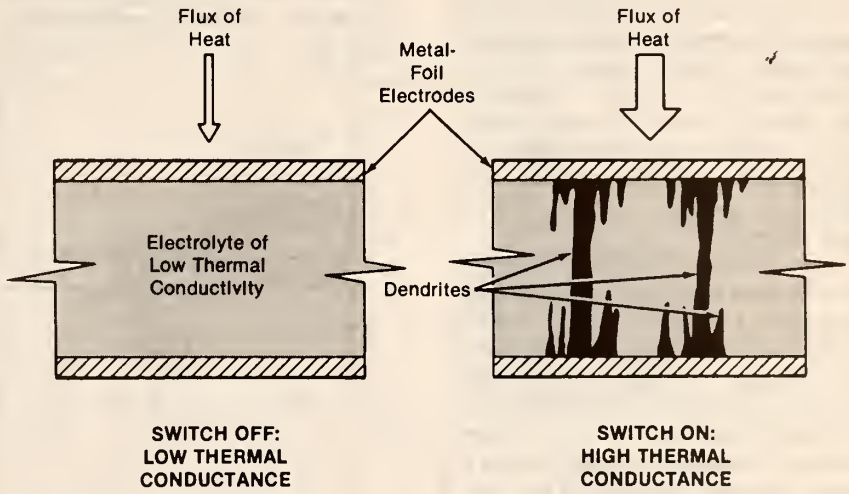

The **Flow of Heat** across the electrolytic heat switch is increased or decreased by the electrochemical deposition or dissolution, respectively, of highly-thermally-conductive metal dendrites across the thermally insulating layer of electrolyte.

As experience was gained during the early experiments, the device evolved through several versions. Because the solid electrolyte was not sufficiently developed for thermal tests, the cells were made with liquid electrolytes filled with porous polymeric materials to reduce thermal conduction and to suppress convection in the electrolytes, which also contributes to the transport of heat. In addition, the anodes were covered by perfluorinated cationic membranes (of a type used as a separator in silver oxide batteries) to assure the reversibility of the electrochemical reactions by preventing the dendrites from penetrating to the anode and thereby causing electrical short circuits.

The design selected for thermal tests included silver electrodes, an electrolyte of silver nitrate in water, and a filler of polypropylene felt. In the tests, the thermal conductivity of the device was increased 21 percent by the deposition of silver dendrites in the inner layer. There is hope for considerable improvement because, according to the projections of a mathematical model, silver dendrites occupying only 1 percent of the area of a cell should increase the thermal conductance by a factor of 10. Furthermore, using data from experiments in electrochemical jigs, it is estimated that the power necessary to operate a typical cell of 20 by 20 cm will be only 2.5 W.

This work was done by Myles Walsh, Gregory D'Andrea, Joseph Adelstein, Brian G. Dixon, and R. Scott Morris of Cape Cod Research for **Marshall Space Flight Center**. *MFS-26074/TN*

FOR ADDITIONAL INFORMATION: *Contact: Director, Technology Transfer Division, P.O. Box 8757, BWI Airport, MD 21240; (301) 621-0100 Ext. 241*
REFER TO THE NUMBER LISTED AT THE END OF THIS ARTICLE

NASA Tech Brief
National Aeronautics and
Space Administration
NASA's Jet Propulsion Laboratory, Pasadena, California

Jacobi-Bessel Analysis of Antennas with Elliptical Apertures

A coordinate transformation improves convergence in pattern analysis of elliptical-aperture antennas.

A modified version of the Jacobi-Bessel expansion for the vector diffraction analysis of reflector antennas uses a coordinate transformation to improve convergence with elliptical apertures. The usual Jacobi-Bessel expansion converges rapidly (i.e., requires relatively few terms) for antennas with circular apertures, but less rapidly for elliptical apertures.

Because the modified Jacobi polynomials (related to Zernike functions) used are orthogonal functions over circular regions, it is natural to apply them to circular apertures. To apply these functions to an elliptical aperture, the aperture is considered to be circumscribed by a circle of diameter equal to the major elliptical axis, and the induced current on the portion of the reflector surface between the circle and the ellipse is assumed to be zero. Because of this discontinuity in the integrand, more terms of the series than would otherwise be needed must be computed to achieve adequate convergence.

The lack of convergence can be remedied by the use of a coordinate transformation that re-expresses the elliptical case in a form that is circular in the new variable space. The radiation integral can be tailored for an elliptical projected aperture with major and minor axes of 2a and 2b by the following change of variables in the integrand

$$x' = at\cos\Psi$$
$$y' = bt\sin\Psi, \text{ and}$$
$$dx'\,dy' = abt\,dt\,d\Psi$$

where x′ and y′ are the original orthogonal coordinates in the aperture plane and Ψ is the azimuthal angle in the transformed aperture plane.

After applying this transformation, performing a Taylor-series expansion with a central plane chosen to be as close to the reflector rim as possible, incorporating the Jacobi-Bessel expansion, and some additional manipulations, the resulting expansion converges much more rapidly than does the original expansion (see figure). It is a simple matter to modify existing circular Jacobi-Bessel computer programs to incorporate the elliptical algorithm.

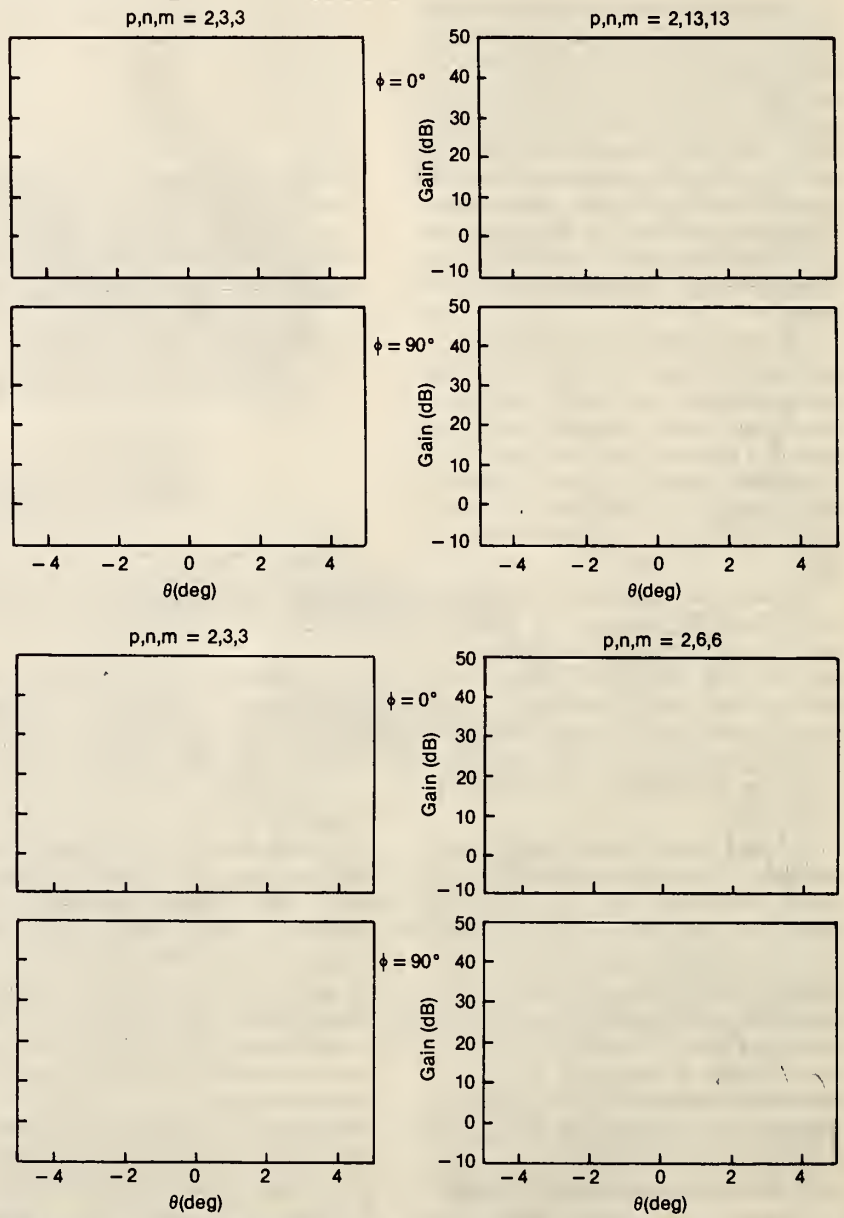

The **Difference in Convergence Behavior** between the circular Jacobi-Bessel (top) and the elliptical Jacobi-Bessel (bottom) algorithms is indicated by the highest values of the indices m, n, and p (indicative of the order of the expansion) required to achieve the same accuracy in the computed radiation pattern of an offset paraboloidal antenna with an elliptical aperture.

This work was done by Y. Rahmat-Samii of Caltech for **NASA's Jet Propulsion Laboratory**. *NPO-16967/TN*

FOR ADDITIONAL INFORMATION: *Contact: Director, Technology Transfer Division, P.O. Box 8757, BWI Airport, MD 21240; (301) 621-0100 Ext. 241*
REFER TO THE NUMBER LISTED AT THE END OF THIS ARTICLE

NASA Tech Brief
National Aeronautics and
Space Administration
Lewis Research Center, Cleveland, Ohio

Multiple-Beam Communications Antenna

This system has both fixed-spot and scanning coverage.

Advanced offset-fed spacecraft antenna systems operating in the 30/20 GHz frequency bands have been developed that can provide multiple-radiating fixed-spot and regional-coverage scanning beams for use on communications satellites. These antennas, operating at the higher frequencies, will provide alternate frequency bands for expansion of existing satellite services as well as achieving frequency reuse capability for conservation of the frequency spectrum.

The satellite antenna configuration uses separate uplink and downlink antennas. Each antenna provides narrow fixed-spot beams to major cities of the continental United States (CONUS) and scanning beams that cover wide-angle geographic areas (sectors) of the CONUS. The spot beams provide the communications coverage for high-volume traffic between major cities, where each beam will cover an area approximately 200 m (322 km) in diameter, and the spacing of the spots across the country allows reuse of the same frequency in many beams. The scanning beams provide coverage for direct-to-user services to remotely located areas according to the demands of the users.

The primary function of the multiple-beam antenna system is to receive the message traffic from the major trunk-beam cities and scanning areas, route this information through an onboard switch or message-processing system, and then transmit these messages to their respective destinations.

The antenna system will provide 18 trunking beams to preassigned major cities of the CONUS and 6 scanning beams, each covering approximately one-sixth of the CONUS. The separate receiving and transmitting antennas are operationally similar except for frequency scaling of dimensions. Each antenna beam has a beam width of 0.3° and a gain of 50 to 53 dB or more. They will provide isolation of 30 dB between individual spots. The control system for the scanning beams allows any one uplink or downlink beam to be independently sequenced to any one of its positions. The dwell time at each position is programmable between 10 and 100 μs, and the switching time between beam positions is less than 0.5 s.

Both the 20-GHz-transmitting, 30-GHz-receiving antennas use unique concepts in

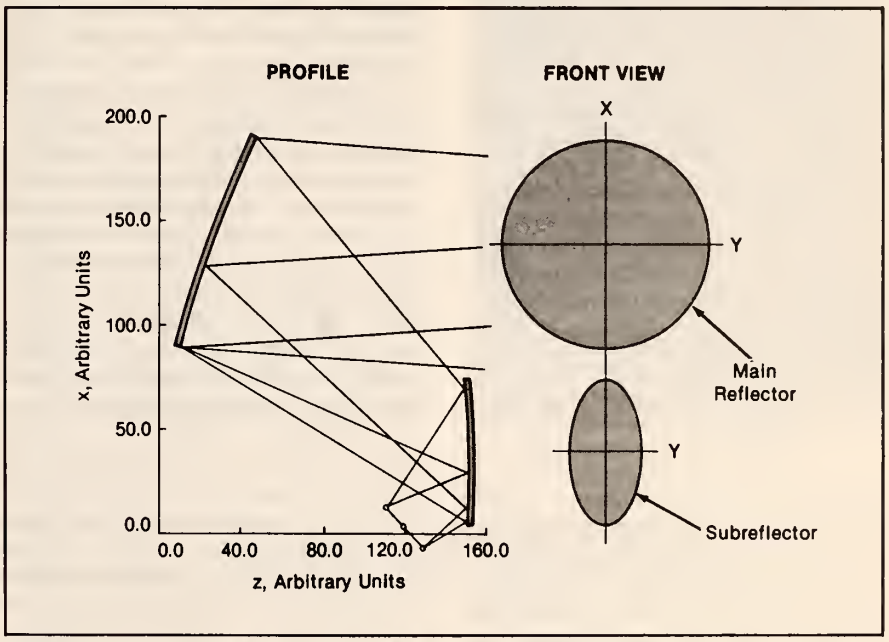

Figure 1. The **20-GHz Transmitting Antenna,** shown schematically here, is an offset-fed, dual-reflector configuration.

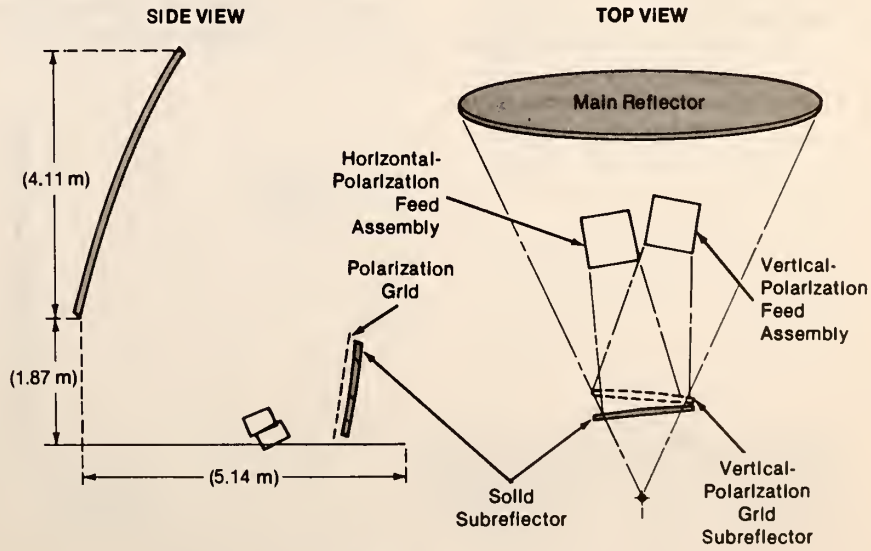

Figure 2. The **30-GHz Receiving Antenna** has orthogonal polarized feeds, hyperbolic reflectors, and two subreflectors.

achieving the goals for meeting the requirements for multiple-beam, high-gain, and optimum-beam isolation. The feed network arrays use multiple horns per beam; sharing of horn clusters for trunk and scan beams; orthomode junctions for dual polarization; diplexers for dual frequency use; and high-speed, low-loss ferrite circulator switches, variable power dividers, and variable phase shifters.

The 20-GHz transmitting antenna (see Figure 1) is an offset-fed dual-reflector microwave optical system with planar-array feed consisting of a multiple-port beam-forming-network (BFN). To form the narrow 0.3° beams, the main reflector is 13.5 ft (4.1 m) in diameter, and the subreflector is a nominal 9.5 ft (2.9 m) in diameter. A unique feature of this hardware model is the shaped main and subreflector surfaces to minimize losses over the required field of view. Thus, the reflectors are not portions of a figure of revolution but are each doubly curved surfaces that have no true focal point at the zero-scan beam position, so that defocusing at the edges of the scan field of view is minimized.

The feed assembly BFN lattice uses seven-element, coherently driven horn clusters for each beam. For beam switching, the ferrite circulator switches, variable power dividers, and variable phase shifters have switching energies as low as 40 μJ and weights as low as 12 g. As a result, large numbers of switch components can be used to provide the required multiple beams, the off-axis scan capability, and both vertically and horizontally polarized beams. All results met or exceeded the design goals.

The 30-GHz-receiving-antenna system is of a similar geometry, but uses hyperbolic reflectors, two subreflectors stacked to form a double-layer bifocal subreflector system, and two orthogonally polarized feed assemblies diplexed by a front wire-grid subreflector (Figure 2). To form the narrow receiving-frequency beams, the main reflector is 9.5 ft (2.9 m) in diameter, and the subreflectors are 5.0 ft (1.5 m) in diameter.

The two orthogonally polarized feeds are completely separated into two focal-point-fed areas for higher gains to compensate for the increased scan losses of the off-axis beams. Similarly, the ferrite switching devices scaled to the 30 GHz frequency band used in the receiving feed array have short switching times, low energy input, low losses, and low weight.

The 30- and 20-GHz antenna systems demonstrated that high-frequency, precise-reflector optical systems can be fabricated and that the feed-beam-forming networks can produce very narrow beams for use on geostationary satellites. As a result, advanced communication satellites will expand existing satellite services by means of narrow spot beams and frequency reuse techniques.

This work was done by R. W. Myhre of **Lewis Research Center,** *T. E. Roberts of Ford Aerospace & Communications Corp., and W. C. Wong of TRW, Inc.*

LEW-14190/TN

FOR ADDITIONAL INFORMATION: *Contact: Director, Technology Transfer Division, P.O. Box 8757, BWI Airport, MD 21240; (301) 621-0100 Ext. 241*

REFER TO THE NUMBER LISTED AT THE END OF THIS ARTICLE

NASA Tech Brief
National Aeronautics and
Space Administration
Langley Research Center, Hampton, Virginia

Reflection-Zone-Plate Antenna

A microwave antenna is based on reflection holography.

A new type of microwave antenna, based on reflection holography, has been designed and tested. The design can be modified to produce arbitrary beam patterns by controlling the relief pattern, and the antenna can be planar or contoured to the supporting structure. The antenna has a low off-axis radar cross section at frequencies removed from the operational frequency.

Many large-aperture microwave antennas are adaptations of optical systems, the most common being parabolic reflectors used for satellite reception. However, the state of the art in the design of optical elements now extends to holography. The interference pattern produced by a spherical wave intersecting a plane wave consists of concentric circles similar to Newton's rings. This pattern is identical to that of a Fresnel zone plate, which has lens properties. A plane wave incident on such a hologram, or zone plate, is focused to a point.

Figure 1 shows an edge-on sectional view of a zone plate that consists of alternating transparent and opaque concentric circles. If the opaque circles are made from a highly reflective metal, the transmitted energy of the incident plane wave is focused to a point to the right of the plate, and the equivalent reflected energy is focused to a point to the left.

The efficiency of this device as a reflection-zone plate can be doubled by modifying the transmissive areas to introduce a phase reversal to the reflected energy. One way is to place a continuous reflecting plane one-quarter wavelength behind the zone plate. Energy passing through the transmissive circles is reflected back after traveling a total of one-half wavelength, equivalent to a phase change of 180°. Figure 2 shows a 13-zone, phase-reversal antenna 36 in. (0.91m) in diameter mounted in an anechoic test chamber. A single conical horn illuminates the antenna at the design microwave frequency of 11.8 GHz.

The axial chromatic aberration of a zone plate is not a serious problem in microwave applications, where the signals are typically monochromatic. In fact, chromatic aberration becomes an advantage in that unwanted frequencies are not focused at the feed as they are in parabolic reflectors. This reduces the level of interference and drastically reduces the off-axis radar cross section of the antenna at frequencies removed from the operating frequency.

Furthermore, although the zone plate can be difficult to construct for portions of the electromagnetic spectrum, it is easier to fabricate than is a parabolic reflector or lens in the wavelength range of interest. The flat surfaces are obviously more readily machinable than are parabolic surfaces and are easier to mount and verify for installed-surface accuracy. Finally, off-axis and specially-shaped beam designs can be obtained by the use of existing computer codes for binary holograms.

Figure 2. This **Reflection-Zone, Phase-Reversal Antenna** is made by bolting aluminum rings to an aluminum plate.

This work was done by John M. Franke and Bradley D. Leighty of **Langley Research Center**. *LAR-13537/TN*

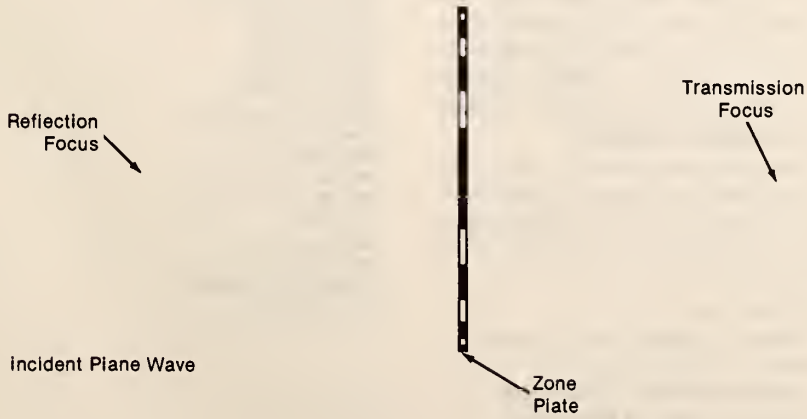

Figure 1. The **Reflective Efficiency** of this simple device can be doubled by modifying the transmissive rings to phase-shifted reflective rings.

FOR ADDITIONAL INFORMATION: *Contact: Director, Technology Transfer Division, P.O. Box 8757, BWI Airport, MD 21240; (301) 621-0100 Ext. 241*
REFER TO THE NUMBER LISTED AT THE END OF THIS ARTICLE

NASA Tech Brief
National Aeronautics and Space Administration
NASA's Jet Propulsion Laboratory, Pasadena, California

Licensing Opportunity

Photodiode-Coupled Light Modulator

The absorption of one light beam would control the transmission of another.

A proposed high-performance monolithic light modulator would comprise a p-doped/intrinsic/n-doped (PIN) GaAs photodiode grown directly over an InAs/GaAs PIN multiple-quantum-well (MQW) diode (see figure). The construction of the new modulator depends on recent advances in molecular-beam epitaxy, which make possible the growth of such new types of InAs/GaAs strain-layer semiconductor microstructures as MQW's and compositional superlattices that have enhanced electro-optical properties. Standard lithographic and etching techniques could be used to form two-dimensional arrays of the modulator elements for use as spatial light modulators. These would be useful in the processing of images or other arrays of data at very high throughput rates. Metal/semiconductor field-effect-transistor circuitry could be included on the periphery of the GaAs chip for control of voltage and frequency to the array.

In the new modulator, the "writing" (modulating) signal would be a beam of light of photon energy greater than the GaAs bandgap, while the "reading" signal (the signal to be modulated) would be a light beam of photon energy less than the bandgap and at the exciton level of the MQW's. The "writing" signal would be absorbed in the upper diode: this would charge the n^+/p^+ node with the integrated photocurrent and thus increase the voltage across the MQW diode. This increase in voltage increases the electric field. Acting on the MQW's and via the quantum confined Stark effect, modulates the transmission of the reading signal through the MQW diode. The information written in the modulator is erased when the applied voltage V is set to zero. Therefore, the integration time (or sensitivity) and frequency response can be selected for a given application.

Since this modulator is transparent to the reading signal, it is practical to transmit the reading signal through the GaAs substrate without having to make membrane structures (by etching the substrate), as is done in the case of AlGaAs/GaAs MQW's.

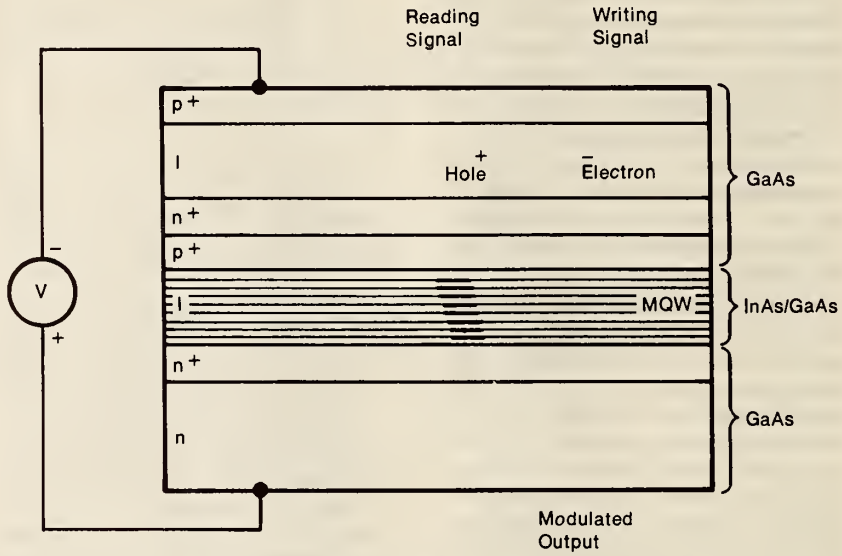

A **Photodiode-Coupled Multiple-Quantum-Well Modulator** would include advanced semiconductor microstructures that have enhanced electro-optical properties. Using standard lithographic and etching techniques for defining picture elements, such structures could be fabricated into two-dimensional arrays for use as spatial light modulators.

The use of the InAs/GaAs for the MQW's offers the flexibility of tailoring the quantum level and, hence, the wavelength of the reading beam to the longer wavelengths associated with fiber optics; e.g., 1.3 or 1.55 μm. Its use in conjunction with <111> oriented substrates offers potential of enhanced electro-optic effects due to strain.

This work was done by Joseph Maserjian and Sverre T. Eng of Caltech for **NASA's Jet Propulsion Laboratory**.

In accordance with Public Law 96-517, the contractor has elected to retain title to this invention. Inquiries concerning rights for its commercial use should be addressed to

Edward Ansell
Director of Patents and Licensing
Mail Stop 301-6
California Institute of Technology
1207 East California Boulevard
Pasadena, CA 91125

Refer to NPO-16298/TN

Jet Propulsion Lab.
NASA Resident Office
Technology Utilization Officer: Gordon S. Chapman
Mail Stop 180-801
4800 Oak Grove Drive
Pasadena, CA 91109
(818) 354-4849
Patent Counsel: Paul F. McCaul
Mail Code 180-801
4800 Oak Grove Drive
Pasadena, CA 91109
(818) 354-2734
Technology Utilization Mgr. for JPL: Norman L. Chalfin
Mail Stop 156-211
4800 Oak Grove Drive
Pasadena, CA 91109
(818) 354-2240

FOR ADDITIONAL INFORMATION: *Contact: Director, Technology Transfer Division, P.O. Box 8757, BWI Airport, MD 21240; (301) 621-0100 Ext. 241*
REFER TO THE NUMBER LISTED AT THE END OF THIS ARTICLE

Transferring Lens Prescriptions Between Lens-Design Programs

Most data are transferred automatically, and the user is notified of those that are not.

The Optical Lens Prescription Data Formatter computer program enables the user to transfer complicated lens prescriptions quickly and easily from one major optical-design program to another and back again. Thus, one can take advantage of the inherent strength of either program. The programs are ACCOS V from Scientific Calculations, Inc., of Fishers, NY, and CODE V from Optical Research Associates of Pasadena, CA.

The translation program works quite well for most lens prescriptions. On all tested lenses, it correctly translates the radii, thicknesses, polynomial aspheric data, tilts, decenters, and aperture sizes of the lenses. Limitations occur for special types of surfaces and some data pickups because the design programs are not fully equivalent. In these cases, the translation program translates all the data it can and prints comments mentioning the rest. The user can then manually adjust the lens to model the system correctly.

This program is available in two machine versions: PRIME and DEC VAX. The PRIME version is written in FORTRAN and requires approximately 64K of 8-bit bytes. The VAX version is written in FORTRAN and requires 64K of 8-bit bytes but has been fully tested in only one direction — ACCOS V to CODE V. At some installations, differences in lens-data files may require modification of format statements. The program was released in 1987.

This program was written by John E. Stacy of Caltech, Laura Wooley of the University of Rochester, and Brian Carlin of Santa Barbara Research Center for **NASA's Jet Propulsion Laboratory**.
NPO-17092/TN

NPO-17093/TN

FOR ADDITIONAL INFORMATION

CONTACT:
COSMIC®
112 Barrow Hall
University of Georgia
Athens, GA 30620
(404) 542-3265

NASA Tech Brief
National Aeronautics and
Space Administration
Lewis Research Center, Cleveland, Ohio

Licensing Opportunity

Optoelectronic Technique Eliminates Common-Mode Voltages

Small signals can be transmitted between circuits at large differences of potential.

An optoelectronic technique lends itself well to the accurate measurement of any electrical parameter and the display of its value. The technique can accommodate a broad range of measured values from millivolts to hundreds of volts and can provide unlimited electrical isolation. In this technique, the measured parameter is converted to the duration, proportional to its value, of a pulse of light. The pulse is transmitted along an optical fiber to or from the isolated circuit.

At the transmitter, the measured parameter is converted to the durations of pulses in a common digital panel meter. It is necessary only to locate the point in the meter circuit where there is a correspondence between the measured parameter and the durations of pulses. This point is not normally used to obtain output from the meter. The signal at this point is suitably conditioned by added transistors to drive the transmitter at one end of the optical fiber.

Power to operate the additional components is supplied by the meter. The components of the optical link include low-cost, snap-in, transmitter/receiver pairs connected with 1-mm-diameter plastic-fiber cable. These devices are relatively new, very rugged, able to operate from dc to 5 MBd, and require little electrical current.

At the receiver, the pulse of light in the fiber is converted back into an electrical pulse, the duration of which is measured by counting the number of clock pulses accumulated in a 12-bit binary counter during the pulse time. On the falling edge of the pulse, the count is strobed into a 12-bit digital-to-analog converter to provide an analog output of 0 to 10 volts proportional to the count. The scale of the digital and analog values is easily changed by changing the clock frequency: The analog output is proportional to the clock frequency.

This technique could be used wherever it is desired to measure, record, and/or control parameters of circuits that are floating at high voltages. It could also be used to prevent ground loops in low-voltage applications. In addition, two circuits, one in each direction, could be used in a control-loop configuration.

Some specific applications could be in the operation of traveling-wave tubes (TWT's) or other electron-gun devices that include filaments at cathode potential. This potential, generally about 10 kV, prevents the direct recording of filament voltage (6 V) or filament current (0.2 to 5 A). Another TWT application is the measurement of control-grid voltage, which controls the beam current and which is established with respect to the cathode.

The technique can be used for the optimization and testing of depressed-collector/microwave-tube combinations. Yet another possible application is in the measurement of current from, or the control of, series stacked power supplies.

This work was done by Gary G. Lesny of **Lewis Research Center**. *No further documentation is available.*

Inquiries concerning rights for the commercial use of this invention should be addressed to the Patent Counsel, Lewis Research Center Refer to LEW-14529/TN

Lewis Research Center
Technology Utilization Officer: Daniel G. Soltis
Mail Stop 7-3
21000 Brookpark Road
Cleveland, OH 44135
(216) 433-5567
Patent Counsel:
Gene E. Shook
Mail Code 301-6
21000 Brookpark Road
Cleveland, OH 44135
(216) 433-5753

FOR ADDITIONAL INFORMATION: *Contact: Director, Technology Transfer Division, P.O. Box 8757, BWI Airport, MD 21240; (301) 621-0100 Ext. 241*
REFER TO THE NUMBER LISTED AT THE END OF THIS ARTICLE

NASA Tech Brief
National Aeronautics and Space Administration
NASA's Jet Propulsion Laboratory, Pasadena, California

Licensing Opportunity

Measuring Shapes of Reflectors by Microwave Holography

Theoretical and practical aspects of microwave holographic metrology are discussed.

A pair of reports discusses the theoretical foundation and recent theoretical and practical developments in the use of microwave holography to measure the surfaces of microwave antennas. (The second report is an abbreviated version of the first report.) Microwave holographic measurements provide acceptable accuracy and are more convenient and less time consuming than optical and mechanical measurements, especially where measurements have to be repeated. The microwave holographic metrology of large reflectors, first reported in 1976, has been improved into an accurate technique with potential industrial applications.

In microwave holographic metrology, one first measures the far-field amplitude and phase (or Fresnel-zone) pattern of the radiation from the antenna or else constructs the far-field quantities from near-field measurements (see figure). One then uses the Fourier-transform relationship between the far-field pattern and a function related to the distribution of electric current on the reflector or on an equivalent aperture to reconstruct that function. From the phase information in the reconstructed function, one can determine the local deviation of the surface of the reflector from the assumed paraboloid.

The first report derives the fundamental equations of the holographic technique, using the customary formulation of physical optics. It describes the conditions under which the Fourier-transform relationship applies and shows the inverse Fourier transform that yields the deviation of the surface. In practice, an approximate numerical inversion is performed by a suitable algorithm that incorporates a discrete or fast Fourier transform. The choice of algorithm depends on the nature of the available measured or simulated data; for example, if the measurements are taken at nonuniformly spaced points, one must incorporate a nonuniform-sampling interpolation formula. The texts discuss these and the related topics of choosing sampling positions and intervals to suppress spurious results.

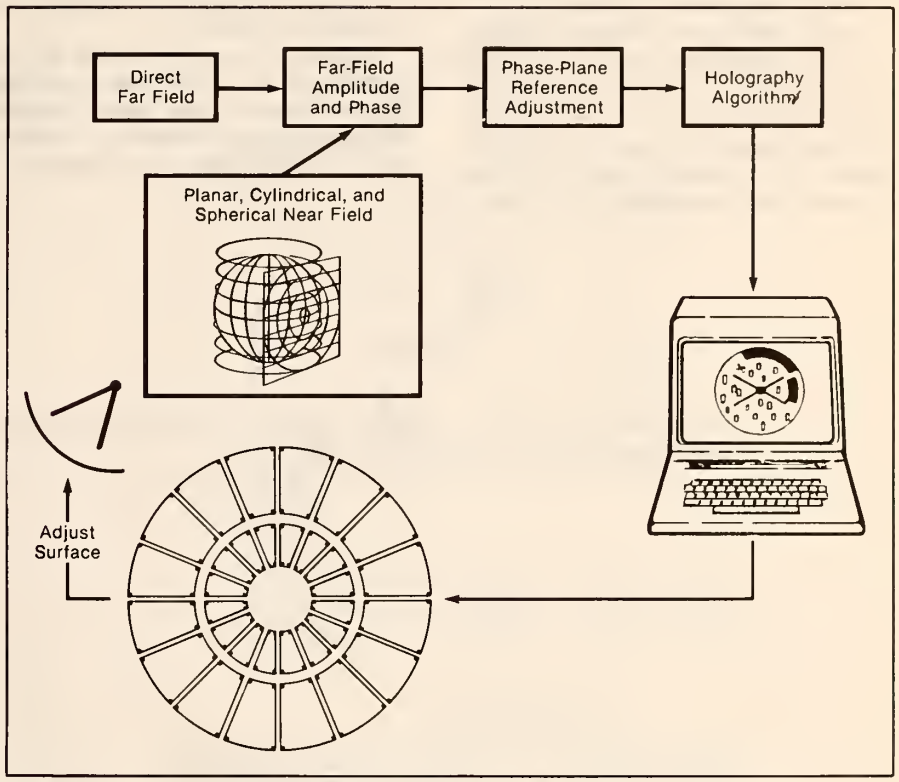

Methodology of Applying Microwave Holographic Diagnosis to complex (amplitude and phase) far-field data, either directly measured (using far-field or compact ranges) or constructed from near-field measurements.

It is also necessary to account for the infinite extent of the Fourier transform of a function that, like the current density, has finite support. Toward this end, the reports discuss an iterative procedure to synthesize far-field measurements outside the region around the antenna boresight where measurements are taken. This extrapolation may be required to increase the spatial resolution of the reconstructed current and deviation of the surface.

The first step in the iterative procedure is to extend the domain of the field-measurement region by pretending that the field is zero out there. The inverse transform is performed over the enlarged domain, and the resulting function is truncated at the edge of the antenna. The forward Fourier transform of the truncated function extends out to the unmeasured domain and there constitutes the extrapolation. Using the measured field in the measurement domain and the extrapolated field elsewhere, the procedure is repeated until the desired improvement is obtained.

The next topic is methods of numerical simulation of possible measurement scenarios. The objective of such studies is to establish the bounds on the accuracy of the reconstructed surface in the presence of various random and systematic errors in the measurements. The first report presents theoretical considerations involved in the use of aperture-simulation models and the results obtained from some of these models. It also discusses the use of more-realistic reflector-simulation models — in particular, those involving displaced surface panels.

The results of far-field measurements on a 64-m-diameter antenna of the Deep

Space Network are reported. Subject to further refinements in the mathematical model of diffraction effects and to corrections for measurement errors, the map of the surface reconstructed from a set of measurements at 11.45 GHz shows deviations of the surface in the range of ±5.09 mm, with resolution of panels as small as 1 m.

Also reported are novel measurements on a 156-cm-diameter reflector at 11.3 GHz in a near field. One set of measurements was performed on the original antenna; another set was performed with four bumps attached to the reflector. The holographic reconstruction showed the bumps clearly. This combination of near-field measurement and holographic reconstruction can be a very powerful diagnostic tool.

This work was done by Y. Rahmat-Samii of Caltech for **NASA's Jet Propulsion Laboratory**. *"Antenna Diagnosis by Microwave Holographic Metrology" and "Microwave Holographic Metrology for Antenna Diagnosis."*

Inquiries concerning rights for the commercial use of this invention should be addressed to the Patent Counsel, NASA Resident Office-JPL. Refer to NPO-17382/TN and NPO-17268/TN.

Jet Propulsion Lab.
NASA Resident Office
Technology Utilization Officer: Gordon S. Chapman
Mail Stop 180-801
4800 Oak Grove Drive
Pasadena, CA 91109
(818) 354-4849
Patent Counsel: Paul F. McCaul
Mail Code 180-801
4800 Oak Grove Drive
Pasadena, CA 91109
(818) 354-2734
Technology Utilization Mgr. for JPL: Norman L. Chalfin
Mail Stop 156-211
4800 Oak Grove Drive
Pasadena, CA 91109
(818) 354-2240

FOR ADDITIONAL INFORMATION: *Contact: Director, Technology Transfer Division, P.O. Box 8757, BWI Airport, MD 21240; (301) 621-0100 Ext. 241*

REFER TO THE NUMBER LISTED AT THE END OF THIS ARTICLE

NASA Tech Brief
National Aeronautics and Space Administration
Marshall Space Flight Center, Alabama

Licensing Opportunity

Spectrograph Measures Contamination of Optical Elements

Reflectance and transmittance are measured over a range of wavelengths.

A scanning-monochromator spectrograph has been designed to measure contamination on the surfaces of optical elements as a function of time. The spectrograph repeatedly exposes samples to the environment, then measures their transmittances or reflectances over a range of wavelengths. The spectrograph is intended for use at vacuum-ultraviolet wavelengths to evaluate the effects of outgassing, heating, and cooling on optical instruments. However, the principle of operation is also applicable to the spectral monitoring of time-dependent contamination at other wavelengths and in laboratory, industrial, or other settings.

The spectrograph (see figure) includes an intense source of light with an exit slit that serves as the entrance slit to the monochromator. For the vacuum-ultraviolet wavelength range, the source could be a deuterium lamp with a magnesium fluoride window. The slit is typically 1 mm wide. The ribbon-shaped beam of light emerging from the slit is dispersed in wavelength by a holographic grating, which is rotated to scan in wavelength or fixed in orientation to select a fixed wavelength that falls on the exit slit of the monochromator. A ribbon of light at the wavelength of interest emerges from the exit slit of the monochromator and travels toward the test position.

A wheel that holds several sample optical components rotates until the desired sample is at the test position. If the transmittance of the sample is to be measured, then the photodetector remains at the position shown in solid lines while the photodetector output is measured as a function of wavelength. For calibration, this measurement can be taken without any sample obstructing the light. If the reflectance of the sample is to be measured, the photodetector is rotated to the position shown by dashed lines, and the sample wheel is tilted to the position shown by dashed lines to reflect light toward the photodetector. When samples are not being tested, the sample wheel can be rotated to expose samples to the environment.

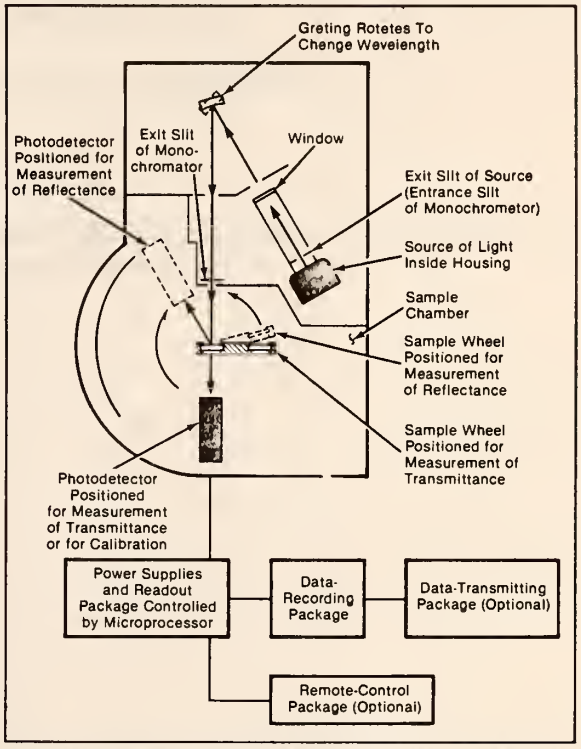

The Contamination-Measuring Instrument contains a scanning-monochrometor spectrometer that meesures spectral reflectance or transmittance. This is one of several versions thet differ with respect to the placement of sampies, detectors, and/or auxiliery reflectors for the two kinds of meesurements.

The grating, detector, and sample wheel are positioned by motors under the control of a microprocessor. The data on these positions and the photometer-output data are synchronized with time signals of the system and recorded together in an attached memory unit for subsequent processing. Alternatively, the spectrograph can be controlled remotely and/or the data can be transmitted to an external memory or processor.

This work was done by Bruce K. Flint, Robert D. Fancy, and Robert V. Jarratt, Jr., of Acton Research Corp. for **Marshall Space Flight Center**.

Inquiries concerning rights for the commercial use of this invention should be addressed to the Patent Counsel, Marshall Space Flight Center Refer to MFS-26076/TN

George C. Marshall Space Flight Center
Technology Utilization Officer: Ismail Akbay
Code AT01
Marshall Space Flight Center,
AL 35812
(205) 544-2223
Patent Counsel:
Leon D. Wofford, Jr.
Mail Code CC01
Marshall Space Flight Center,
AL 35812
(205) 544-0024

FOR ADDITIONAL INFORMATION: *Contact: Director, Technology Transfer Division, P.O. Box 8757, BWI Airport, MD 21240; (301) 621-0100 Ext. 241*
REFER TO THE NUMBER LISTED AT THE END OF THIS ARTICLE

Energy

0639 Axial-Gap Permanent Magnet Motor

0640 Bipolar Battery Using Conductive-Fiber Composite—Improved lead/acid battery features reduced weight and increased energy and power densities. (Licensing Opportunity)

0641 New Eyes for Wind Turbines Designers

Other Items of Interest

0679 Multiple-Purpose Rigid Foam Insulation—Properties can be adapted to a variety of demanding applications.

Department of Energy

Technology Application

Oak Ridge National Laboratories

Axial-Gap Permanent Magnet Motor

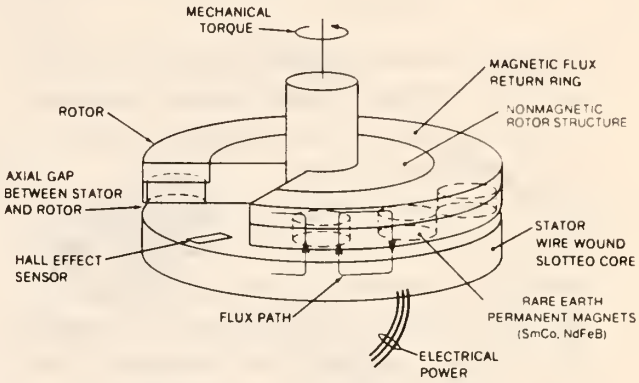

Fig. 1. Conceptual design of the axial-gap permanent magnet motor/generator.

Most of the high-speed (>3600 rpm) rotating machines in the United States use gearbox speed increasers or belt-and-pulley systems coupled to relatively slow synchronous motors. However, high-speed, direct-drive motors can drive these machines more efficiently and more reliably. The axial-gap permanent magnet motor, developed by researchers at ORNL, the Oak Ridge Gaseous Diffusion Plant, and the University of Tennessee, represents the ideal configuration for direct drive of such high-speed machinery (Fig. 1).

Speeds in excess of 40,000 rpm and power densities greater than 5 kW/kg have been demonstrated with this motor. In one application of this design, a direct-drive motor is being used to drive a 30-hp gas compressor. Elimination of the gearbox in the drive train has resulted in an immediate savings of 25% in energy consumption, reduced downtime for repairs and preventive maintenance, and reduced vibration and audible noise.

The motor's rotor consists of eight cylindrical neodymium alloy magnets (2.8 in. diam, 0.25 in. thick) mounted on a maraging steel rotor, which provides structural integrity under stress as well as a return path for magnetic flux. An aluminum cartridge separates the magnets. The stator has a slotted core, constructed of tape-wound, 0.005-in.-thick silicon steel. Hand-formed copper windings are installed, and an epoxy is applied to contain the windings and to conduct heat to the motor periphery (Fig. 2).

The permanent magnet concept has resulted in motor efficiencies of ~95%. Research has shown that the use of a relatively large number of circular magnets results in a minimum of magnetic material in the motor. In addition, circular magnets provide for smooth transition of rotor poles over the stator slots; the combined effect is to minimize eddy-current losses.

A highly efficient adjustable speed drive system was developed to control the motor's speed and torque. The drive package power section consists of a pair of switching regulators and output inverters. Each switching regulator operates at 1 kHz with a variable pulse width, thereby controlling the voltage applied to the associated inverter. Each inverter produces a six-step output waveform, which is phase-locked to the rotor by

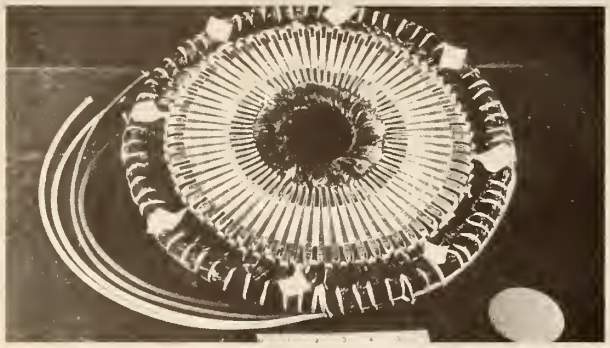

Fig. 2. Stator assembly, showing teeth and windings, before encapsulation in epoxy.

means of a single Hall probe signal and control circuitry. All control signals between the power section and controller are isolated by optical fibers or magnetic circuits.

The controller, built around a Motorola 68701 microprocessor, maintains optimum stator field phasing, controls motor current, performs numerous self-checks, and responds as necessary to power-section faults. It also provides for self-starting of the rotor. The single Hall probe, mounted on the stator, develops a rotor-position reference signal, which is phase shifted by a programmable counter. Phase-locked loop circuitry multiplies the shifted reference, and combinational logic provides the six-step waveforms necessary to control the power inverter. Optimum phase angle, based on motor speed and current, is continually maintained, thereby maximizing motor efficiency.

A second programmable counter is used to develop a variable-pulse-width, fixed-frequency switching regulator control signal. This signal yields direct motor-current control with sufficient resolution to achieve speed regulation greater than 0.002% over the full range of motor loads.

The axial-gap permanent magnet motor can drive compressors, pumps, machine tools, electronic chip "spinners," and a wide variety of high-speed equipment. In addition, the configuration is ideally suited for use as a generator when the prime mover is a high-speed turbine. Reversible "motor-generator" combinations have been demonstrated by ORNL staff. Variations include addition of a second stator, which effectively doubles the torque output of the motor with ~50% weight gain, and a counterrotating motor for slow- and high-speed applications.

This type of motor could provide exceptional slow-speed torque control for marine applications demanding two output shafts for power transfer. In addition, this design could be used for slow-speed industrial processes such as the production of textiles, pulp, and paper. The industrial sector may find a wide range of applications, at slow and high speeds, when precise torque (tension) and speed control are required for process or product quality.

Additional information:

Office of Technology Applications
Martin Marietta Energy Systems, Inc.
P.O. Box 2008
Oak Ridge, TN 37831-6257

Telephone: (615) 574-4192; FTS 624-4192

NASA Tech Brief
National Aeronautics and Space Administration

Licensing Opportunity

NASA's Jet Propulsion Laboratory, Pasadena, California

Bipolar Battery Using Conductive-Fiber Composite

Improved lead/acid battery features reduced weight and increased energy and power densities.

In an improved version of the bipolar lead/sulfuric acid battery, electrically-conducting fiber/polymer composite substrates are used in place of metallic substrates. Sealing and corrosion problems associated with metallic substrates are thereby reduced. Other benefits include a halving of weight, increased energy and power densities, and a much lower gassing rate.

A conventional bipolar battery includes electrodes on which positive active material (PbO_2) forms one surface and negative active material (Pb) forms the opposite surface. Sandwiched between the two surfaces is a substrate, usually a metal, that conducts electrons but not electrolyte ions. Bipolar electrodes are stacked into a multicell battery such that the electrolyte and separators lie between adjacent electrodes. The end electrodes are unipolar, of course.

In the improved bipolar battery (see figure), the conductive biplates and bipolar separators are made from a composite — typically, 50 percent by weight of graphite fibers embedded in polyethylene. Electrical contact between the biplate and the active material is achieved by narrow lead stripes plated onto the biplate surfaces.

Each bipolar separator is composed of a sheet of the composite, on each side of which is bonded a porous graded glass-fiber mat. The glass mats hold the positive and negative electrode materials in place. They provide transverse porosity for H_2 and O_2 gases and add to the axial compliance of the bipolar stack, thus assuring uniform clamping pressure. The positive-side mat also protects the separator from oxidation by contact with the PbO_2.

As shown, the entire assembly is clamped between pressure plates. The axial pressure helps to contain active material and to maintain electrical contact between the active material and the biplates.

The amount of H_2 and O_2 gases given off depends on the amount of antimony in the grid structure. Antimony is normally added to give structural strength and to improve adhesion of the PbO_2 to the grid. The improved battery uses no antimony and no grid, with the result that gas is evolved at about one-tenth of the usual rate. Thus, electrolyte needs to be added at about a tenth of the usual frequency, and safety is increased because of the reduction in hydrogen gas.

Sealing problems are largely eliminated

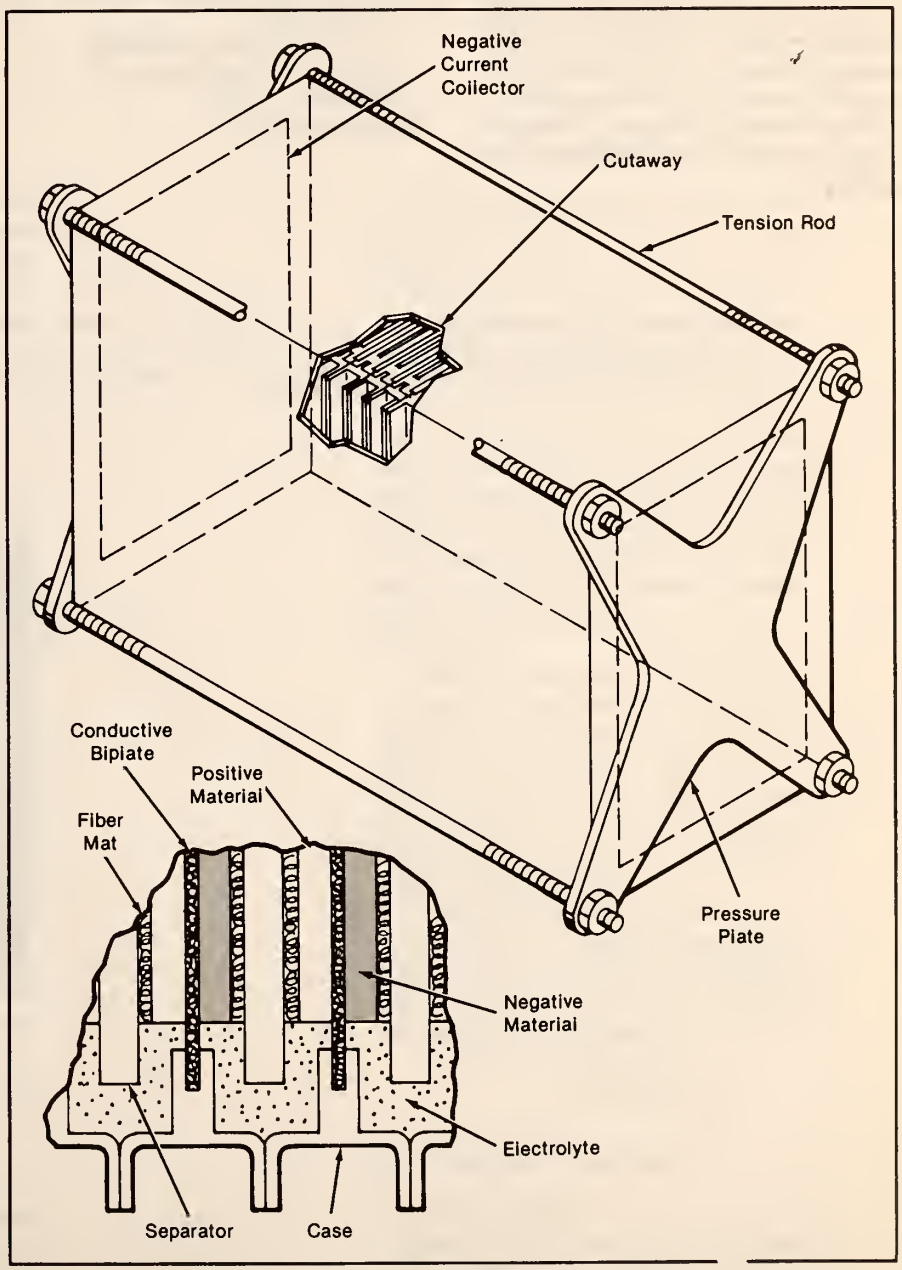

A **Bipolar Lead/Acid Battery** using the new composite materials contains un. cells clamped together between pressure plates. Among other benefits conferred by the new approach, the clamping pressure improves the retention of the electrode materials.

since, unlike metals, the fiber composite is easily bonded to the non-conductive plastics used to construct the battery case. Improved energy and power densities are due, in part, to the elimination of the grid masses and grid losses and to the use of reduced active-material thickness and improved surface-to-volume ratios.

The improved bipolar battery can be used in all customary storage-battery applications. Because of its improved energy-to-weight ratio, it should be especially important for electric-vehicle development.

This work was done by Wally E. Rippel of Caltech for **NASA's Jet Propulsion Laboratory**.

Title to this invention, covered by U.S. Patent No. 4,353,969, has been waived under the provisions of the National Aeronautics and Space Act [42 U.S.C. 2457(f)]. Inquiries concerning licenses for its commercial development should be addressed to

Edward Ansell
Director of Patents and Licensing
Mail Stop 301-6
California Institute of Technology
1207 East California Boulevard
Pasadena, CA 91125

Refer to NPO-14994/TN

Jet Propulsion Lab.
NASA Resident Office
Technology Utilization Officer: Gordon S. Chapman
Mail Stop 180-801
4800 Oak Grove Drive
Pasadena, CA 91109
(818) 354-4849
Patent Counsel: Paul F. McCaul
Mail Code 180-801
4800 Oak Grove Drive
Pasadena, CA 91109
(818) 354-2734
Technology Utilization Mgr. for JPL: Norman L. Chalfin
Mail Stop 156-211
4800 Oak Grove Drive
Pasadena, CA 91109
(818) 354-2240

FOR ADDITIONAL INFORMATION: *Contact: Director, Technology Transfer Division, P.O. Box 8757, BWI Airport, MD 21240; (301) 621-0100 Ext. 241*

REFER TO THE NUMBER LISTED AT THE END OF THIS ARTICLE

New Eyes for Wind Turbines Designers

What does the wind look like? How does a wind turbine respond to changes in the wind? SERI researchers are answering these questions with a pioneering experiment that promises to lead to improved wind turbine blade and rotor designs.

SERI technicians adjust the video camera boom at the hub of the wind turbine. The boom must hold the camera absolutely still so that "tufts" indicating air flow are properly imaged.

Visualizing the wind's interaction with aircraft wings, buildings, and other man-made objects can be done with models in wind tunnels. However, visualizing the wind's interaction with a rotating wind turbine in the turbulent atmosphere presents so many problems that few have attempted the feat and none have really succeeded—until now.

During the first phase of an experiment conducted by SERI's Wind Research Branch, high-resolution videotapes were made of small "tufts" mounted on a wind turbine rotor blade. Observations from the tapes can be correlated with wind inflow, air pressure, and blade strain data, and measurements of the blade's angle of attack with respect to the wind. The result is a total picture of the wind's interaction with the wind turbine rotor. This information will help designers understand what happens when complex aerodynamic states such as dynamic stall occur along the blade surface.

The experiment required painstaking preparation. The camera boom was only one of the pieces of equipment fabricated at SERI specifically for the experiment. It keeps the video camera aimed at the tufts with no out-of-plane movement as it twirls at more than 80 rpm in high winds.

Preliminary videotapes and other data have already been viewed by researchers from across the country. The consensus is that SERI has provided new "eyes" for the wind turbine designer.

Contact: C.P. Butterfield
(303) 231-1171

For Additional Information:

Mr. Dana Moran
Research & Technology Application
Solar Energy Research Institute
1617 Cole Boulevard
Goldon, CO 80401-3393
(303) 231-7115

Refer to Volume X, Number 3/TN

Engineering

0642 Coefferdams—Answer to Underwater Window Repair—Divers can control temperature and water quality during repair

0643 Navy Personal Computers Challenge the High Sees

0644 Crimping Wires in Cramped Spaces

0645 A Device that Rigidly Assembles Interlocking Parts

0646 Special Plug Lets Researchers 'See' Inside Auto Engines

0647 The Beam-Raising Vehicle

0648 Beneficiation Technique Provides a Means for Capitalizing on Domestic Sources of Cobalt

0649 Novel Foam Application Lowers Longwall Dust

0650 High-Capacity Heat-Pipe Evaporator—The cylindrical configuration increases the contact conductance.

0651 High Temperature Gas-Gap Thermal Switch

0652 Optimizing Locations of Nodes to Reduce Vibrations

0653 Venting Gases with Minimum Loss of Heat—The design of a vent reduced radiative transfer of heat.

0654 Video Alignment System for Remote Manipulator—Crosshairs and a mirror provide angular references. (Licensing Opportunity)

Software

0655 Unified Engineering Software System—A collection of computer programs performs diverse functions in prototype engineering.

Testing & Instrumentation

0656 In Situ Measurement of Rock Stress with Hydraulic Borehold Pressure Cells

0657 Borescope Inspects with Visible or Ultraviolet Light—Quartz optical fibers improve performance at ultraviolet wavelengths.

0658 Densitometry by Acoustic Levitation—Detailed knowledge of the acoustic field is not necessary.

0659 Measuring Thermal Conductivities of Rough Specimens—Cost is reduced and accuracy and repeatability increased.

Other Items of Interest

0660 Emulsion-Phase Contactor

0661 New Inland Oil Skimmer

0665 Compliant Robot Wrist Senses Deflections and Forces—Precise parts can be assembled without damage.

0670 Strain-Gaged Bolt Process for the Direct Measurement of Valve-Stem Thrust

0700 Acoustical Measurement of Furnace Temperatures—Simple probes withstand severe conditions, yet give spatially-resolved temperature readings. (Licensing Opportunity)

0704 Injected Water Augments Cooling in Turboshaft Engine—Additional cooling enables operation at higher than usual power.

NAVY
Domestic Technology Transfer Fact Sheet

Coefferdams--Answer to Underwater Window Repair

Divers can control temperature and water quality during repair

When a ship runs over debris, underwater sonar dome rubber windows are often damaged and must be repaired immediately. A newly developed, fresh water cofferdam allows divers to control water quality and temperature, permitting effective underwater repair.

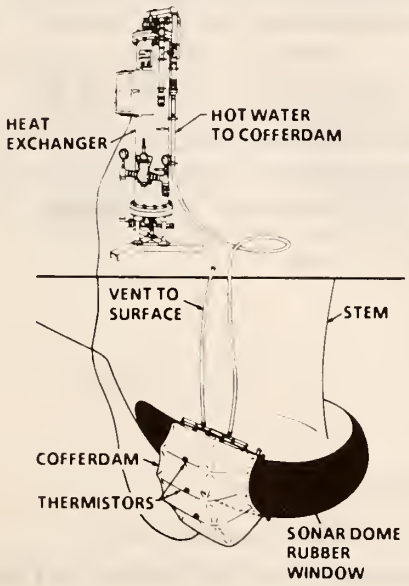

Consisting of a tubular frame covered by stretched fabric, a watertight enclosure has room for two divers and is easily attached by straps to the outside of the windows. Fresh water is heated and pumped down into the cofferdam, displacing the heavier salt water. This provides an environment that ensures a firm epoxy bond and cure. (From *Deckplate*, NAVSEA)

For Additional Information:

Backup material on this effort is available from:

Navy Domestic Technology Fact Sheet Reader Reply Service
Code E211
Naval Surface Weapons Center
Dahlgren, VA 22448-5000
(703) 663-8921

Refer to 140303/TN

Navy Personal Computers Challenge the High Sees

You cannot fight a sea battle in a typhoon. Just trying to keep the ship afloat in any of the higher sea states may be top priority.

Recent technological advances may improve the Navy's fighting capability in the higher sea states. Tests, conducted by the David Taylor Research Center, Bethesda and Annapolis, Maryland, under Office of Naval Technology sponsorship, have verified that a new, innovative approach to ship control can potentially achieve as much as 40-percent reductions in ship roll amplitudes for seaways up to Sea State 5.

The new approach reduces ship roll motion by using desktop personal computers (PCs). The specially modified PCs provide digital control inputs to the rudder, sending commands designed to directly compensate for the wave-induced forces and moments affecting the ship. The feasibility of this new control concept was recently demonstrated through more than 200 hours of roll stabilization while at sea on the USS CUSHING (DD 985). The 17-day demonstrations were part of antisubmarine warfare (ASW) exercises conducted by the Pacific Fleet that spanned a full range of ASW operating conditions.

A 40-percent roll-motion reduction can extend important ship-platform operations including helicopter launch and recovery, weapons delivery accuracy, and crew fatigue levels by as much as one sea state. Based on these results, the Navy is performing longer-term evaluations of ship roll stabilization by actively controlling the rudder systems on both the USS CUSHING and on an AEGIS-class cruiser operating in the North Atlantic.

For Additional Information:

Backup material on this effort is available from:

Navy Domestic Technology Fact Sheet Reader Reply Service
Code E211
Naval Surface Weapons Center
Dahlgren, VA 22448-5000
(703) 663-8921

Refer to 131002/TN

Department of Energy

Technology Application

Fermi National Accelerator Laboratory

Crimping Wires in Cramped Spaces

Sometimes the seemingly smallest advances can have large impacts. Crimping continuous wire strips might seem to be as routine an operation as clipping one's fingernails, until the wires to be crimped are in a tight environment; in a dot-matrix printer, for example.

A non-terminating wire crimper developed at Fermilab solves this problem neatly. While no commercial crimper exists that can crimp wires closer together than approximately 1 inch, the Fermilab version is designed to crimp wire as close as 0.200 in. on center. Additionally, the crimper can be used without cutting the wire, so that wires can be crimped anywhere along their length.

This device is in use at Fermilab for the construction of drift chambers for Fermilab experiments. The ORTA projects potential commercial application in areas where wires must be fastened in the afore-mentioned close quarters or where an intermediate fastener is needed far from both ends of a wire or cable.

For Additional Information:

Office of Research and Technology Applications
Fermi National Accelerator Laboratory
P.O. Box 500
MS 208
Batavia, IL 60510
(312) 840-3333

Refer to FAA-290/TN

A Device that Rigidly Assembles Interlocking Parts

A method has been devised for clamping two layers of identical parts in a zipper-like fashion to form a rigid structure requiring fasteners at one end only. The first use of this concept proposed interlocking extruded tubes used in drift-chamber systems for Fermilab experiments.

The technique makes use of special extrusion shapes that interlock and exploits the fact that high-precision parts can be economically made using extrusions. The self-locking concept makes this system applicable to any configuration.

The system has proven to be a vehicle for flights of practical fancy. An industrial design class at the University of Illinois-Chicago (under the auspices of the State of Illinois Technology Commercialization Program) proposed such uses as decorative panels and construction of boat docks. Other potential applications include assembling modular components for pneumatic, hydraulic, or electronics systems.

For Additional Information:

Office of Research and Technology Applications
Fermi National Accelerator Laboratory
P.O. Box 500
MS 208
Batavia, IL 60510
(312) 840-3333

Refer to FAA-268/TN

Special Plug Lets Researchers 'See' Inside Auto Engines

A spark plug fitted with fiber-optic "eyes" is being used to probe combustion problems inside auto engines while they are running.

The new diagnostic tool is in use now at Sandia National Laboratories' Combustion Research Facility (CRF) in Livermore, and all of the "big three" U.S. auto makers may soon be using similar ones in their engine research programs. The fiber-optic spark plug was devised and built at the CRF, which is operated by Sandia for the Department of Energy (DOE).

Sandia developed the fiber-optic plug as a result of a direct inquiry from Chrysler, which was interested in studying the causes of rough idling in automobile engines — a problem that concerns the entire automotive industry. Auto makers obviously would like to solve this problem and produce engines that run as smoothly and efficiently as possible.

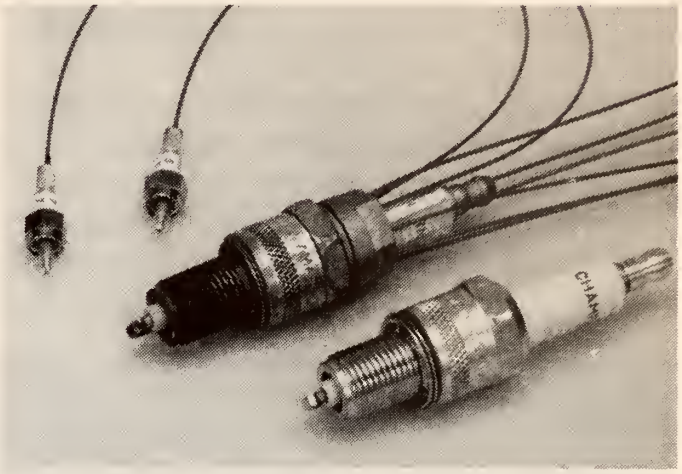

Sandia's fiber-optic spark plug that allows researchers to "see" inside running engines is shown beside a standard plug. When the special plug is used, each of the eight fiber-optic cables leads outward to separate light detectors in an analyzer apart from the engine.

Works on unmodified engines

Because the special plug was built using a standard 14-mm spark plug, it can be used to test unmodified, production-model automotive engines. In normal operation, the cylinders of an internal combustion engine fire one by one in a precise, recurring cycle. As each cylinder fires, a small explosion occurs, driving a piston attached to the crankshaft. This turns the crankshaft, transferring energy to the rest of the drivetrain.

The efficiency of this process can vary greatly. The primary variables are the design of the combustion chamber and the chemistry of the air/fuel mixture. The special spark plug was developed in order to measure the way in which the flame of the explosion grows in the first moments following ignition. Researchers call the infant flame a kernel.

Sandia researchers Peter Witze and Matthew Hall — working with visiting scientist James Wallace of the University of Toronto — devised the optical probe. It consists of a standard spark plug in which a ring of eight 1-mm (0.039-in.) holes have been drilled through the threaded metal housing that screws into the combustion chamber.

Each hole contains an optical fiber that is cut off flush with the base of the plug so that it "looks" down into the combustion chamber. Each fiber leads up through the plug to a separate light detector, in this case a photo-multiplier tube located in an analyzer away from the engine. (An optical fiber is a light guide that can transmit light over large distances with high transmission efficiencies.)

Using the specialized spark plug, researchers are able to record the shape of the flame kernel by analyzing the outputs from the eight detectors. Because each optical fiber transmits the light it "sees" from moment to moment, the speed at which the flame grows in different directions can be plotted with the help of a computer program.

Witze and Hall say measurements of this type are useful for comparing the effect on combustion of the many variables that can occur within the cylinder following ignition.

The optically instrumented spark plug is particularly valuable because it can be placed in the engine without changing the geometry of the engine. It is, in effect, an invisible observer that provides information while the engine operates exactly as it normally would.

May help optimize engine designs

The Combustion Research Facility team believes the special plug can help optimize engine designs and is cooperating with engine designers and researchers at Chrysler, Ford, and General Motors. Witze says all three auto makers are now tracking the team's progress on the fiber-optic spark plug.

Michal Dyer, supervisor of Sandia's Combustion Application Division, believes the fiber-optic plug has a lot of potential as a research tool. "This is truly an exciting development that should give us substantial insight into the workings of production engines. No wonder industry is optimistic about using it in their own engine research programs," he says.

The fiber-optic plug also is being used at the CRF to study lean combustion in natural gas engines. This work is being done by Hall, a postdoctoral fellow supported by the Gas Research Institute, Chicago, Ill.

Witze will explain the development of the fiber-optic spark plug and how it is used at the International Fuels and Lubricants meeting of the Society of Automotive Engineers in Portland, Ore., October 10-13.

The plug was developed with funding from DOE's Office of Conservation and Renewable Energy. Under that office's Combustion Technology Program, Sandia has worked cooperatively with industry for the past 10 years to develop advanced techniques to measure, analyze, and understand engine combustion processes.

FOR ADDITIONAL INFORMATION

Public Information Division,
Code 3161,
Department of Energy,
Sandia National Laboratories,
Albuquerque, NM 87185-5800
(505) 844-4207
Refer to announcement 23, No. 6

Technology News

From the Bureau of Mines, United States Department of the Interior

The Beam-Raising Vehicle

Objective

Reduce the potential for injuries in underground mines by providing an alternative to manually lifting and holding heavy roof-support beams.

The Problem

I-beams, rail sections, and wooden cross-beams are often used in mine haulageways where extensive roof support is needed. Studies by the Bureau of Mines have shown that many mines must resort to manually lifting, moving and installing these beams. Such manual-handling activities have the potential for causing injury to mine workers, particularly back injuries. I-beams used for roof support can typically weigh from 400-500 lbs. Rail sections weigh about the same as the I-beams. Wooden beams can weigh from 200 to 300 lbs. To lift a single beam usually requires the efforts of 3 to 5 mine personnel.

Approach

The Bureau of Mines investigated this problem and designed a special multi-purpose vehicle which lifts and positions wooden cross-beams, sections of rail, or I-beams needed for roof support.

Beam-raising vehicle being used underground to raise a 500-lb section of rail for roof support.

How It Works

The beam-raising vehicle can be either rail-mounted or equipped with rubber tires. It uses a movable hydraulic jack to safely lift beams to the mine roof and to position them for permanent installation. When it is not needed for beam installation, the hydraulic jack is recessed into the vehicle so that the beam-raiser can be used as a flat car for hauling supplies. In addition, the jack can be rolled back and forth along the length of the car while the jack arm is in a raised position. This allows a beam to be positioned without moving the entire car. The end of the arm supporting the beam can be rotated through 360 degrees in a horizontal plane (parallel to the floor and roof). This rotation capability increases the ease with which the heavy, awkward beams can be maneuvered. The device will permit beams to be safely installed by only two workers--one to balance the beam on the support head of the vehicle and the other to operate the jack to raise the beam to the roof.

Test Results

The beam-raising vehicle is currently being tested underground in an eastern Ohio coal mine. Test results thus far have been very favorable. The vehicle has been used almost daily by the timber crew during the past 15 months to install hundreds of sections of rail.

Patent Status

The U.S. Department of the Interior has applied for a patent on the beam-raising vehicle. Information about the patent or on licenses when the patent becomes available can be obtained by contacting the Bureau of Mines, Branch of Technology Transfer, 2401 E Street NW, Washington, D.C. 20241.

For More Information

Additional information about the beam-raising vehicle can be obtained by writing the co-principal researchers for this work, Mr. Richard L. Unger or Mr. Thomas G. Bobick, at the Bureau's Pittsburgh Research Center, P.O. Box 18070, Cochrans Mill Road, Pittsburgh, PA 15236.

Technology News

From the Bureau of Mines, United States Department of the Interior

Beneficiation Technique Provides a Means for Capitalizing on Domestic Sources of Cobalt

Objective

Develop new technolgies and techniques which enable recovery of strategic and critical minerals such as cobalt from domestic resources, thereby easing the U.S. dependence upon foreign producers for these valuable commodities.

Approach

The Bureau of Mines, through research, developed a process which uses mineral beneficiation techniques to recover cobalt-rich products from Missouri lead ores. Before development of this process, cobalt was lost as an impurity in the copper, lead, and zinc concentrates and in the mill tailings because the technology to recover it with minimum impact on present production did not exist.

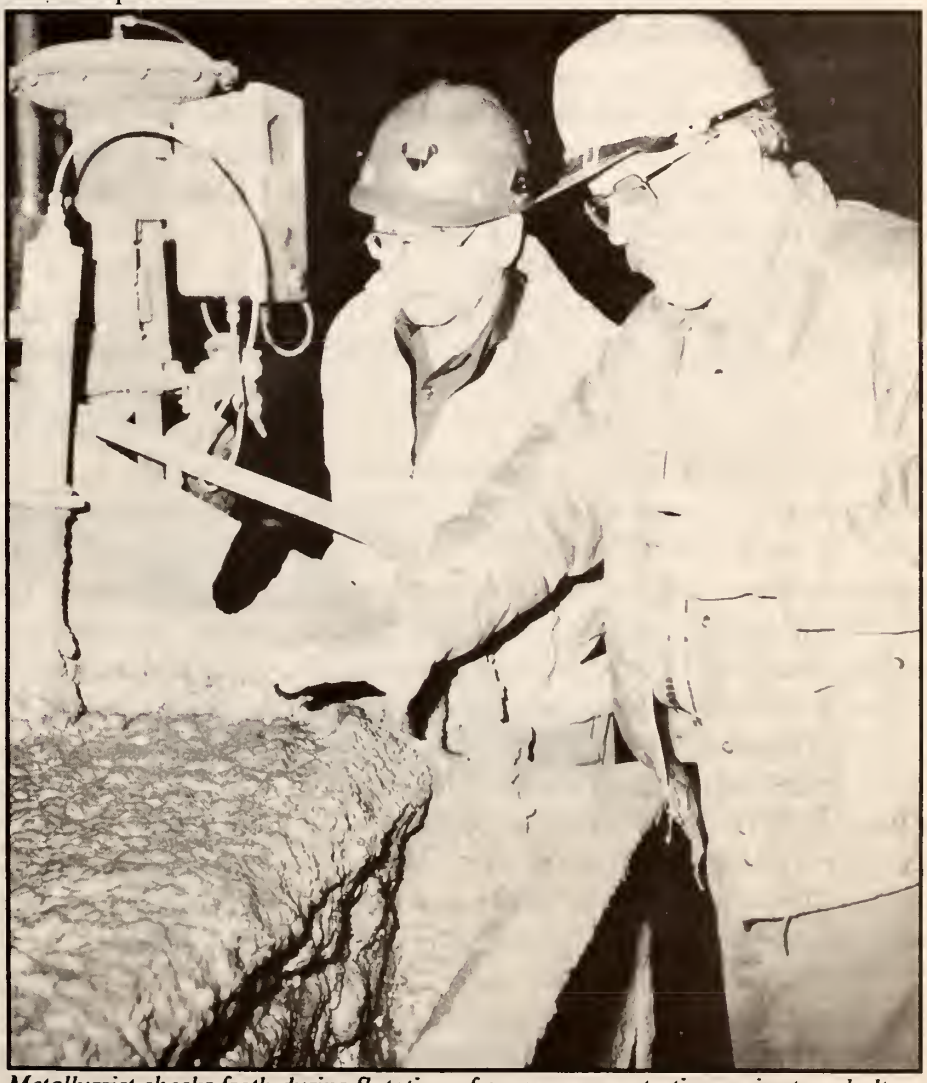

Metallurgist checks froth during flotation of copper concentrations prior to cobalt separation.

Recovering Valuable Cobalt from Domestic Sources

Over 2.7 million lbs of cobalt, equivalent to about 15 pct of the Nation's annual consumption, are lost each year due to a lack of technology permitting its recovery from Missouri lead ores. These ores are now being mined for lead, copper, and zinc. The Bureau of Mines developed a process which fills this technology gap and allows for an alternative domestic source in the event that foreign supplies are suddenly cutoff. Currently cobalt is used in the manufacture of jet engines. At present the United States must rely upon Africa for sufficient quantities of this important metal.

The new cobalt recovery technique is a beneficiation process which uses a combination of fine grinding and froth flotation. The new process enables recovery of about 60 pct of the cobalt that winds up in copper concentrates made from the lead ores. The concentrates are first ground to an average size of 10 um. After grinding, the slurry is scrubbed to polish the mineral surfaces and a flotation collector is added. The collector adsorbs on the fresh mineral surfaces, causing the copper mineral to float away from the cobalt mineral. As flotation proceeds, additional collectors are added to enhance the process. Separation occurs in a stagewise fashion, with about 98 pct of the cell feed floated away as a copper concentrate and the combined tailings becoming an enriched cobalt product. The floated material goes to the next stage and is refloated with the same product as the previous stage. Six stages of flotation will recover 60 plus pct of the cobalt and increase the grade of the cobalt by 4 to 6 times to a range of 2.5 to 4.0 pct. The recovered grade is comparable to the cobalt concentrates produced in Africa. Recovery could be increased by adding additional stages.

The recovery method can be incorporated as an add-on to existing plants and will not interfere with in-place processes. Costs are incremental since the feed material for this process is an existing product. Removing cobalt as a separate product also enhances the original copper concentrate by removing not only the cobalt but by reducing the magnesium oxide and iron contents.

Test Results

The cobalt recovery process has been tested at an operating Missouri lead mine using a continuous flotation unit with very good results. Tests have resulted in development of a flowsheet that allows for the recovery of 70 pct or more of the cobalt in Missouri lead ore copper concentrates, at grades greater than 3 pct Co or 7 pct combined Ni-Co. This was accomplished on feeds grading as low as 0.25 pct Co. In addition, the flowsheet, which involves stagewise separations, has proven to be much more flexible than the classic rough, scavenge, and clean configuration.

Patent Status

The U.S. Department of the Interior has not applied for any patents on the Bureau's cobalt recovery process.

For More Information

A description of initial studies to recover cobalt from Missouri lead ores may be obtained in Bureau Report of Investigations (RI) 9072 entitled, "Continuous Flotation Testing to Recover Cobalt from Missouri Lead Ores." A free single copy of the RI may be obtained by writing the Bureau of Mines, Publication Distribution Section, P.O. Box 18070, Cochrans Mill Road, Pittsburgh, PA 15236. Additional information or answers to technical questions may be obtained by contacting the principal researcher for this process:

William L. Cornell
Bureau of Mines Rolla Research Center
P. O. Box 280, 1300 Bishop Avenue
Rolla, MO 65401
Tel: (314) 364-3169

Technology News

From the Bureau of Mines, United States Department of the Interior

Novel Foam Application Lowers Longwall Dust

Objective

Reduce the dust exposure to the operator of a longwall shearer with a novel foam spray system.

Approach

Discharge foam through the nozzles of a shearer drum so that foam and coal are better mixed.

How It Works

Bureau of Mines research showed that two very important principles for successful application of foam are: (1) moisture distribution and (2) degree of mixing. Foam can distribute a given quantity of moisture much more evenly over a large surface area. Successful Bureau tests of foam for dust control always involve a high degree of mixing between the foam and the material. Mixing permits a greater distribution of foam throughout the mined product. The most suitable location of foam application would be at the point where the dust is generated, before the dust becomes airborne. Foam nozzles located in the cutter drum (pick face foaming or ejecting foam through scroll sprays) will suppress dust close to its source.

Underground Test Results

A compressed air foam system was field tested at three longwall operations using double drum shearers. At two of the mines surveyed, foam had a significant effect on dust levels when discharged through 10 to 12 large diameter nozzles in each shearer drum. Shearer operator

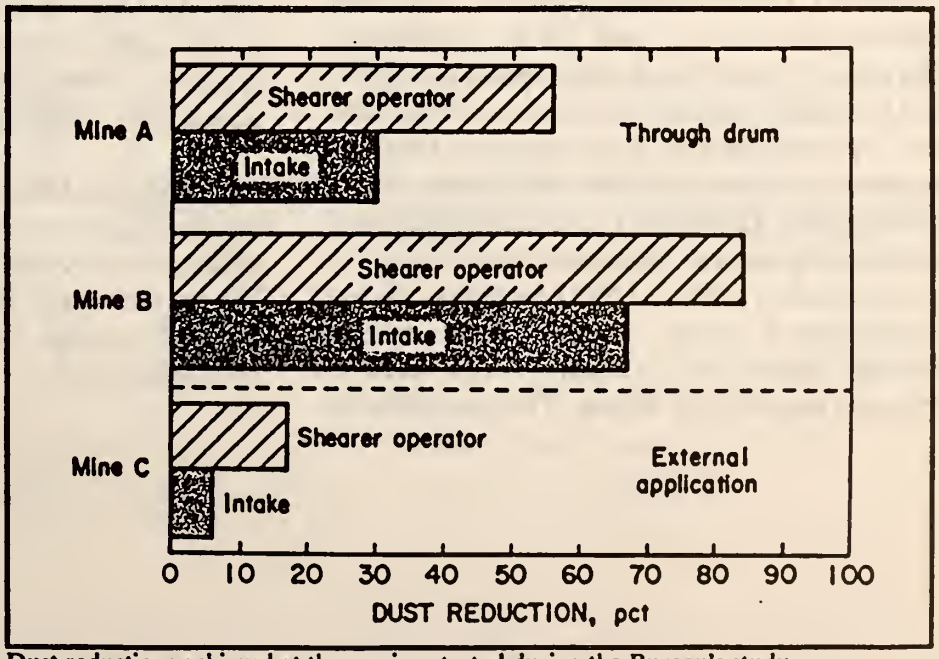

Dust reductions achieved at three mines tested during the Bureau's study.

exposure was reduced by 70 pct on the average. Dust concentrates upwind of the shearer and at the shearer operator position were obtained to determine the relative effectiveness of the foam system over the water spray system. No change was made to the external water spray system when using foam.

The first underground test was conducted in a northern West Virginia mine with workings in the Pittsburgh seam (Mine A). Seam height and face length were approximately 56 in and 600 ft, respectively. The shearer utilized 42 scroll sprays on each drum, as well as external sprays for dust control. The total quantity of water used for dust suppression was about 80 gpm.

Results showed the foam system reduced operator dust exposure by 56 pct. The foam system used 50 pct less water, and reduced intake dust concentrations by approximately 30 pct. Lower intake dust levels are attributed to the improved distribution of moisture throughout the mined product which minimized dust generated by coal transport, stageloader, and crusher.

The second field evaluation occurred at a mine in southwestern Virginia operating in the Pocahontas No. 3 seam (Mine B). Seam height and face length were 60 in and 500 ft, respectively. The shearer used 45 pick-point sprays per drum, and 6 external hollow cone sprays for dust control. A less expensive high-expansion foaming agent was used to minimize overall cost of the foam system. Laboratory tests conducted prior to the study showed the agent produced good quality foam at a ratio of 750:1 (water to agent). Underground results showed foam output through nozzles on the shearer drum reduced operator exposure by 84 pct. This method also reduced dust concentrations at the headgate and tailgate by 54 and 78 pct, respectively. Foam was produced with mix ratios varying from 500:1 to 700:1, and used 30 pct less water. A third field test was conducted at a mine in Utah working the Blind Canyon seam (Mine C). Mining height varied between 96 and 120 in. Face length was 550 ft. External spray nozzles located on the head and tail sides of the shearer discharged the majority of foam. The results showed that external nozzle application is not as effective as through-the-drum discharge. For this test, poor water circuitry restricted the amount of foam that could discharge through the drums, resulting in low dust reductions. Cost of the foam system for the first and third underground studies was $0.25 and $0.84 per ton of raw coal, respectively. By using a less expensive foam agent at higher mix ratios, costs for the second study were lowered to between $0.07 and $0.08 per ton of raw coal.

For More Information

Additional information about Bureau of Mines research performed to determine optimum water spray systems for shearer dust control are described in Technology News Nos. 112, 113, 118, 150, 155, 244, 245, and 246. Copies of these issues can be obtained by writing to the Bureau of Mines, Office of Technology Transfer, 2401 E Street, NW, Washington, D.C. 20241.

For additional information about this Technology News, please contact the technical project officer, John J. McClelland, at the Bureau of Mines, Pittsburgh Research Center, P.O. Box 18070, Pittsburgh, PA 15236, or telephone him at 412/892-6690.

NASA Tech Brief
National Aeronautics and
Space Administration
Lyndon B. Johnson Space Center, Houston, Texas

High-Capacity Heat-Pipe Evaporator

The cylindrical configuration increases the contact conductance.

A heat pipe with a cylindrical heat-input surface has a higher contact thermal conductance than does a comparable one with the usual flat surface. Because the cylindrical heat absorber promotes the nearly uniform flow of heat into the pipe at all places around the periphery of the pipe, it helps to eliminate hotspots on the heat source.

The cylindrical heat absorber, an extruded aluminum tube with internal lugs, is the housing for the heat-pipe evaporator (see figure). A porous wick of polyethylene or sintered metal powder extends from the heat-pipe condenser into the round center channel of the evaporator tube, fitting snugly against the ends of the lugs. Arteries in the wick carry the working liquid from the condenser to the evaporator.

The liquid moves through the 80- and 120-μm-wide capillaries to the surface of the wick. There, heat from the lugs, conducted by the aluminum tube from the external heat source, causes the liquid to evaporate. The vaporized working fluid returns to the lower pressure condenser through the open passages between the lugs.

A cylindrical evaporator with a 1.75-in. (4.4-cm) diameter using ammonia as the working fluid would be able to transfer heat at a rate of 7,500 watts. This capacity is far higher than that of all known heat pipes now in operation.

This work was done by J. A. Oren, R. J. Duschatko, F. E. Voss, and L. W. Sauer of LTV Corp. for **Johnson Space Center**.

MSC-21272/TN

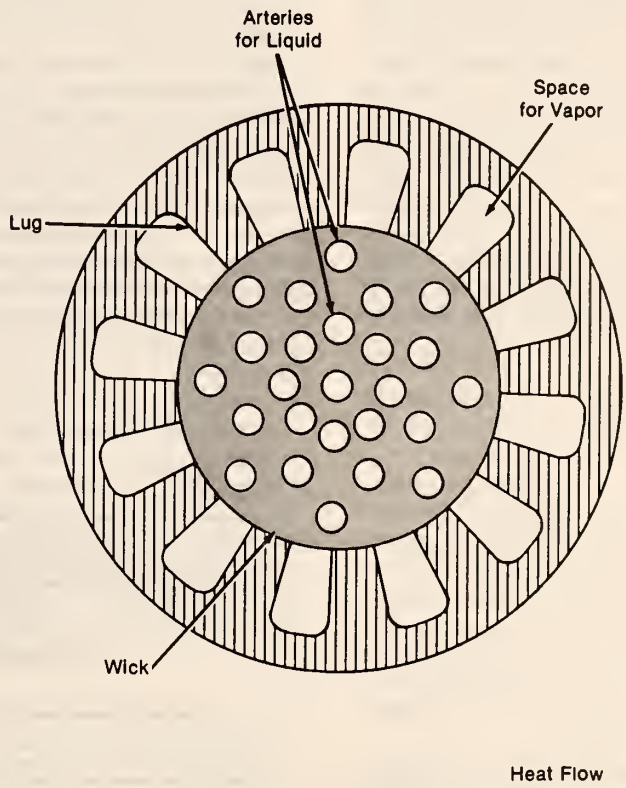

Lugs in an Aluminum Pipe carry heat from the outer surface to the liquid oozing from the capillaries of the wick. The liquid absorbs the heat, evaporates, and passes out of the evaporator through the interlug passages.

FOR ADDITIONAL INFORMATION: *Contact: Director, Technology Transfer Division, P.O. Box 8757, BWI Airport, MD 21240; (301) 621-0100 Ext. 241*
REFER TO THE NUMBER LISTED AT THE END OF THIS ARTICLE

NASA Tech Brief
National Aeronautics and
Space Administration
NASA's Jet Propulsion Laboratory, Pasadena, California

High Temperature Gas-Gap Thermal Switch

The flow of heat is varied at will.

A simple device can be set to allow heat to flow across a gap (switch "on") or to decrease the rate of transfer of heat to a relatively low value (switch "off"). The device — a gas-gap heat switch — operates at temperatures in the approximate range of 100 to 1,500 °C.

Although similar heat switches have been made for operation at lower temperatures, they rely on the variation of only the conductive component of the transfer of heat; the designs of these units do not provide for the suppression of the thermal radiation, which contributes significantly to the transfer of heat at temperatures above about 100 °C. Consequently, these switches cannot be turned "off" at higher temperatures.

The principle of operation is illustrated in the figure, which shows a cylindrical version of the switch surrounding a cylindrical object that is to be thermally connected to or disconnected from the environment. The gap between the inner and outer sleeves of the switch is filled with layers of low-emissivity and low-absorptivity nickel, molybdenum, or zirconium foil to suppress the radiative transfer of heat across the gap. The spaces between the layers of foil are filled with woven quartz fibers to prevent the layers from touching, thereby reducing thermal conduction.

To turn the switch "off" — for example, to insulate the inner cylinder so that it can be heated, the gap in the switch is evacuated. To turn the switch "on" — for example, to allow the inner cylinder to shed its heat to the environment, the gap in the switch is filled with a gas. Any of a large number of gases can be used, such as helium, hydrogen, nitrogen, and argon. The pressure of the gas in the gap has to be only about 1 torr (about 130 Pa) to provide substantial conduction of heat across the gap.

The vacuum to turn the switch "off" can be provided by an ordinary laboratory vacuum pump. A more novel approach that requires no moving parts would involve the use of a sorption pump to control the pressure in the switch. A bed of sorbent material (charcoal, zeolite, hydrides, or oxides) would be heated to drive the gas into the gap or cooled to absorb the gas from the gap at low pressure.

An experimental switch was made with a gap 0.095 in. (2.41mm) wide filled with 5 layers of 0.001-in. (0.025-mm) nickel foil. When tested at temperatures of 300 to 650 °C, using nitrogen as the heat-transfer gas and a cryopump as the source of the vacuum, the switch exhibited a switching ratio of 16. The switching ratio is defined as the ratio of thermal resistance in the "off" state to the "on" state. Calculations show that a decrease in the width of the gap to 0.05 in. (1.27 mm), coupled with the use of helium instead of nitrogen, should increase the switching ratio to 400.

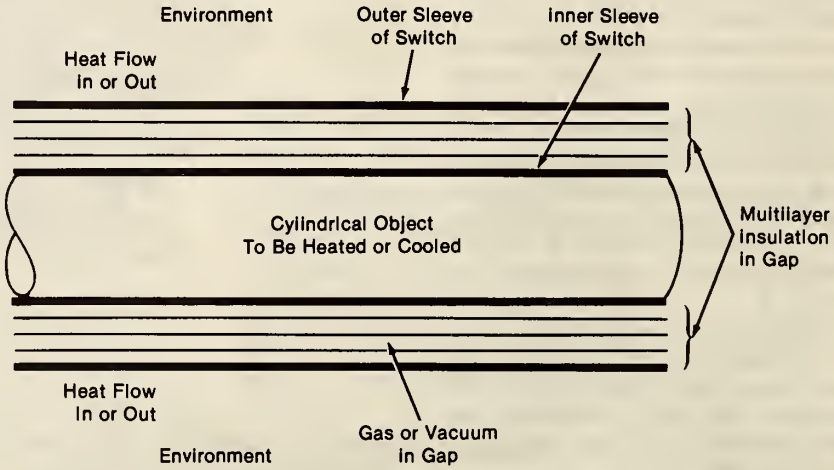

The **Central Cylindrical Object** is thermally connected to (or disconnected from) the environment by filling the gap between the inner and outer sleeves of the switch (or evacuating the gap) to increase (or decrease) the thermal conduction across the gap.

This work was done by Steven Bard of Caltech for **NASA's Jet Propulsion Laboratory.**
NPO-17163/TN

FOR ADDITIONAL INFORMATION: *Contact: Director, Technology Transfer Division, P.O. Box 8757, BWI Airport, MD 21240; (301) 621-0100 Ext. 241*
REFER TO THE NUMBER LISTED AT THE END OF THIS ARTICLE

NASA Tech Brief
National Aeronautics and
Space Administration
Langley Research Center, Hampton, Virginia

Optimizing Locations of Nodes To Reduce Vibrations

The distribution of mass is modified to move the nodes to desired locations.

The current trend in the design of aircraft and spacecraft is to incorporate, in an integrated manner, various design requirements at an early stage in the design process. The conventional approach to meeting vibration requirements has been to correct a design for vibration, sometimes after a serious problem has been detected. Advances in technology are leading to more-complicated aircraft and spacecraft, with higher required speed and performance. Therefore, it is more important to include vibration requirements early in the design process.

Recently, the concept of modal shaping has been proposed as a method to reduce structural vibration. The current optimization technique deals with the placement of nodal points, which is related to modal shaping and consists of modifying the distribution of the mass of a structure to place the node of a mode at a desired location. The key to this optimization procedure is the analysis of the sensitivity of the locations of nodes, which provides straightforward expressions for the derivatives of the locations of the nodes.

The process of optimization uses added lumped masses on the structure as design variables to move the node to a preselected location. For example, the node can be moved to a point where low response amplitude is required or to a point that makes the shape of the mode nearly orthogonal to the distribution of force, thereby minimizing the generalized force and overall response. The formulaton of the optimization leads to values for added masses that adjust the location of a node while minimizing the total amount of mass required to do so

In one example, the node of the second mode of a cantilever box beam is relocated to coincide with the centroid of a prescribed distribution of force, thereby reducing the generalized force substantially without adding excessive mass. A comparison with an optimization formulation that directly minimizes the generalized force indicates that the appropriate placement of the node gives essentially a minimum generalized force.

This work was done by Howard M. Adelman of **Langley Research Center**, *Jocelyn I. Pritchard of USAARTA-AVSCOM, and Raphael T. Haftka of Virginia Polytechnic Institute and State University. Further information may be found in NASA TM-87763 [N86-31069/NSP], Price Code A02 "Sensitivity Analysis and Optimization of Nodal Point Placement for Vibration Reduction."*

Copies may be purchased from the National Technical Information Service, Springfield, Virginia 22161, Telephone No. (703) 487-4650. Rush orders may be placed for an extra fee by calling (800) 336-4700. *LAR-13716/TN*

FOR ADDITIONAL INFORMATION: *Contact: Director, Technology Transfer Division, P.O. Box 8757, BWI Airport, MD 21240; (301) 621-0100 Ext. 241*
REFER TO THE NUMBER LISTED AT THE END OF THIS ARTICLE

NASA Tech Brief
National Aeronautics and
Space Administration
Goddard Space Flight Center, Greenbelt, Maryland

Venting Gases With Minimum Loss of Heat

The design of a vent reduces radiative transfer of heat.

A venting system allows gases to escape while minimizing the loss of heat by radiation. By allowing the gases to escape, venting prevents an excessive buildup of internal pressure on the thermal blanket. Developed to permit outgassing from thermal-blanket-covered spacecraft during passage from the atmosphere of the Earth to the vacuum of space, the venting approach may be adaptable to thermal insulation in laboratory vacuum systems.

The system provides paths that allow gases to flow but occlude radiation from the inside to the outside. The system consists of vent modules, each folded from a sheet of polyimide laminate into a long, slender box (see figure). The box is pierced on top and bottom by four holes, which allow the free exchange of air or other gases between the inside and the outside. In a representative application, a box is 8.4 in. (21.3 cm) wide, 0.3 in (.76 cm) high, the holes are 1 in. (2.54 cm) in diameter, and nine boxes are used.

The exterior of the box is covered with polyimide tape on which a gold film has been vapor-deposited. The film ensures low infrared emissivity. Nonmetallic spacers of low thermal conductivity are positioned between the upper and lower surfaces of the box at six points. The spacers enable the mounting of the box on lugs and maintain dimensional stability under pressure loads resulting from the inflow and outflow of gases.

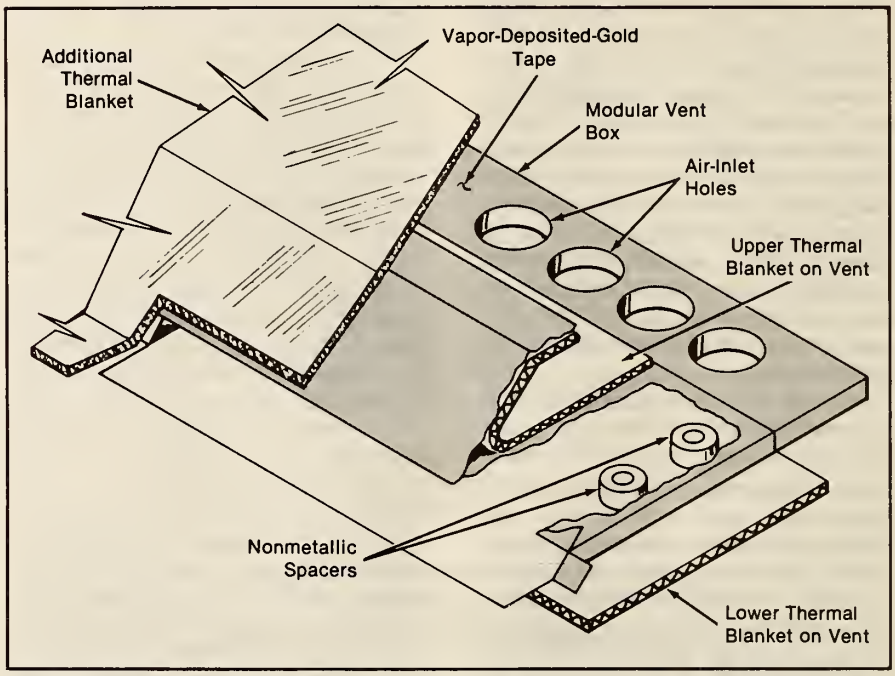

The **Polyimide Box** serves as a modular vent. Many such modules can be combined to suit the gas-flow requirements of the equipment. Indirect flow paths, external thermal control film, and thermal blankets reduce the radiative loss of heat from the interior.

The outer surfaces of the box are covered with multilayer thermal blankets. Each blanket consists of 10 layers of aluminized polyimide interleaved with polyester netting.

This work was done by James R. O'Coin and Joseph Genovese of United Technologies Corp. for **Goddard Space Flight Center**. *GSC-13133/TN*

FOR ADDITIONAL INFORMATION: *Contact: Director, Technology Transfer Division, P.O. Box 8757, BWI Airport, MD 21240; (301) 621-0100 Ext. 241*
REFER TO THE NUMBER LISTED AT THE END OF THIS ARTICLE

NASA Tech Brief
National Aeronautics and Space Administration
Lyndon B. Johnson Space Center, Houston, Texas

Licensing Opportunity

Video Alignment System for Remote Manipulator

Crosshairs and a mirror provide angular references.

A video system enables an operator to align a remote manipulator with objects to be grasped. Unlike the alignment system that it is intended to replace, the new system does not rely on aligning protuberances on the objects. Consequently, it becomes possible to eliminate such protuberances and the mechanical interferences that they cause.

The end effector on the manipulator holds a television camera that views the object to be grasped. Crosshairs on the camera lens intersect at the center of the lens. The lens reticle also includes a circle and a rectangle centered on the optical axis. The object has a reflector on its surface, also with crosshairs at its center.

The remote-manipulator operator views the image from the camera on a television monitor, which displays another set of crosshairs that intersect at the point corresponding to the optical axis of the camera.

The operator moves the end effector to bring the three sets of crosshairs into alignment. Before the camera is centered on the reflector, two sets of crosshairs appear displaced on the monitor (see figure). When the camera is centered on the reflector but the surface of the reflector is not perpendicular to the optical axis of the camera, the crosshairs of the object in the television image align with the crosshairs of the monitor, but the television image (if any) of the crosshairs in the lens remains off center or out of sight. When the surface of the reflector is made perpendicular to the optical axis, the view of the crosshairs on the lens is reflected back along the optical axis into the camera, and these crosshairs then align with the others in the television image.

The alignment system could be automated by using pattern-matching algorithms to control the orientation of the camera or object or both. With the addition of range-measuring instrumentation, the end effector could also be moved automatically to the object while the proper orientation is maintained.

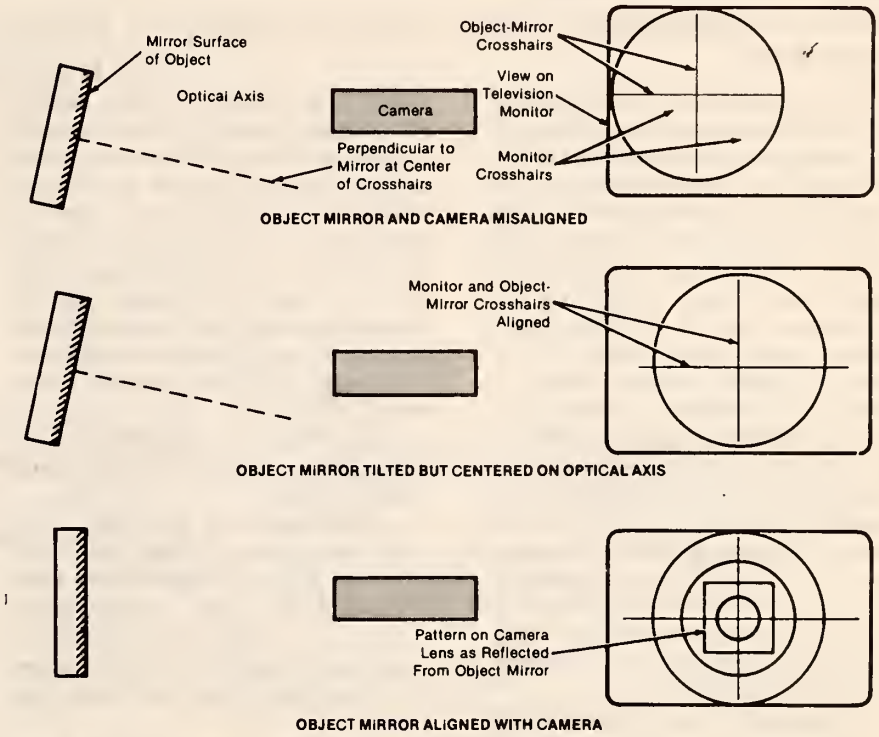

The **Display on the Television Monitor** reveals the orientation of the television camera with respect to crosshairs on a mirror on an object with which the camera is to be aligned.

This work was done by Leo G. Monford of **Johnson Space Center**.

Inquiries concerning rights for the commercial use of this invention should be addressed to the Patent Counsel, Johnson Space Center [see page 18]. . Refer to MSC-21372.

Lyndon B. Johnson Space Center
Technology Utilization Officer: Dean C. Glenn
Mail Code IC
Houston, TX 77058
(713) 483-3809
Patent Counsel: Edward K. Fein
Mail Code AL3
Houston, TX 77058
(713) 483-4871

Unified Engineering Software System

A collection of computer programs performs diverse functions in prototype engineering.

NEXUS, the NASA Engineering Extendible Unified Software system, is a research set of computer programs designed to support the full sequence of activities encountered in NASA engineering projects. This sequence spans preliminary design, design analysis, detailed design, manufacturing, assembly, and testing. NEXUS primarily addresses the process of prototype engineering, the task of getting a single or small number of copies of a product to work.

The spinoff benefits of automating prototype engineering are significant because prototype engineering is a critical element of large-scale industrial production. The time and cost needed to introduce a new product are heavily dependent on two factors: (1) how efficiently required prototypes of the product can be developed and (2) how efficiently required production facilities, also a prototype engineering development, can be completed.

The extendability and unification of NEXUS are achieved by organizing the system as an arbitrarily large set of computer programs to which access can be gained in a common manner through a standard user interface. The NEXUS interface is a multipurpose interactive graphics interface called NASCAD (NASA Computer Aided Design). NASCAD can be used to build and display two- and three-dimensional geometries; to annotate models with dimension lines, text strings, and the like; and to store and retrieve such information related to a design as names, masses, and power requirements of components used in the design.

From the user's standpoint, NASCAD enables the construction, viewing, modification, and other processing of data structures that represent the design. Four basic types of data structures are supported by NASCAD: (1) three-dimensional geometric models of the object being designed, (2) alphanumeric arrays to hold data ranging from numeric scalars to multidimensional arrays of numbers or characters, (3) tabular data sets that provide a relational-data-base capability, and (4) procedure definitions to combine groups of system commands or other user procedures to create more powerful functions. NASCAD has extensive abilities to handle IGES format data, including proposed solid-geometry formats. This facilitates interfaction with other CAD systems.

NEXUS/NASCAD supports the activities encountered in various engineering projects as follows:

1. In preliminary design, geometric models can be built from points, lines, arcs, splines, polygons, drive surfaces, ruled surfaces, and bicubic spline surfaces. Geometric models can be displayed in any view (including removal of hidden lines and surfaces) to check design features.
2. In the analysis of design, geometric models and related data structures can be used to build a NASTRAN data deck. Calculated stress data can be added to model data structures and displayed as variations of color on the geometric model.
3. In detailed design, the geometric model is dimensioned and annotated, and manufacturing and assembly drawings are generated.
4. In manufacturing, the geometric model and related data structures developed by NASCAD can be used to build input for the APT program, which generates the cutter-location (CL) file that describes the required motions of a machine tool.
5. In assembly, a plan for a robot to put together or take apart (repair) a set of mechanical components can be generated on the basis of an IGES solid-geometrical description.
6. In testing, data from measurements can be correlated with predictions made during the design-analysis phase.

NEXUS/NASCAD is available by license for a period of 10 years to approved licensees. The licensed program product includes the source, executable code, command streams, and one set of documentation. Additional documentation may be purchased separately at any time. The NASTRAN and APT programs are distributed separately from the NEXUS/NASCAD system: Call or write to COSMIC for details.

The NEXUS/NASCAD system is written in FORTRAN 77 and PROLOG with command streams in DEC Control Language (DCL) for interactive execution under VMS on a DEC VAX-series computer. All of the PROLOG code deals with the robot strategy planner feature. A minimum recommended configuration is a DEC VAX 11/750 with 8 megabytes of real memory, 250 megabytes of disk storage, and a floating-point accelerator. For interactive graphics, NEXUS/NASCAD currently supports Tektronix 4114, 4016, 4115, and 4095 terminals; Lexidata Solidview terminals; and Ramtek 9400 terminals. Most features are supported on the VT 125, and the nongraphics features are available from a standard ASC II text terminal. The NEXUS/NASCAD system was first released in 1984 and was last updated in 1986.

This program was written by L. R. Purves, S. Gordon, A. Peltzman, and M. Dube of **Goddard Space Flight Center**. *GSC-12900/TN*

FOR ADDITIONAL INFORMATION

CONTACT:

COSMIC®
112 Barrow Hall
University of Georgia
Athens, GA 30602
(404) 542-3265

Technology News

From the Bureau of Mines, United States Department of the Interior

In Situ Measurement of Rock Stress with Hydraulic Borehold Pressure Cells

Objective

Develop a new technique of in situ rock stress measurement which can be used when and where the conventional methods, such as the overcoring stress relief methods and the hydrofracturing method, cannot be effectively applied.

Approach

The Bureau of Mines developed basic principles to determine existing biaxial stresses in rock mass by using an instrumentation package consisting of one 3.8-cm-diameter hydraulic cylindrical pressure cell (CPC) and two 5.7-cm-diameter cement-capsulated flat hydraulic borehole pressure cells (BPC) to be installed in a single drill hole.

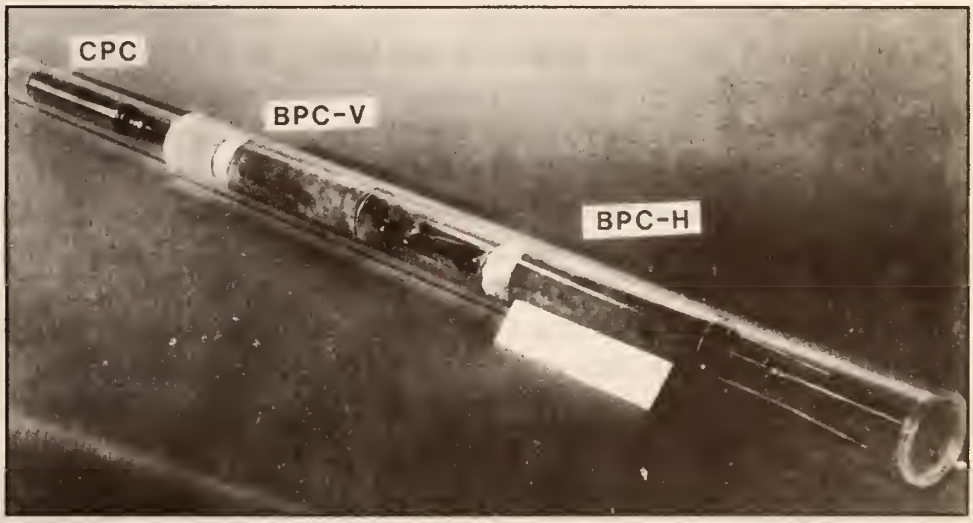

A combination of one 3.8 cm diameter cylindrical (CPC) and two 5.7 cm diameter cement-capsulated flat (BPC) hydraulic borehole presssure cells to be installed in one hole to measure biaxial stresses in rock.

How It Works

A test hole, preferably BX size, is drilled to the approximate depth of the measuring point. The last portion of the hole is then drilled with a combination bit of EX (for CPC) and BX (for BPC's) size for the cells to be installed.

The sum of the biaxial stresses is obtained from the CPC measurement through a simple alge-

braic equation derived from the elastic theories of plates and thick-walled cylinders. The ratio of the biaxial stresses is obtained from the two BPC measurements through another simple algebraic equation. Thus, the biaxial stresses (two unknowns) can be obtained by solving these two equations.

This method is a direct rock stress measuring technique that does not require the rock deformation modulus for back calculation of the rock stresses. The technique can be applied to almost any kind of rock, but it is especially suitable for soft and weak rocks.

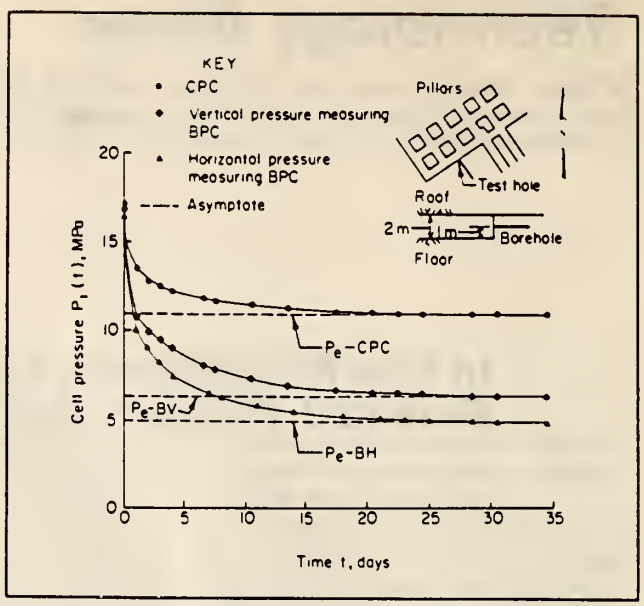

Test results of vertical and horizontal stresses in a potash bed.

Test Results

A package of one CPC and two BPC's was installed in a 34-m-deep horizontal hole drilled into a potash bed under 366 m of overburden to measure existing vertical and horizontal stresses. All three cell pressures, initially set at the same level, converged to the respective equilibrium pressures in 25 to 30 days. With these three equilibrium pressures, the vertical and horizontal rock stresses were calculated as 10.9 MPa and 7.3 MPa, respectively.

Besides potash rock, this technique has been applied to many other types of rocks such as coal, salt, trona, fractured monzonite porphyry, and metamorphic rocks. With the same instrumentation, changes in biaxial stresses also can be determined. If the response factor between rock stress and the BPC pressure is predetermined, a combination of two BPC's alone is sufficient to determine the same biaxial rock stresses.

Patent Status

The U.S. Department of the Interior is not applying for a patent on this novel technique and device.

For More Information

Bureau of Mines' Report of Investigation (RI) 8929, which includes as appendices, A) Theoretical Considerations for Determination of Ground Pressure Existing in a Viscoelastic Rock Mass by Use of Hydraulic Borehole Pressure Cells, and B) Basic Concepts of Mining-Induced Stress Measurement With Hydraulic Borehole Pressure Cells, is available. To obtain a single free copy of this report, please write the Bureau of Mines, Publication Distribution Section, P.O. Box 18070, Cochrans Mill Road, Pittsburgh, PA 15236. For the answers to technical questions or for additional information, contact the Bureau's principal investigator for this research:

Dr. Paul H. Lu
Denver Research Center
U.S. Bureau of Mines
Bldg. 20,Denver Federal Center
Denver, CO 80225
(303) 236-0745

NASA Tech Brief
National Aeronautics and
Space Administration
Marshall Space Flight Center, Alabama

Borescope Inspects With Visible or Ultraviolet Light

Quartz optical fibers improve performance at ultraviolet wavelengths.

A borescope can be used to inspect the interior of small-diameter tubing by both "white" (visible) light and "black" (ultraviolet) light. The borescope (see figure) employs quartz fibers to conduct the ultraviolet light as well as the visible light with high efficiency. In fact, the intensity of the ultraviolet output far exceeds that of other commercial borescopes of the same diameter. The ultraviolet output exceeds 1,000 $\mu W/cm^2$.

The borescope probe is 4 mm in diameter. It is intended for inspecting the interior surfaces of tubes with the aid of fluorescent penetrant dyes. The tubing, which is only 0.190 in. (4.83 mm) in inside diameter, is used in heat-exchanger coils. Gradient optics provide excellent images of internal defects illuminated with visible or ultraviolet light.

This work was done by Orlando G. Molina of Rockwell International Corp. for **Marshall Space Flight Center**. *No further documentation is available.*
MFS-29369/TN

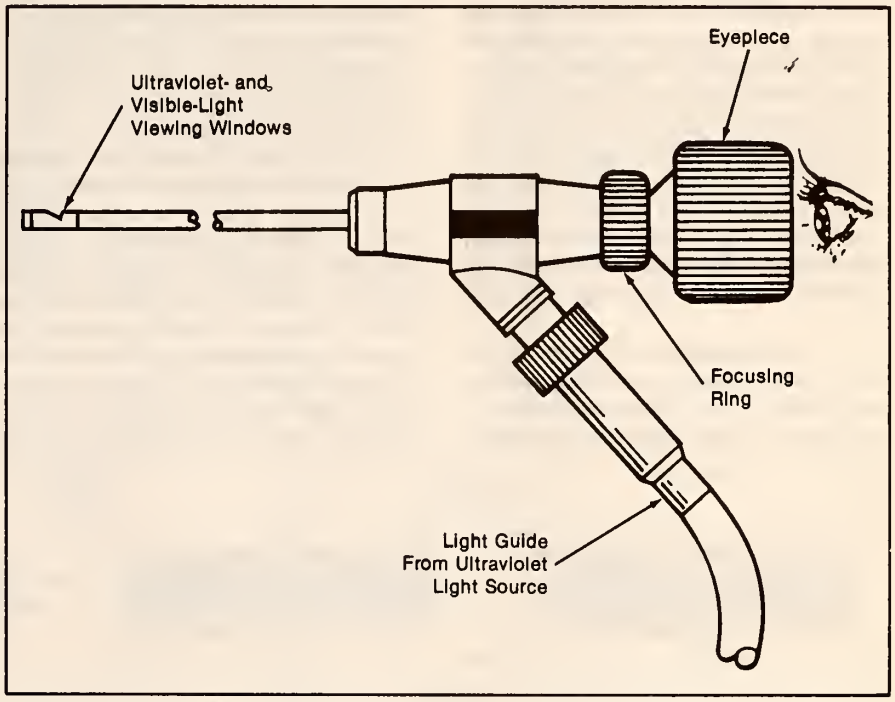

The **Thin Probe of the Borescope** enables inspection of small-diameter tubing.

FOR ADDITIONAL INFORMATION: *Contact: Director, Technology Transfer Division, P.O. Box 8757, BWI Airport, MD 21240; (301) 621-0100 Ext. 241*
REFER TO THE NUMBER LISTED AT THE END OF THIS ARTICLE

NASA Tech Brief
National Aeronautics and
Space Administration
NASA's Jet Propulsion Laboratory, Pasadena, California

Densitometry by Acoustic Levitation

Detailed knowledge of the acoustic field is not necessary.

"Static" and "dynamic" methods have been developed for measuring the mass density of an acoustically levitated solid particle or liquid drop. These methods have several advantages over conventional density-measuring techniques: the sample does not have to make contact with a container or other solid surface, the size and shape of the sample do not affect the measurement significantly, the sound field does not have to be known in detail, and the sample can be smaller than a microliter.

The "static" method (see Figure 1) is an extension of a prior gravitational method for measuring the "compressadensity," a composite quantity related to the density and the adiabatic compressibility. In practice, sample materials often have adiabatic compressibilities so low that they can be ignored to a first approximation, enabling the interpretation of the measurements in terms of the densities alone.

In the "static" method, the unknown density of a sample is found by comparison with another sample of known density. First, one sample is levitated to the desired height in the acoustic-levitation chamber, and the voltage on the acoustic transducers is recorded. The other sample is then acoustically levitated and the transducer voltage adjusted until the sample is held at the same height as that of the previous sample. Then assuming that the amplitude of the acoustic field is proportional to the transducer voltage, the density ϱ_2 of the unknown sample is related to the density ϱ_1 of the known sample by

$$\varrho_2 = \varrho_1(V_2/V_1)^2$$

where V_1 and V_2 are the transducer voltages for the known and unknown samples, respectively.

The "dynamic" method (see Figure 2) can be practiced with or without a gravitational field. The acoustic levitating field serves, in effect, as a spring instead of as a measure of gravitational force. The acoustic field is amplitude modulated by a few percent to make the sample oscillate about the equilibrium levitation position. The modulation frequency is varied until the resonant frequency of the oscillation is found, as indicated by the maximum amplitude of the excursions of the sample from the equilibrium position.

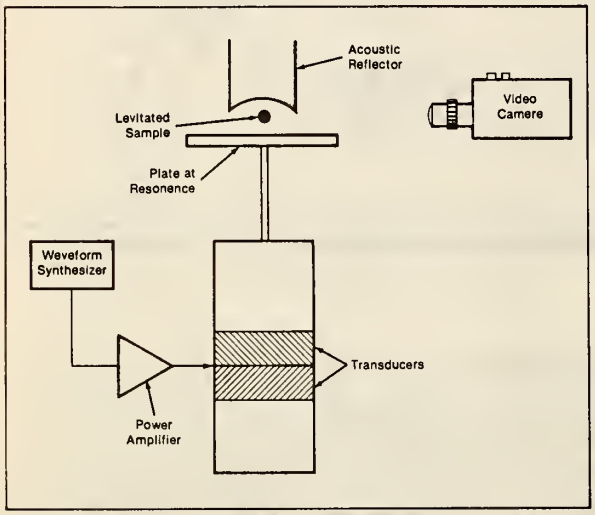

Figure 1. A **Sample Is Acoustically Levitated**, and the position of the sample is measured. The voltage on the transducers is recorded when the sample lies at the desired height.

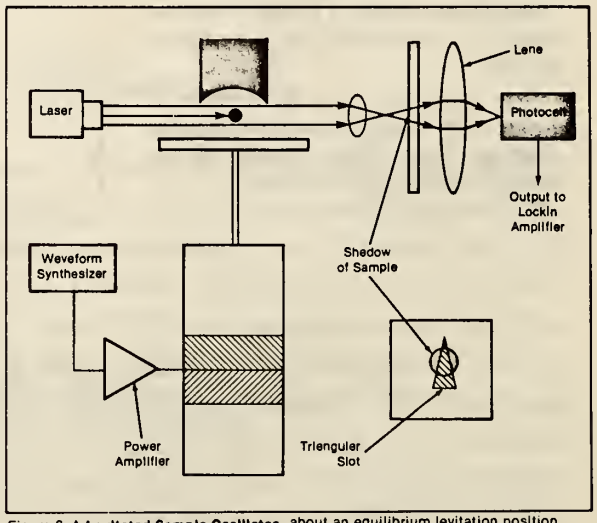

Figure 2. A **Levitated Sample Oscillates** about an equilibrium levitation position. The amplitude of oscillation is measured optoelectronically. The transducer voltage and oscillation frequency are also recorded.

If known and unknown samples are levitated to the same equilibrium position and made to oscillate, then the density of the unknown sample can be found from

$$\varrho_2 = \varrho_1(V_2 f_1/V_1 f_2)^2$$

where f_1 and f_2 are the resonant frequencies of the known and unknown samples, respectively. In the absence of a gravitational field, the equilibrium position would not depend on the voltage, and the equation would be simplified to

$$\varrho_2 = \varrho_1(f_2/f_1)^2$$

This work was done by Eugene H. Trinh of Caltech for **NASA's Jet Propulsion Laboratory**. *NPO-16849/TN*

FOR ADDITIONAL INFORMATION: *Contact: Director, Technology Transfer Division, P.O. Box 8757, BWI Airport, MD 21240; (301) 621-0100 Ext. 241*
REFER TO THE NUMBER LISTED AT THE END OF THIS ARTICLE

NASA Tech Brief
National Aeronautics and
Space Administration
Lyndon B. Johnson Space Center, Houston, Texas

Measuring Thermal Conductivities of Rough Specimens

Cost is reduced and accuracy and repeatability increased.

The thermal conductivity of an irregularly surfaced specimen can be measured more accurately and reliably than before by use of a heat-transfer adhesive that establishes contact between the specimen and the reference standards. The method is also useful when the specimen must be made up of fragments of material. The adhesive ensures good thermal contact to pieces that do not match the others in height (see figure).

Previously, the standard practice was to machine each specimen to a smooth, flat surface and load it in compression between the reference standards. The machining was costly and time consuming, and compressive loading did not ensure consistency of the contact thermal resistance.

The adhesive is cupric oxide cement, which has high thermal conductivity and bonds to many materials. It is usable at temperatures up to 500 °C and can be readily removed from glass or metal reference standards after the measurements are completed.

The assembled specimen and the reference standards are simply bonded together with the cement, which cures at room temperature. The reference standards are of identical size and shape and similarly instrumented with thermocouples. The sandwich structure consisting of the specimen between the two reference standards is placed between the upper and lower heaters and mounted on a liquid-cooled heat sink. A guard heater is placed around the setup, and the space around it and between it and the apparatus is filled with alumina insulation.

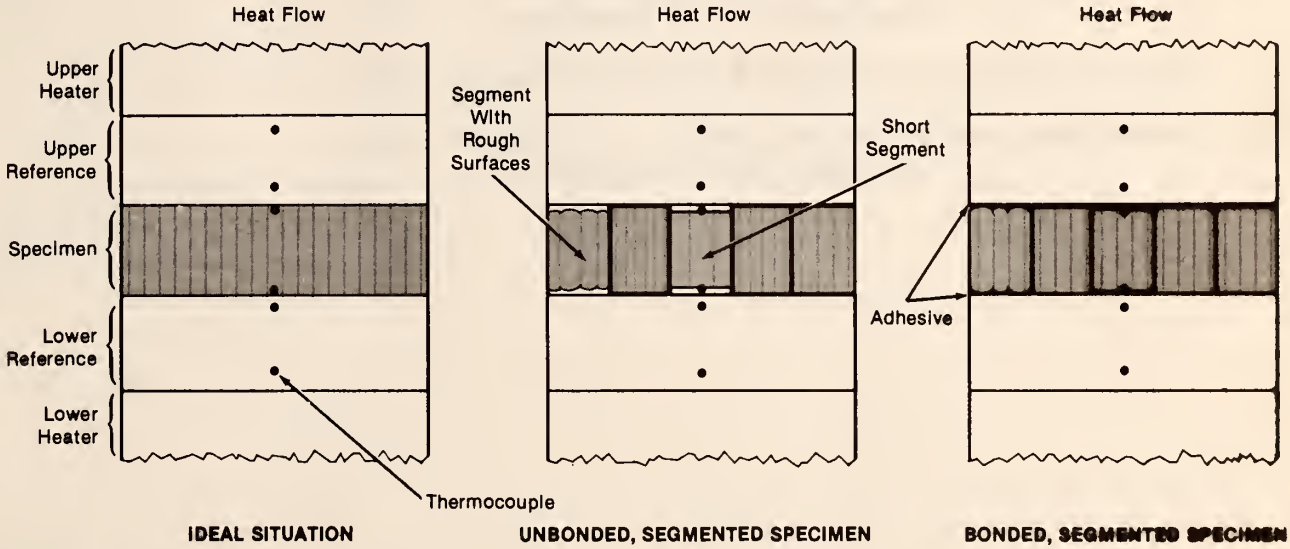

Ideally, Heat Flows Uniformly through a specimen (left). In rough-surfaced or unequally sized specimens, however, the heat-flow pattern becomes distorted, and temperatures at the measurement points do not accurately represent those throughout the reference standards and specimen. Filling the voids with a conductive adhesive restores the nearly uniform distribution of the heat flow.

The upper heater is set to a temperature higher than that of the lower heater to establish a controlled vertical temperature gradient in the sandwich. (The guard heater and the insulation nearly eliminate the radial gradient.) The temperatures of the specimen and of the reference standards are measured at various points. The thermal conductivity of the specimen is calculated from the temperatures and the distances between the measurement points.

In a comparison of measurements with and without the adhesive, the apparent thermal conductivities were higher in the adhesive-bonded specimens. For an advanced carbon/carbon composite material, for example, the thermal conductivity at room temperature was 147 Btu•in./h•ft^2 • °F (21.2 J/m • °C) for a bonded specimen and 49 Btu•in./h•ft^2• °F (7.1 J/m• °C) for an unbonded specimen.

This work was done by Aloys H. Striepens and Chi-Wang Chang of Rockwell International Corp. for **Johnson Space Center**.

MSC-21333/TN

FOR ADDITIONAL INFORMATION: *Contact: Director, Technology Transfer Division, P.O. Box 8757, BWI Airport, MD 21240; (301) 621-0100 Ext. 241*
REFER TO THE NUMBER LISTED AT THE END OF THIS ARTICLE

Environmental Science & Technology

0660 Emulsion-Phase Contactor

0661 New Inland Oil Skimmer

Testing & Instrumentation

0662 In Situ Groundwater Detection of Chloroform and Trichloroethylene

Other Items of Interest

0695 The Determination of pH by Flow Injection Analysis and by Fiber Optrode Analysis (Licensing Opportunity)

0698 Fourier Transform Infrared Spectrometry of Ambient Aerosols

0699 Investigation 2,4-Dinitrophenylhydrazine Impregnated Adsorbent Tubes for the Collection of Airborne Aldehydes

Emulsion-Phase Contactor

The electrically driven countercurrent solvent-extraction process uses high-voltage electric fields to form an emulsion between two immiscible phases in a contacting vessel (Fig. 1). This process is used to transfer solute from one phase to another. The process promotes efficient extraction by creating a large interfacial surface area and by promoting coalescence of the droplets formed.

Commercial solvent-extraction systems are limited by the mass-transfer rates of one or more chemical species between a continuous phase and a dispersed phase. Parameters of these species that limit mass-transfer rate include surface area, convection, diffusion through each of the two phases, reaction rate, and differing chemical activities in the two phases. Generally, vigorous mechanical mixing is used to create small droplets; this mixing increases the surface area and local convection. However, mechanical mixing involves bulk movement of the continuous phase and reduces the energy efficiency of the extraction.

At ORNL, imposition of both ac and dc electric fields into a contacting vessel was shown to create small droplets having high surface-to-volume ratios and to coalesce the droplets. The aqueous dispersed phase is fed through a nozzle located in a high-voltage electric field. Shear stresses at the nozzle cause the formation of

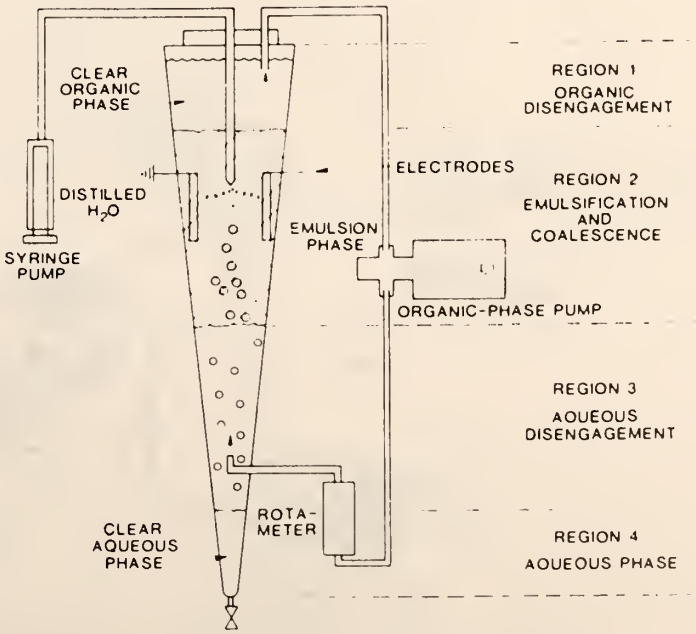

Fig. 1. Schematic diagram of the electrically driven solvent-extraction process. The distilled water (aqueous phase) is injected into the organic compound 2-ethyl-1-hexanol (organic-continuous phase), forming an emulsion (Region 2). Because of the presence of an electrical field, the water droplets mix efficiently and then coalesce, the coalesced water collects in the bottom, forming Region 4. The result is an energy-efficient method of mass transfer between phases and subsequent phase separation.

small (1-5 μm) droplets. The electric field tends to promote electrodynamic flow and maintain a high concentration of droplets near the electrodes. An upflow of the continuous phase in the presence of the electric field produces countercurrent convection that is more efficient than mechanical mixing. The same electric field induces the droplets to coalesce and fall through the organic phase, thus separating into another phase and providing countercurrent solvent extraction and phase separation.

The electrically driven countercurrent solvent-extraction process was developed specifically for solvent extraction processes that mix and separate aqueous-dispersed and organic-continuous phases. This process can also be used for small-scale radioisotope production. Research is under way to develop large-scale applications of this technology. Because of its greater efficiency, this process may result in energy savings of an estimated 70-90% over conventional separation processes while operating at mass-transfer efficiencies that are potentially an order of magnitude higher than present-day devices.

T. C. Scott and R. M. Wham, "An Electrically Driven Multistage Countercurrent Solvent Extraction Device: The Emulsion Phase Contactor," *Ind. Eng. Chem. Res.* (submitted).

Additional information:

Office of Technology Applications
Martin Marietta Energy Systems, Inc.
P.O. Box 2008
Oak Ridge, TN 37831-6257

Telephone: (615) 574-4192; FTS 624-4192

NCEL
Techdata Sheet

NAVAL CIVIL ENGINEERING LABORATORY
PORT HUENEME, CALIFORNIA 93043

New Inland Oil Skimmer

A new oil skimmer has been procured for the Navy to clean up small (less than 200 gallons) oil spills in inland areas and hard to access locations in harbors. This skimmer was selected to meet two basic Navy needs in small oil spill clean up:

- Reduce cost and manpower
- Improve performance

The new oil skimmer is the Crowley Environmental - Alden Industries Model A-4 (Figure 1). This skimmer has two 4-inch-diameter propylene mop ropes that pick up floating oil from the water. The ropes are connected to an aluminum frame supported between two 5-foot-long pontoons. Oil is squeezed from the ropes by a set of rollers and then pumped to a separate oil

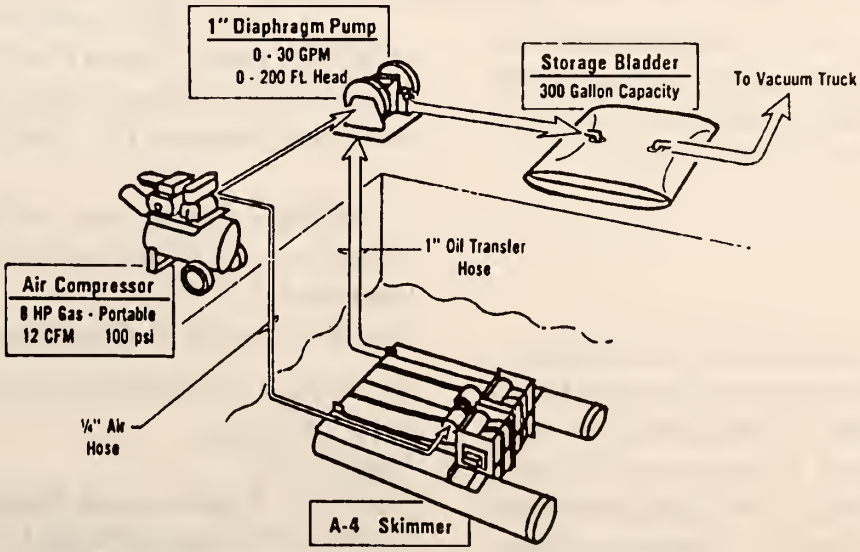

Figure 2. Typical operational setup of Crowley-Alden A-4 oil skimmer.

storage bag. The ropes and pump are driven by a gasoline-powered air compressor. The primary characteristics of the A-4 are:

- rapid setup time (less than 20 minutes)
- lightweight and compact (fits into a pickup truck)
- can be handled by two people
- very high oil content in the discharge (70 to 90%)
- good performance in harbor chop up to 1 foot
- capable of operating unattended

The A-4 is used after the spill has been contained within oil spill booms. Figure 2 shows how the skimmer would typically be setup in the field. Additional details on the A-4 can be found in References 1 and 2.

Uses

The A-4 is intended as the new generation replacement for the existing small (SLURP) and medium (JBF DIP 1001) oil skimmers. The A-4 can be used to clean up any oil, but especially JP-5 and Diesel Fuel Marine spills. The skimmer is primarily designed for spills of between 50 and 200 gallons (20% of Navy spills), but can be used for smaller or larger spills. The areas where the skimmer will be most useful are near piers, berthed ships, ditches, ponds, and shore areas with water depths of less than 4 feet.

Tests

The A-4 has been tested under simulated conditions in an EPA test tank and in the field at 30 Navy activities. The A-4 performed very well, meeting or exceeding 15 performance criteria that defined Navy needs. Ten of the quantitative criteria are listed in Table 1. The results of these tests were used to slightly modify the A-4 to match Navy needs even better.

Table 1. Small Skimmer Performance Parameter Range

Criteria	Desired	Actual Results[a]
Self Sufficient System	Yes	Yes
Operating Manpower	None	None
Recovery Rate	120 gph	120 gph
Deployment Time	20 min	20 min
Wave Impact	1 ft/80%	1 ft/70%[b]
Proven Equipment	Tested	EPA tested
Oil Recovery Efficiency	80%	65-95%
Portability	1/2-ton truck	1/2-ton truck
Maintainability	Easy	Easy
Set-up Manpower	2 people	2 people

[a]Results are for both DFM and JP-5.
[b]Acceptable performance when combined with calm water performance.

Military Specification

Modifications to the existing specification on small oil skimmers have been proposed in Reference 2. These modifications will bring the specification into conformance with the new inland oil skimmer.

References

1. NCEL Contract Report CR 87.003. Crowley Alden A-4 Oil Skimmer Operational Test Report. Port Hueneme, CA. Oct 1987.

2. Military Specification Mil-0-29155(YD), Amendment 1: Oil Spill Retrieval System, Small Inner Harbor, 17 May 1976.

For Additional Information:

To discuss this effort further, contact:

Jerry Dummer
Code L03C
Facilities Engineering Support Office
Naval Civil Engineering Laboratory
Port Hueneme, CA 93043
(805) 982-4070

Refer to Techdata sheet 89-04/TN

Lawrence Livermore National Laboratory

In Situ Groundwater Detection of Chloroform and Trichloroethylene

The long-term objective of research is to develop a fiber-optic-based system for monitoring contaminant species in groundwater. These efforts require the development of optical chemical sensors (optrodes) that are compatible with optical fiber spectrometers. A new fluorescence-based chemical test for detecting chloroform and trichloroethylene (TCE) was developed. The fluorescent products of this assay have been isolated and these compounds have been identified using modern spectroscopic analyses. A report describes the details of this reaction, its putative reaction sequences with chloroform and TCE, and present an analysis of the spectral data obtained from the reaction products.

The researchers have exploited this new fluorescence-based test for chloroform and TCE and have incorporated it into a fiber optic chemical sensor (optrode) that was developed for monitoring groundwater contamination. The configuration of the optical sensor is described and the methods to improve the transduction mechanism are discussed. A technique permits the selective detection of chloroform in the presence of TCE and have detailed approaches to selectively measure TCE in the presence of chloroform. Finally, the syntheses of several compounds to be evaluated to improve the luminescence properties of the fluorescence-based test for chloroform and TCE are reported.

FOR ADDITIONAL INFORMATION: A copy of the report is available from NTIS, Springfield, VA 22161; (703)487-4600.
NTIS order number: DE88-016646NAC.
Price code: A03.

Manufacturing, Machinery & Tools

0663 Automated Chemical Analysis for Process Solutions

0664 PARDS to be Used in National Institute of Standards & Technology Research

0665 Compliant Robot Wrist Senses Deflections and Forces—Precise parts can be assembled without damage.

0666 Gray-Scale Processing for Tracking of Welds—Digital analysis of video images provides information for control of a welding robot. (Licensing Opportunity)

0667 Plating Repair of Nickel-Alloy Pressure Vessels—Localized plating builds up wall thickness.

Testing & Instrumentation

0668 Double-O-Ring Plug for Leak Tests—A verifiable redundant seal contributes to testing and assurance of safety.

0669 Identification of Anomalies in Welds—Advanced techniques are combined with conventional analytical methods.

0670 Strain-Gaged Bolt Process for the Direct Measurement of Valve-Stem Thrust

Other Items of Interest

0625 Adaptive Force and Position Control for Robots—Precise knowledge of manipulator and environment is not required. (Licensing Opportunity)

0654 Video Alignment System for Remote Manipulator—Crosshairs and a mirror provide angular references. (Licensing Opportunity)

Automated Chemical Analysis for Process Solutions

The development of four measurement devices for use in automated monitoring of the concentration of specific chemicals in multi-layer printed wiring board (PWB) plating baths was recently completed. The measurement devices, known as optrodes, will be key elements of the Automated Chemical Analysis for Process Solutions (ACAPS) system. ACAPS is a computer controlled system which will continuously, automatically, and accurately control the copper and solder plating solutions used in electroplating PWBs.

The present system for monitoring PWB plating bath process solutions is time consuming, costly, and not conducive to achieving consistent plating results. Since the complex chemistries involved in these solutions can drift rapidly and without warning, monitoring solutions with the current procedure can result in a large time span in which the chemical concentrations deviate, undetected, from their control limits.

The ACAPS project sought to develop optrodes to automatically monitor the eight chemical constitutents most critical to the copper and solder plating baths. The optrode concept is based on remote fiber fluorimetry sensor technology, originally developed by Lawrence Livermore National Laboratory. In a typical system, laser light is focused into the end of a fiber optic cable. The light travels along the fiber to an optrode immersed in the solution to be analyzed. The amount of light absorbed by the solution near the optrode, as detected by the optrode, provides a measure of how much of the particular chemical constituent is present. The intensity of the detected light is converted into a digital signal and transmitted to an HP 1000 computer. There, it is processed by an algorithm and concentration data is developed. If the concentration is low, the HP 1000 computer software will compute the necessary chemical addition to return the parameter to its optimum level.

Development of each constituent-specific optrode requires extensive research into the properties of the constituent ot be measured. For this reason, optrodes for only four of the originally proposed eight chemical constituents have been successfully developed.

The future of optrode technology is very bright in that there are many other processes requiring solutions to be kept within tight concentration tolerances. As this technology is further developed to accommodate some of these applications, DOD contractors and the military will benefit greatly from the results.

FOR ADDITIONAL INFORMATION: Contact, Commander, Naval Air Systems Command, Attn: Mr. Robert Lewandowski (AIR-5143K), Washington, DC 20361-5140; (202) 692-7493, AV222-7493.

PARDS To Be Used in National Institute of Standards & Technology Research

AMRF researchers will test the capabilities of RVSI's (Robotic Vision Systems, Inc.) new Parts Digitizing System (PARDS) for the Naval Supply Systems Command (NAVSUP).

PARDS uses a laser scanning technique and graphic data analysis tools to produce a representation of a mechnical part. The system is designed for use in reverse engineering, i.e., the identification and measurement of the features of an existing part to generate the data required to manufacture functional copies. The part data output will be used in ongoing AMRF research in product representation data and quality assurance.

PARDS graphics utilities are based on Computervision CADDS4X software. AMRF researchers will call on their experience gained using the CADDS4X supplied as part of the Research Associate agreement with Computervision as they test the current capabilities and user features of PARDS. In addition, they will explore areas for suggested technical enhancements to the system such as the use of solid graphics and the production of part representations in the Product Data Exchange Specification (PDES) format.

At the completion of the AMRF effort, PARDS will be transferred to the Naval Ordnance Station, Louisville, Kentucky. Louisville is a Navy site for development and approval of PDES for use in manufacturing spare parts.

FOR ADDITIONAL INFORMATION: To discuss this effort further, contact: Dr. Philip Nanzetta, AMRF Project, Building 220--Room B-1111, National Institute of Standards & Technology, Gaithersburg, MD 20899; (301) 975-3414.

NASA Tech Brief
National Aeronautics and
Space Administration
Goddard Space Flight Center, Greenbelt, Maryland

Compliant Robot Wrist Senses Deflections and Forces

Precise parts can be assembled without damage.

The Goddard Space Flight Center has developed a compliant wrist that will move in any direction and rotate about any axis in response to applied forces. Its deflection is calibrated and instrumented so that a control computer can measure the degree of deflection and derive the magnitude and direction of the applied forces and torques.

Such a compliant wrist brings to robots important capabilities that humans use in manipulating objects. The compliance helps prevent damage to precise, delicate parts during assembly by the robot. A knowledge of the degree of compliance allows the control computer to alter the robot's position to compensate for compliance-induced positioning deviations. The measure of the contact forces allows the system to perform a series of moves, using a force-sensing-search strategy, to determine and correct certain kinds of misalignments between parts being mated or demated.

Tests with the compliant wrist mounted on a computer-controlled manipulator have shown that certain parts with clearances on the order of 0.001 in. (0.025 mm) can be mated with force feedback when the initial errors in relative position are on the order of 0.25 in. (6 mm). Besides permitting error correction, the force/torque-sensing-control software can prevent damage to components and determine the success or failure in carrying out a specified operation.

As shown in the two figures, the compliant-wrist assembly consists of six identical rods that connect two plates. Each rod is essentially a spring-loaded piston. One plate, which serves as the base plate, is rigidly attached to the end of a robot arm and is connected to the rods through universal joints. The other or "compliant" plate is rigidly attached, usually by a gripper, to the object being manipulated and is connected to the other ends of the rods by spherical bearings. The "compliant" plate can move relatively to the robot arm in response to any applied force or torque because the springs in the connecting rods will give, causing changes in the lengths of the rods. A linear displacement transducer measures the change in piston length. The force acting on the rods can be deduced from piston travel if the spring constant is known. It is also possible to use strain gauges to measure the axial forces directly.

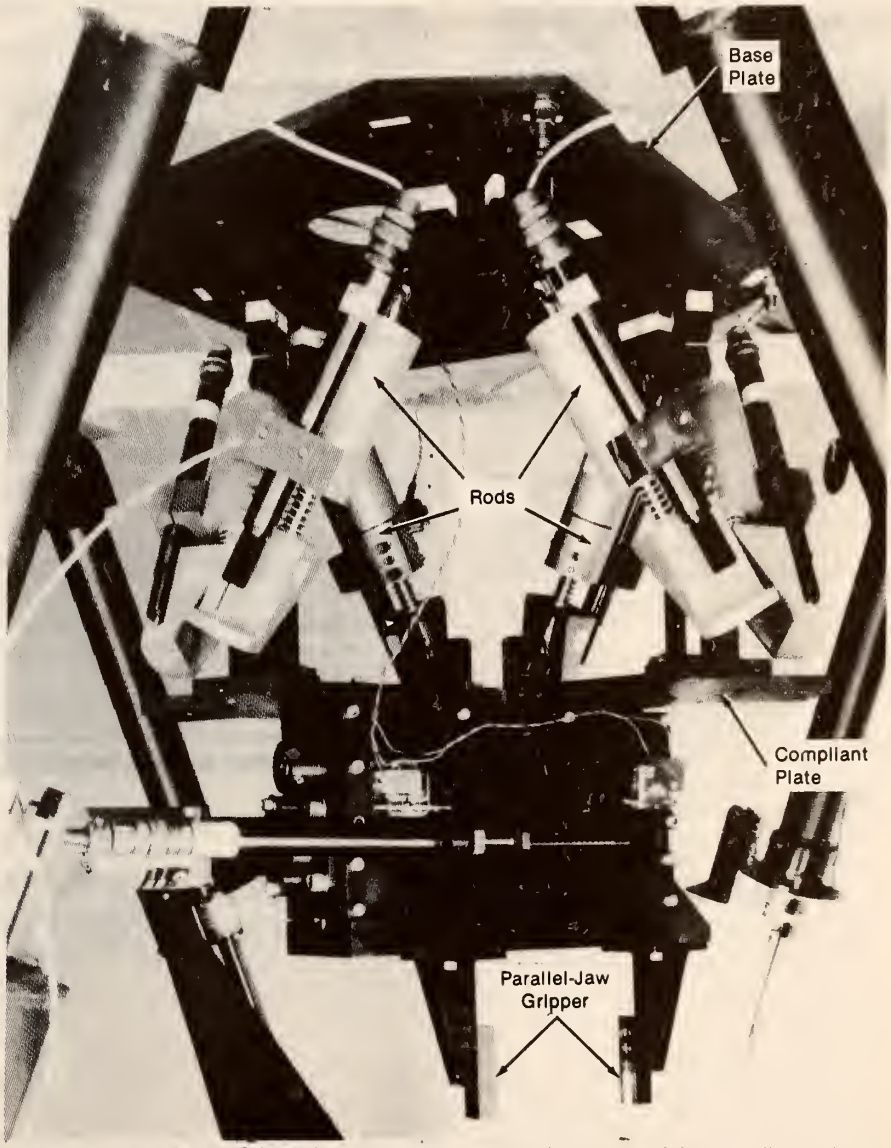

Figure 1. **A Parallel-Jaw Gripper** is mounted on the compliant plate of the compliant-wrist assembly.

The outputs of the transducers are fed to a control computer through a digital-to-analog converter. The computer calculates actual lengths of the rods from these data and uses them to find the position and orientation of the "complaint" plate with respect to the base plate. Since the spring forces act along the rods, their directions are known. From these data the computer finds the vector sums of forces and torques exerted on the "complaint" plate by the rods. Given that the orientation and spatial distribution of the mass of the "complaint"

plate and its associated hardware are known, the gravitational components of the forces and torques can be subtracted to yield only the contact forces and torques. If the wrist were to be used in space, this correction for the gravitational field would not be needed.

In the prototype version, the wrist mechanism can exert a force of about 50 lb (220 N) in any direction and can deflect about 0.375 in. (9.5 mm). The rod lengths, spring stiffnesses, and type of displacement sensor can be changed to suit different applications.

This work was done by Lloyd R. Purves, Franklin Strempek, and Timothy Premack of **Goddard Space Flight Center**.
GSC-12868/TN

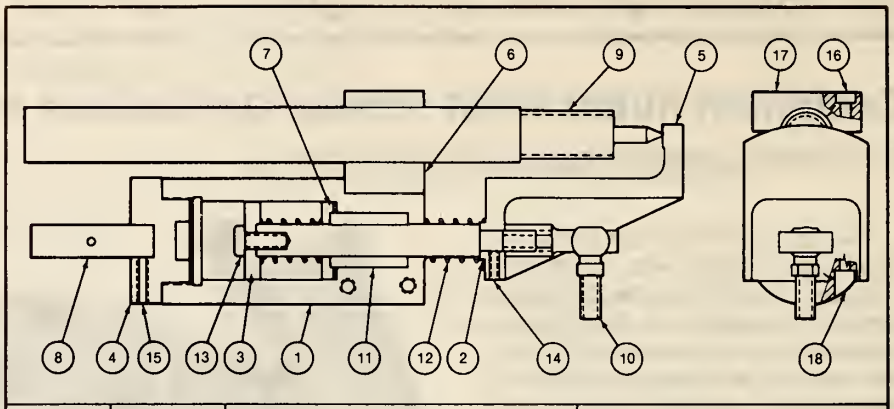

Item	Number of Pieces Required	Description	Material
18	2	Screw, 8-32 UNC-2A × 1.750 in. Long	Corrosion-Resistant Stainless Steel
17	1	Clamping Block, Linear Variable-Differential Transducer	
16	2	S.H.C.S. .164-32 UNC-3A 0.875 in. Long	Corrosion-Resistant Stainless Steel
15	2	SET SCREW .190-24 UNC-3A 0.375 in. Long	Corrosion-Resistant Stainless Steel
14	1	SET SCREW .164-32 UNC-3A 0.375 in. Long	Corrosion-Resistant Stainless Steel
13	1	SCREW .250-28 UNF-2A 0.500 in. Long	Corrosion-Resistant Stainless Steel
12	2	Spring, Compression	
11	1	Adjustable Ball Bushing	
10	1	Ball-Joint Rod End, With Stud	
9	1	Gauging Linear Variable-Differential Transducer	
8	1	Universal Joint, Bored	
7	1	Spring Retainer, Inner	
6	1	Block, Linear Variable-Differential Transducer	
5	1	Flange	
4	1	Plug	
3	1	Spring Retainer	
2	1	Piston Rod	
1	1	Piston Housing	

Figure 2. This **Simplified Assembly Drawing** shows the parts of each of the six identical pistons.

FOR ADDITIONAL INFORMATION: *Contact: Director, Technology Transfer Division, P.O. Box 8757, BWI Airport, MD 21240; (301) 621-0100 Ext. 241*
REFER TO THE NUMBER LISTED AT THE END OF THIS ARTICLE

NASA Tech Brief
National Aeronautics and
Space Administration
Marshall Space Flight Center, Alabama

Licensing Opportunity

Gray-Scale Processing for Tracking of Welds

Digital analysis of video images provides information for control of a welding robot.

A real-time digital video-image-processing system contributes to the automation of weld-seam tracking. The tracking system makes no contact with the seam. A small television camera views the seam just ahead of the point currently being welded. The welding arc provides the illumination. Periodically, a frame grabber digitizes the video image and stores it in a computer memory as gray-scale values. The seam is located by analyzing Hough-transform arrays of derivatives of digitally-filtered image data. The information on the location and orientation of the seam is used as feedback by a welding robot to correct deviations of the electrode from the seam as welding continues.

Standard image-processing techniques are used in the early stages of the analysis. First, the image data are filtered by a 3-by-3 convolution. First and second derivatives of the filtered data are calculated in the direction perpendicular to the direction of motion of the torch. The derivative data are then compared with threshold values and used to calculate three Hough-transform arrays. The first and second arrays correspond to first-derivative data above and below a threshold, respectively; the third array, to second-derivative data below a threshold.

The three Hough arrays are examined to determine the angle having the most entries. That angle corresponds to the angle of the seam in the image. The column in each of the arrays corresponding to that angle is then scanned for the locations of peaks. A set of pattern-matching rules is used to locate specific patterns of peaks. These correspond to various joint profiles; the location of the match indicates the location of the joint in the image.

The system can locate the seam between two metal parts even if they are shiny, and it can detect a smaller gap than could previous systems. The location and angle of the seam can be determined without any advance information. The seam-tracking algorithm is more robust than the previous ones, both in finding the seam and in deciding whether the seam has been found.

This work was done by David A. Gutow of Rockwell International Corp. for **Marshall Space Flight Center**. *No further documentation is available.*

Inquiries concerning rights for the commercial use of this invention should be addressed to the Patent Counsel, Marshall Space Flight Center. Refer to MFS-29433/TN

George C. Marshall Space Flight Center
Technology Utilization Officer: Ismail Akbay
Code AT01
Marshall Space Flight Center,
AL 35812
(205) 544-2223
Patent Counsel:
Leon D. Wofford, Jr.
Mail Code CC01
Marshall Space Flight Center,
AL 35812
(205) 544-0024

FOR ADDITIONAL INFORMATION: *Contact: Director, Technology Transfer Division, P.O. Box 8757, BWI Airport, MD 21240; (301) 621-0100 Ext. 241*
REFER TO THE NUMBER LISTED AT THE END OF THIS ARTICLE

NASA Tech Brief
National Aeronautics and Space Administration
Marshall Space Flight Center, Alabama

Plating Repair of Nickel-Alloy Pressure Vessels

Localized plating builds up wall thickness.

A procedure for the localized electrodeposition of nickel enables the repair of small damaged nickel-based pressure vessels. Electrodeposition can restore weakened areas of a vessel wall to at least their former strength.

The area to be repaired is cleaned and sanded. An open-bottom box is placed around the area to be repaired (see figure). Electroplating solution enters the box, flowing over and under an electrode shaped to accommodate the area to be repaired. Nickel is deposited from the solution onto the wall to a typical thickness of 0.17 to 0.23 in. (4.3 to 5.8 mm). The edge of the plated layer is ground and sanded to blend smoothly into the surrounding unplated surface.

This work was done by Steve K. Ricklefs and Kevin M. Chagnon of Rockwell International Corp. for **Marshall Space Flight Center**.

MFS-29304/TN

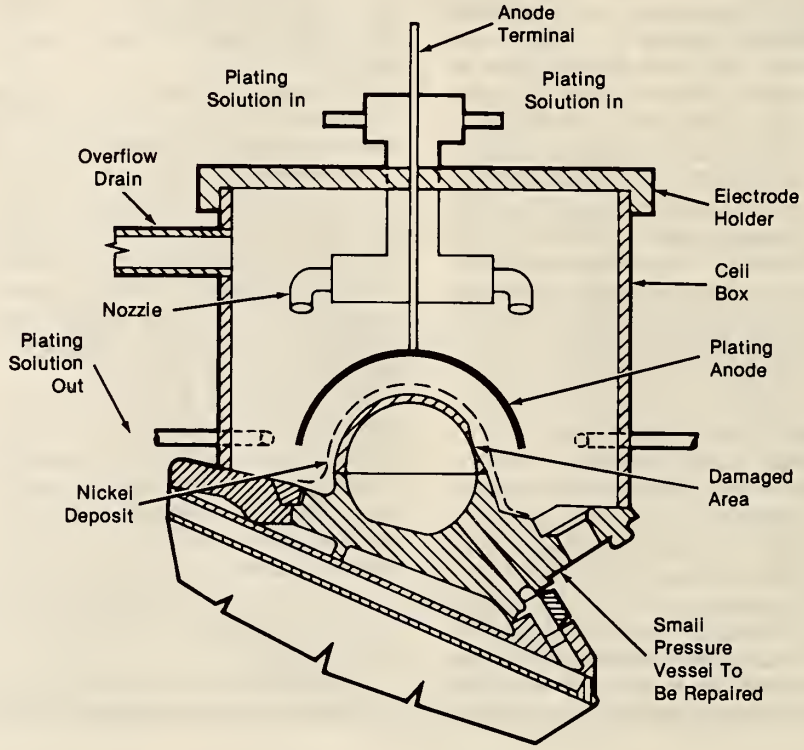

An **Electroplating Box Fits** around the damaged pressure vessel. The plating anode is shaped to cover approximately the area to be plated.

FOR ADDITIONAL INFORMATION: *Contact: Director, Technology Transfer Division, P.O. Box 8757, BWI Airport, MD 21240; (301) 621-0100 Ext. 241*
REFER TO THE NUMBER LISTED AT THE END OF THIS ARTICLE

NASA Tech Brief
National Aeronautics and
Space Administration
Marshall Space Flight Center, Alabama

Double-O-Ring Plug for Leak Tests

A verifiable redundant seal contributes to testing and assurance of safety.

A pressure plug features redundant O-ring bore seals and an axial port that opens laterally into the space between the O-rings to enable testing of the seals (see figure). Designed to plug holes used to test the large O-rings of the Space Shuttle solid rocket boosters, the pressure plug might be useful to seal test or cleanout holes that are normally kept closed in hydraulic actuators, pumps, and other pressurized systems.

After the plug is installed and verified, a sealing ring — essentially an O-ring mounted as a washer — is placed in a recess in the plug and compressed by a screwhead. Thus, the screwhead and sealing ring act as a secondary seal in parallel with the outer O-ring.

This work was done by James H. Greene of United Technologies Corp. for **Marshall Space Flight Center**. *No further documentation is available.*
MFS-28222/TN

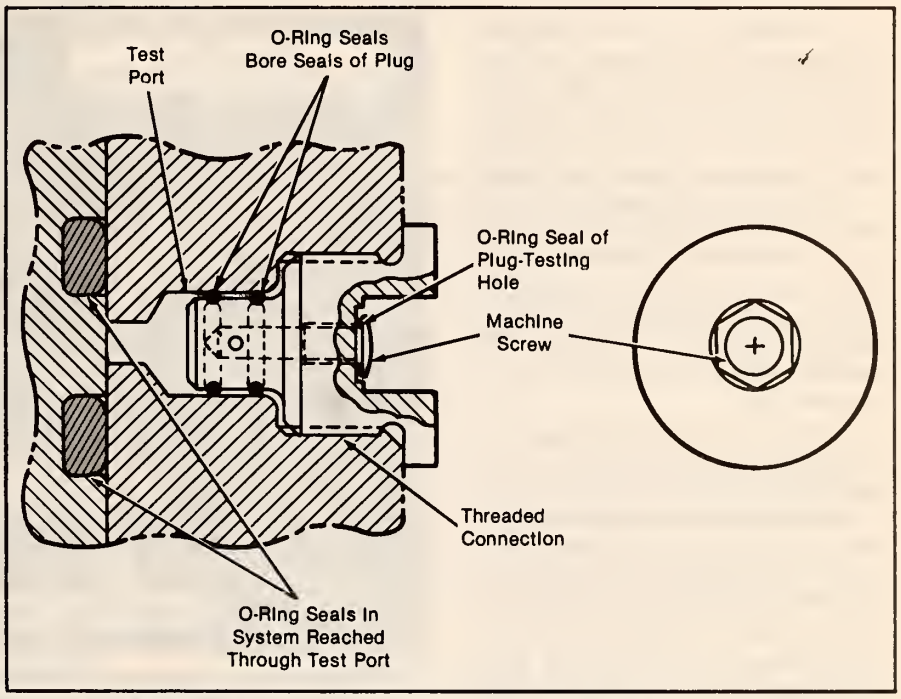

An **Axial Passage** in the plug is connected through a radial passage to the space between the O-rings. The opening is used to test the O-rings, then sealed with a smaller O-ring compressed by a machine screw.

FOR ADDITIONAL INFORMATION: *Contact: Director, Technology Transfer Division, P.O. Box 8757, BWI Airport, MD 21240; (301) 621-0100 Ext. 241*
REFER TO THE NUMBER LISTED AT THE END OF THIS ARTICLE

NASA Tech Brief
National Aeronautics and
Space Administration
Marshall Space Flight Center, Alabama

Identification of Anomalies in Welds

Advanced techniques are combined with conventional analytical methods.

A combination of real-time radiography, scanning electron microscopy, and energy-dispersive spectrometry can identify enigmatic features in radiographs of welds where the standard tensile, hardness, and electrical-conductivity tests and visible-light microscopic and macroscopic examinations are insufficient by themselves. The new combination of techniques was applied successfully to variable-polarity-plasma-arc welds of 2219 aluminum alloy. The joints were subjected to penetration, fill, and weld-repair passes with 2319 aluminum weld wire.

Radiographs of the test welds showed anomalous white dots and lines. These anomalous features were then observed in a scanning electron microscope instrumented with an energy-dispersive spectrometer while the data were processed in real time. This combination of techniques showed that these regions consist of a platelike phase intermixed with the aluminum/copper eutectic (see figure). They also showed that the platelike phase is rich in copper (20 percent), iron (6 percent), and manganese (1.5 percent). These concentrations are many times greater than those in other parts of the weld.

In general, the white lines were located in the zones of fusion between the penetration passes and the base metal. One of the white dots was identified as part of a penetration pass just beneath the zone of fusion between the penetration and fill passes.

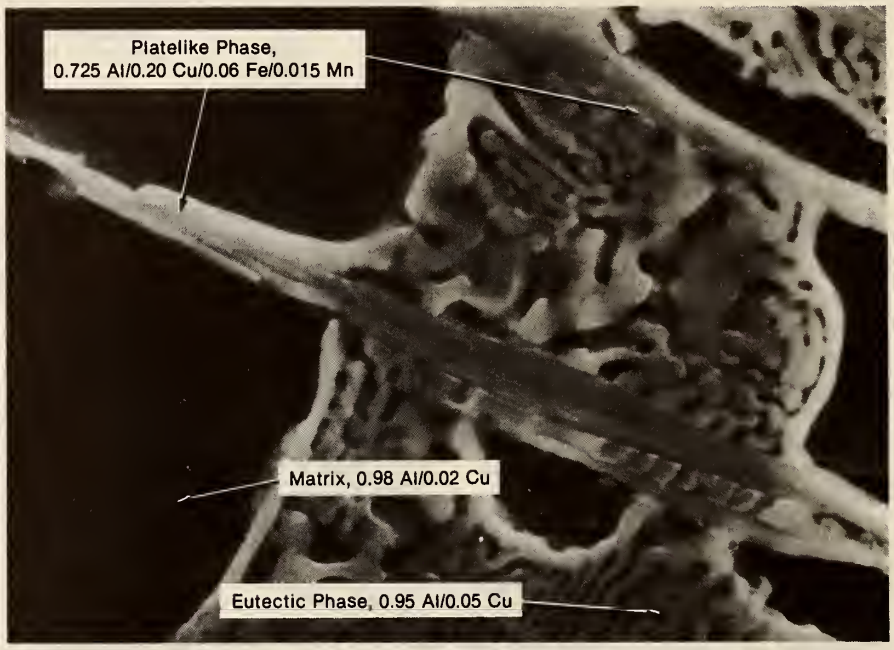

A **Platelike Phase of Aluminum** with copper, iron, and manganese appears mixed with the eutectic phase and extends into the copper/aluminum alloy matrix in this scanning electron micrograph. The composition and nature of the platelike phase could not be determined by ordinary methods.

This work was done by David G. Knichen of Martin Marietta Corp. for **Marshall Space Flight Center.**

MFS-28285/TN

FOR ADDITIONAL INFORMATION: *Contact: Director, Technology Transfer Division, P.O. Box 8757, BWI Airport, MD 21240; (301) 621-0100 Ext. 241*
REFER TO THE NUMBER LISTED AT THE END OF THIS ARTICLE

Strain-Gaged Bolt Process for the Direct Measurement of Valve-Stem Thrust

The strain-gaged bolt process (SGBP) for the direct measurement of valve-stem thrust provides valve owners with a simple, cost-effective means of solving their valve problems. The SGBP was developed at the Paducah Gaseous Diffusion Plant (PGDP) to facilitate the setup, maintenance, and monitoring of the plant's motor-operated valves. Normally, the SGBP can be applied to test any make of valve or actuator, and available accessories permit the stem thrust of any rising stem valve to be measured without closing the valve and disrupting the flow.

The SGBP is applicable to valves or actuators having a bolted thrust plate that bears the axial loads exerted by the valve stem. For motor-operated valves, the SGBP uses a strain-gage bolt, a clamp-on ammeter, a digital storage oscilloscope, and signal-conditioning electronics (Fig. 1) in a process that collects digital data and provides time-based signatures of stem thrust and motor current (Fig. 2).

Fig. 1. Strain-gaged bolt test of a motor-operated valve in progress. The technician is installing the required strain-gaged bolt.

The SGBP produces an accurate and a complete measure of the levels of motor current and stem thrust that occur during a valve's seating stroke. These thrust levels are critical to the performance, maintenance, and service life of many valves. Insufficient thrust may result in leaking valve seats; excessive thrust can damage valves and accelerate their wear. SGBP signatures and data yield significant information concerning these thrust-related problems. Other useful information, such as the running thrust, the inertia thrust, the maximum thrust, and motor current peaks can also be determined from the SGBP data and signatures.

Most valve actuators have a field-adjustable control, which, in effect, limits stem thrust. The actuation of this control does not normally rely on a direct determination of the thrust exerted by the valve stem. When the control actuates, it does so in response to the reaction loads occurring within the actuator's drive train, which constitutes an indirect determination of stem thrust. It forces the assumption that a given control setting will consistently produce a particular level of stem thrust. Evidence suggests that this assumption becomes invalid as valves and actuators age or wear.

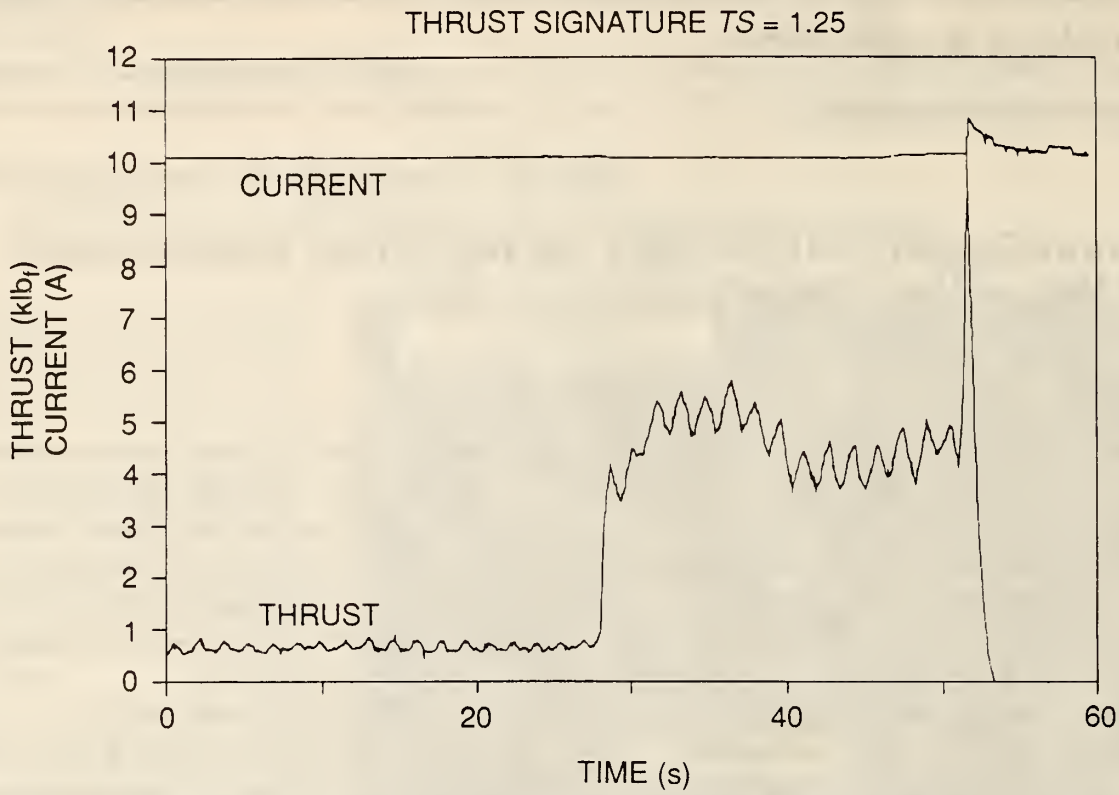

Fig. 2. Typical stem-thrust and motor-current signatures produced using SGBP test data from a 24-in. motor-operated gate valve.

Various factors can permanently decrease or increase the original stem- thrust level associated with any thrust-control setting. As a result, significant valve problems often develop before valve owners discover that their thrust-control settings are inadequate. Application of the SGBP corrects this situation by removing any doubt regarding the level of stem thrust produced by a particular thrust-control setting.

The SGBP offers many benefits. The equipment is easily transported, set up, and operated by a single technician. SGBP tests can be conducted very quickly because no calibration of the equipment is required at the valve site. A two-man crew routinely tests 10 to 15 motor-operated valves during their 8-hour shift at PGDP. The digital storage oscilloscope permits real-time signature analysis, allowing remedial actions to take place at the valve site during SGBP testing. Test data are permanently retained on IBM-compatible floppy disks.

Additional information:

Office of Technology Applications
Martin Marietta Energy Systems, Inc.
P.O. Box 2008
Oak Ridge, TN 37831-6257

Telephone: (615) 574-4192; FTS 624-4192

P. G. Elliott and S. J. Davis, *Evaluation of the Operability and Reliability of Motor-Operated G-17 Gate Valves*, KY/L-1459, Paducah Gaseous Diffusion Plant (October 1987).

P. G. Elliott and S. J. Davis, *Evaluation of Valve Stem Thrust Measurement Processes*, KY/L-1467, Paducah Gaseous Diffusion Plant (November 1987).

Materials

0671 Kenaf Paper: A Forest-Saving Alternative

0672 Low Dislocation Density GaAs Crystals Grown Using Advanced Vertical Gradient Freeze Technique

0673 Eight New High-Temperature Superconductors Produced by Novel Process

0674 Method for Preparing Vanadium

0675 New Model Makes Glass-Fracture Predictions More Reliable

0676 Flexible, Polymer-Filled Metallic Conductors—Combined advantages of metals and polymers are exploited by advanced manufacturing techniques. (Licensing Opportunity)

0677 Fluoroepoxy Adhesives Bond Flouroplastics (Licensing Opportunity)

0678 Low-Thermal-Expansion Filled Polytetrafluoroethylene—PTFE would be made thermally compatible with aluminum without changing its dielectric constant.

0679 Multiple-Purpose Rigid Foam Insulation—Properties can be adapted to a variety of demanding applications.

0680 Polymer Coatings Reduce Electro-osmosis (Licensing Opportunity)

0681 Soluble Aromatic Polyimides for Film Coating—Films are nearly colorless and soluble and exhibit good mechanical properties.

0682 Polymer Lubricants for use in Vacuum—Both solid and film polyimides offer low friction and wear.

Testing & Instrumentation

0683 Measuring Fracture Times of Ceramics—Electrical measurements complement or replace fast cinematography.

0684 Ultrasonic Detection of Transply Cracks in Composites—The densities and propagation of cracks are measured nondestructively.

Other Items of Interest

0626 Advanced Components for Fiber-Optical Systems—This concise review emphasizes highly birefringent fibers, couplers, and polarizers.

0640 Bipolar Battery Using Conductive-Fiber Composite—Improved lead/acid battery features reduced weight and increased energy and power densities. (Licensing Opportunity)

0667 Plating Repair of Nickel-Alloy Pressure Vessels—Localized plating builds up wall thickness.

0669 Identification of Anomalies in Welds—Advanced techniques are combined with conventional analytical methods.

0702 Thermal-Wave Microscope—Images are produced by a modified computer-controlled scanning electron microscope.

Kenaf Paper: A Forest-Saving Alternative

It is the land of cotton and dreams, where generations of farmers have turned to make a living and where generations more are yet to come.

But while cotton generally fares well in Willacy County, Texas, farming is down, oil and gas prices are down, and unemployment, at more than 15 percent, continues to climb. Some in this southern Texas county are placing their hope for better days on a fibrous crop closely related to cotton, a crop some say will not only help Willacy County with its problems but will help meet the nation's growing need for newsprint paper.

The crop is called kenaf, and its future looks as bright as cotton's was 200 years ago.

"We obviously believe it is a very good crop with an excellent future," says Charles S. Taylor, general manager of Kenaf International, a joint-venture partnership based in Bakersfield, California.

"Kenaf is a fiber that is yearly renewable. It can be grown throughout the South, where some papermills already exist to process native hardwood trees. It provides an alternative crop for farmers. It also provides an opportunity to build new mills for paper made from kenaf," he says.

Both pulpy center and fibrous exterior of bamboolike kenaf are used to produce newsprint and other fiber products.

Together with Canadian Pacific Forest Products, the second largest paper manufacturer in North America, Taylor's group expects to break ground later this year in Willacy County for a papermill that will be the first of its kind in the United States. It will take harvested kenaf fiber from the Rio Grande Valley and turn it into massive rolls of newsprint.

Kenaf International is the leader in kenaf commercialization, a relatively slow process that has picked up steam in the last 18 months. Relying on 20 years of research by USDA's Agricultural Research Service, the group hopes to make kenaf a common word among newspaper publishers across America.

There are several factors that make kenaf attractive to private industry. First, it is a fast-growing, highly productive crop. An acre of kenaf reaches a height of 15 to 18 feet in 4

Like cotton, its close relative, kenaf leaves show wide genetic variation in shape ranging from slightly to deeply lobed.

months and yields 7 to 10 tons of dry-weight fiber.

Second, kenaf produces a paper product that is as tough as wood-pulp paper but is generally brighter and more appealing to the eye and doesn't yellow quickly.

"There is also less ink rub-off with kenaf paper," says Dan Kugler, an agriculture economist and manager of USDA's Kenaf Demonstration Program. "The consumer will like that because you can read your newspaper instead of wear it."

Kenaf can tolerate salty water to a certain extent and may be successfully grown without an extensive investment in irrigation equipment. It is easy to store and requires less energy to process than wood pulp.

FOR ADDITIONAL INFORMATION: Contact Marvin O. Bagby, USDA-ARS Oil Chemical Research Unit, Northern Regional Research Center, 1815 North University St., Peoria, IL 61604 (309) 685-4011.

Lawrence Berkeley Laboratory

Low Dislocation Density GaAs Crystals Grown Using Advanced Vertical Gradient Freeze Technique

GaAs single crystals have been grown for the first time using an advanced vertical gradient freeze technique. The technique is unique in its use of a micro-processor controlled multi-heating zone furnace that allows precise and reproducible control of parameters including temperature gradients and crystal growth rate. In addition, the vessel is completely sealed, allowing the crystal growth to proceed in an arsenic atmosphere that can be controlled to achieve any desired stoichiometry of the GaAs melt and of the crystals. (Stoichiometry control has been shown to be of primary importance in reducing the density of structural defects in these crystals.)

Crystals grown using this technique by CAM researchers Edith Bourret and Joe Guitron have been shown to have a very low density of structural defects; more than half the area of wafers cut through them shows a dislocation density below 1,000/cm^2, increasing slightly towards the edges. This is to be compared with the average figure of 50,000-100,000/cm^2 in wafers from crystals produced by the Czochralski technique. Electronic characterization has shown that the electrical resistivity and the doping distribution in these wafers are very uniform, representing another significant improvement over those from crystals grown by traditional techniques. These characteristics are critical to the successful processing of gallium arsenide crystals for both opto-electronic devices and large-scale integrated circuits.

XBB 883-2258

GaAs single crystal grown using an advanced vertical gradient freeze technique. The first crystals produced at CAM were 1.5" in diameter. Facilities to grow crystals 3" in diameter are now under construction.

The crystals are produced in the shape of a cylinder of constant diameter and the periphery is smooth and free of voids or cracks. This geometry is optimum for subsequent, economical fabrication of devices.

For Additional Information:

Office of Research and Technology Application
50A 4112
Lawrence Berkeley Laboratory
Berkeley, CA 94720
Telephone (415) 486-6502

Refer to CAM Volume 2, Number 1/TN

Lawrence Berkeley Laboratory

Eight New High-Temperature Superconductors Produced by Novel Process

A new process for making high-temperature superconducting materials, developed by a scientist at the Lawrence Berkeley Laboratory, has produced an instant family of eight new superconductors-four of which become superconducting at temperatures at or above the boiling point of liquid nitrogen (77 degrees Kelvin, or -319 degrees F).

The new process utilizes high-pressure oxygen during the preparation of the compounds.

The technique yields superconductors "in bulk" (that is, in substantial quantities) and so should improve the availability of high-temperature superconductors for research and technology.

The new high-temperature superconductors developed by Donald E. Morris and his coworkers are compounds of barium, copper, and oxygen, with one additional element.

The first superconducting compound produced by the new process contained yttrium. Thin films of this compound had been made earlier by other researchers, working at Stanford University and Bell Laboratories. The LBL group found that they could substitute any of eight other so-called "rare earth" elements without losing superconductivity. However, each compound has a different transition temperature (the temperature at which superconducting behavior begins). This may help in testing theories of high temperature superconductivity.

FOR ADDITIONAL INFORMATION: Public Information Department, Lawrence Berkeley Laboratory, Berkeley, CA 94720; Telephone (415)486-5771.

Method for Preparing Vanadium

Vanadium metal is a material of great interest in several areas of high technology. It can be used to make superconducting compounds and to make cladding material for fast breeder reactors. But for both of these applications, high quality vanadium must be available. Silicon, which is present in the natural vanadium ore, may be detrimental to the use of vanadium in advanced energy

Efforts to purify vanadium of silicon have proven to be difficult and expensive. The commercial grade vanadium pentoxide generally contains 300-400 parts per million silicon, which carries over to the vanadium metal upon reduction.

Ames Laboratory metallurgists have developed a new method for purifying vanadium. It is simpler and less expensive than the competing electrorefining process, and is based on metallurgical, rather than chemical separation techniques. The new method involves the following process.

Commercial grade vanadium pentoxide, which contains silicon, iron and other impurities, is first mixed with a stoichiometric or slightly deficient amount of aluminum metal. This mixture is heated, causing a reaction that produces a vanadium-aluminum alloy containing silicon and iron impurities, along with an excess of oxygen.

This alloy is again heated to a temperature that vaporizes the aluminum and causes part of the excess oxygen to react with the silicon and form SiO. The SiO vaporizes away from the metal, thereby removing the silicon. The remaining oxygen is removed from the vanadium metal by adding calcium, which forms calcium oxide. This results in a high purity, low silicon vanadium metal.

Literature: O. N. Carlson and F. A. Schmidt, "Preparation of Low-Silicon Vanadium Metal," Proceedings of the Vacuum Metallurgy Conference on Specialty Metals, Melting and Processing, June 11-13,1984, Pittsburgh, Pennsylvania.

Patent/License Status: U.S. Patent No. 4,610,720.

Potential Application/Spinoffs: This technology is of interest to the nuclear power industry, where high purity vanadium based alloys are needed for making nuclear cladding material in fast breeder reactors and as a first wall in fusion reactors.

For More Information on this Technology: Contact Daniel E. Williams, Office of Research and Technology Application, Ames Laboratory, 119 Office and Laboratory, Iowa State University, Ames, Iowa 50011 (515)294-2635.

AL 88-03

Sandia National Laboratory

New Model Makes Glass-Fracture Predictions More Reliable

A model that explains how glass cracking and eventual failure occur for many types of glass has been developed at Sandia National Laboratories. The new model is unique because it offers a first-time explanation of how chemical reactions that modify the glass surface structure and composition can control how fast cracks grow, or whether they grow at all.

"The ability to reliably predict long-term behavior of glass will help designers produce better optical fibers, ceramic bone replacements, insulators for high-performance batteries, solar collector covers, underwater windows, and many other items made of glass or ceramics," says Terry Michalske, supervisor of Sandia's Surface Science Division. (Michalske is a recent recipient of the prestigious Woldemar A. Weyl International Glass Science Award.)

Michalske and Bruce Bunker developed the model, which has as its key an ability to explain the impact of alteration layers on long-term performance of chemically complex, commercially important glasses, such as the widely used borosilicate family.

Glass is intrinsically one of the strongest materials known. Flaw-free glass - under high-vacuum conditions - can withstand stress greater than two million pounds per square inch. "But," says Michalske, "it is almost impossible to produce a piece of glass that does not have microscopic surface flaws or cracks."

When glass is stressed, chemicals such as water can react with and rupture bonds in the silicon-oxygen-silicon glass molecules existing in microscopic surface flaws. When this occurs, cracks grow. The rate of this so-called "slow crack growth" controls the extent to which glass strength decreases with time. This reaction also can result in catastrophic "delayed failures" in which glass breaks completely after several years under stress.

An award-winning silica-glass crack-growth model developed by Michalske and Bunker in the mid-1980s predicts crack velocities as a function of stress levels and chemical environments, and reliably predicts times-to-failure for design engineers.

This early silica-glass model explains crack velocity measurements that have been under controlled conditions. "Unfortunately," says Michalske, "cracks that move fast enough to see in the laboratory are much faster than those which cause many delayed failures."

"To make lifetime predictions [10-25 years into the future] in such situations," he adds, "we often extrapolate from the minimum velocity we can measure in the laboratory - one atomic bond broken per second - to velocities that are 100,000 times slower."

While such extrapolations appear valid for silica glass, errors associated with chemically complex glasses have long plagued design engineers.

The new Michalske-Bunker model extends crack growth understanding from pure silica to more complicated glasses. "Relatively simple crack-growth models developed for pure silica are unable to predict delayed failures in complex glasses," explains Bunker, supervisor of Sandia's Electronic Ceramics Division. "That's because many chemically complex glasses show a different stress dependence for crack growth at low crack velocities than they do at high crack velocities."

For these glasses, extrapolations of measured crack growth data to lower crack velocities can lead to serious errors. "Some glasses, such as window glass, exhibit a so-called stress corrosion limit, or stress below which cracks stop growing," Bunker explains. "Other glasses crack and fail even when no stress is applied."

"For us," he continues, "the key to understanding unusual crack growth behavior of complex glasses was a realization that alteration layers can control crack growth when it occurs at low velocities."

Alteration layers form when some elements in the glass composition dissolve faster than others. For instance, reactions between a sodium borosilicate glass and water can dissolve away boron and sodium, leaving behind a porous, water-filled silica-rich layer called a "gel" layer (for its resemblance to silica gel).

Alteration layers can influence crack growth in two ways. First, glass-composition changes that occur during layer formation can cause the layer to expand or contract relative to the unaltered glass below. This creates either compressive or tensile stresses within the alteration layer.

Sandia researchers now know that borosilicate crack growth slows, and can even stop, if alteration layers develop internal compressive stresses when they form. If alteration layers are in internal tension, they literally pull themselves apart. That permits cracks to grow from surface flaws in the absence of external stresses.

Second, glass corrosion processes can change the shape of the crack tip. This can change crack growth velocities by affecting how external stresses focus on reactive bonds at the crack tip. For example, silica dissolving from the walls of a crack can redeposit at the crack tip. This blunts the tip, which makes conditions less suitable for continued crack growth.

In order to make quantitative predictions of how alteration layers influence crack growth, Bunker and Michalske conducted experiments to relate glass corrosion processes to crack propagation. The experiments involved the use of binary alkali silicate glasses, soda-lime window glass, and several sodium borosilicate glasses.

First, they measured how fast alteration layers form on glass surfaces and determined their compositions in various chemical environments. Next, they measured the amount of surface stresses generated in alteration layers as a function of time. Finally, they measured crack growth velocities in the same glasses as a function of applied stress. Results show that deviations in crack growth behavior seen at low crack velocities can be predicted for complex glasses, provided that the alteration layer properties are understood.

Because of these and other advances, models now exist which offer the promise of accurately predicting long-term performance (20 years into the future, for instance) of glass families whose crack growth speed is not governed simply by stress-activated chemical reactions between water and silicon-oxygen bonds. The models also pave the way for the development of techniques to tailor glasses that are more resistant to slow crack growth, and are more reliable and well suited for special applications.

FOR ADDITIONAL INFORMATION: Public Information Division, Code 3161, Department of Energy, Sandia National Laboratories, Albuquerque, NM 87185-5800; (505) 844-4207. Refer to announcement 24, No. 4.

NASA Tech Brief
National Aeronautics and Space Administration
Lewis Research Center, Cleveland, Ohio

Licensing Opportunity

Flexible, Polymer-Filled Metallic Conductors

Combined advantages of metals and polymers are exploited by advanced manufacturing techniques.

A procedure has been developed to make materials that are both flexible and reasonably good electrical conductors. Heretofore, electrical conductors for power and signal applications have been manufactured from pure metals and metal alloys because these materials possess the requisite electrical conductivity. Unfortunately, the repeated flexure of these metals in ordinary handling produces stress fatigue and, ultimately, mechanical failure.

Polymers that have much better flexure durability have been tried, but they are inadequate because of their very low electrical conductivity. Furthermore, because they have low thermal-decomposition temperatures, the polymers cannot be heated to a liquid state and mixed with molten metals to produce metal-organic materials that might have improved stress-fatigue properties.

In the new manufacturing procedure, a metal or a polymer sheet substrate is cleaned with a beam of energetic inert-gas ions to remove adsorbed gases and contaminants from its surface. After this cleaning, the substrate is coated by cosputter deposition of both a conductive metal and a flexible polymer. The substrate is then removed by either a mechanical or a chemical-dissolution technique, and the resulting flexible metal/polymer conductor can then be bonded at low temperature to conductor-surface contacts. Material thus produced exhibits both adequate electrical conductivity to convey power or signals and a flexibility that is superior to that of conventional metal conductors.

To demonstrate the beneficial properties of such a material, a mixture of 76 volume percent gold and 24 volume percent polytetrafluoroethylene approximately 8,000 Å thick was codeposited by ion-beam sputtering on a Kapton® polyimide substrate 0.0005 in. (12.7 μm) thick. The resulting laminate was capable of being bent (with the coating in tension) on a radius of curvature of 0.17 mm without either cracking or crazing the conductive coating. However, a 100-percent-gold coating of the same thickness was found to craze at a radius of curvature of 1.6 mm. Furthermore, the addition of the 24 percent of polymeric constituent raised the resistivity to only 3.7 times that of the pure gold.

This work was done by Bruce A. Banks and Diane M. Swec of **Lewis Research Center**. *No further documentation is available.*

Inquiries concerning rights for the commercial use of this invention should be addressed to the Patent Counsel, Lewis Research Center Refer to LEW-14161/TN

Lewis Research Center
Technology Utilization Officer: Daniel G. Soltis
Mail Stop 7-3
21000 Brookpark Road
Cleveland, OH 44135
(216) 433-5567
Patent Counsel: Gene E. Shook
Mail Code 301-6
21000 Brookpark Road
Cleveland, OH 44135
(216) 433-5753

FOR ADDITIONAL INFORMATION: *Contact: Director, Technology Transfer Division, P.O. Box 8757, BWI Airport, MD 21240; (301) 621-0100 Ext. 241*
REFER TO THE NUMBER LISTED AT THE END OF THIS ARTICLE

NASA Tech Brief
National Aeronautics and Space Administration
Goddard Space Flight Center, Greenbelt, Maryland

Licensing Opportunity

Fluoroepoxy Adhesives Bond Fluoroplastics

Etching or other special preparation is unnecessary.

Experiments have shown that some fluoroepoxy compounds of high fluorine content adhere to fluoroplastics, without prior etching or other treatment of the fluoroplastic surfaces. Previously, fluoroplastics with high fluorine contents could be bonded with epoxies or other adhesives only after severe etching, usually by a corrosive sodium/naphthalene complex. The etching weakened the surface layers and made the bonds vulnerable to degradation by moisture, oxygen, and ultraviolet light.

A representative fluoroepoxy compound could be made from a fluorodiepoxide resin cured by an adduct diamine (see figure). The adduct diamine could be made by reacting the same or a different diepoxide with an excess of ethylenediamine. Other curing agents — for example, 3,3,4,4,5,5,6,6-octafluorooctamethylenediamine — could be used, as long as it is compatible with the particular fluoroepoxy resin.

The use of fluoroepoxies is most advantageous in bonding polymers that have fluorine contents of 55 percent or more; for example, polytetrafluoroethylene (76 weight percent fluorine). Almost any of the variety of suitable fluorinated epoxy resins and curing agents can be selected. The main requirement is to obtain adherence without the need for treatment of the surface, and the experiments show that this is achieved by using an epoxy compound with a fluorine content of at least 46 weight percent.

While higher fluorine contents are clearly advantageous in fluoroepoxies used to bond fluoroplastics with high fluorine contents, they are less advantageous in fluoroepoxies used to bond fluoroplastics with lower fluorine contents. For example, in experiments on an ethylene/tetrafluoroethylene copolymer that contains 54.4 percent fluorine, a commercial nonfluorinated epoxy bonded somewhat more strongly [tensile strength of 743 ± 142 psi (5.12 ± 0.99 MPa)] than three fluoroepoxies [tensile strengths of 573 ± 160, 586 ± 188, and 567 ± 200 psi (3.95 ± 1.10, 4.04 ± 1.29, and 3.91 ± 1.38 MPa), respectively].

Depending on the specific parts to be bonded and the curing process desired, either or both the fluoroepoxy resin and curing agent chosen could be liquid or solid. For example, to make a laminate of large area, a mixture of solid resin and solid curing agent could be pressed between the layers to be bonded and heated to make the compounds react. In this case, one of the main requirements is that at some time during the process the fluoroepoxy compound be sufficiently liquid or at least able to flow under pressure and wet the surfaces of the fluoroplastic parts.

This work was done by Sheng Yen Lee of **Goddard Space Flight Center.**

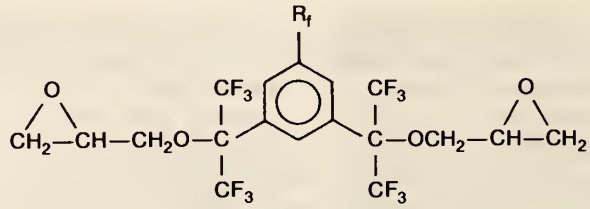

FLUORODIEPOXIDE RESIN

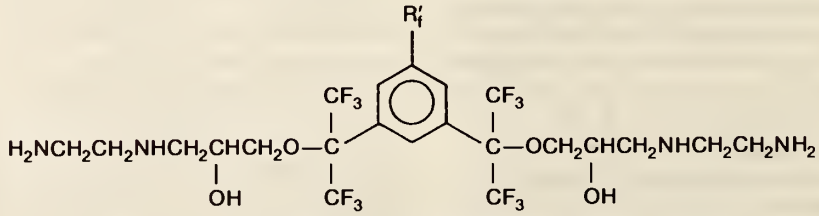

ADDUCT DIAMINE CURING AGENT

These **Compounds Are Mixed With Each Other** in approximately stoichiometric amounts and react to produce fluoroepoxy compounds that adhere to fluoroplastics. The fluorine content is governed primarily by the selection of R_f and R'_f, which are perfluoroalkyl groups of general formula C_nF_{2n+1} (where n is an integer).

This invention is owned by NASA, and a patent application has been filed. Inquiries concerning nonexclusive or exclusive license for its commercial development should be addressed to the Patent Counsel, Goddard Space Flight Center Refer to GSC-13072/TN

Goddard Space Flight Center
Technology Utilization Officer: Donald S. Friedman
Mail Code 702
Greenbelt, MD 20771
(301) 286-6242
Patent Counsel:
R. Dennis Marchant
Mail Code 204
Greenbelt, MD 20771
(301) 286-7351

NASA Tech Brief
National Aeronautics and
Space Administration

NASA's Jet Propulsion Laboratory, Pasadena, California

Low-Thermal-Expansion Filled Polytetrafluoroethylene

PTFE would be made thermally compatible with aluminum without changing its dielectric constant.

According to a proposal, polytetrafluoroethylene (PTFE) would be manufactured with fillers and pores to reduce its coefficient of thermal expansion by a factor of 6 to match that of aluminum. The new material would retain the 2.1 dielectric constant of pure PTFE.

Heretofore, the great difference in expansion rates precluded the use of PTFE insulation in aluminum coaxial connectors, unless temperature could be restricted to a narrow range. Previous efforts to reduce the thermal expansion of PTFE also changed the dielectric constant, and the resulting material therefore could not be used as a direct substitute for pure PTFE in existing designs for 50-Ω coaxial connectors. For example, the addition of 50 percent mica or silica filler to reduce thermal expansion increases the dielectric constant to about 3.7. The introduction of micropores to reduce the expansion also decreases the dielectric constant to 1.5.

The new material combines the filler and micropore concepts. The filler and micropores are expected to function synergistically; less filler and fewer micropores should be needed than if either were used alone to reduce the thermal expansion.

Particles of mica, fused silica, or other suitable low-expansion material would be blended with finely-ground hydrocarbon powder and powdered PTFE. The mixture would be heated to fuse the PTFE granules and the filler particles with the PTFE. With continued heating to a temperature not to exceed 550 °F (288 °C) (the maximum usable temperature of PTFE), the hydrocarbons would evaporate and escape from the PTFE matrix, leaving interconnected voids (see figure). Because the fillers and voids increase and decrease the dielectric constant, respectively, the amounts of each can be chosen to leave the dielectric constant unchanged.

From previous experience, it is known that the mica particles accept the compression forces created when the PTFE shrinks at low temperatures. At high temperatures, the PTFE becomes pliable, and the voids take up the excess volume so that the PTFE does not exert excessive tensile forces on the mica particles. With the blending of suitable proportions of the two fillers, it should be possible to balance these effects so that the filled, porous PTFE will have the correct dielectric constant and subject aluminum parts to little or no tensile or compressive stress as it shrinks or expands with falling or rising temperatures.

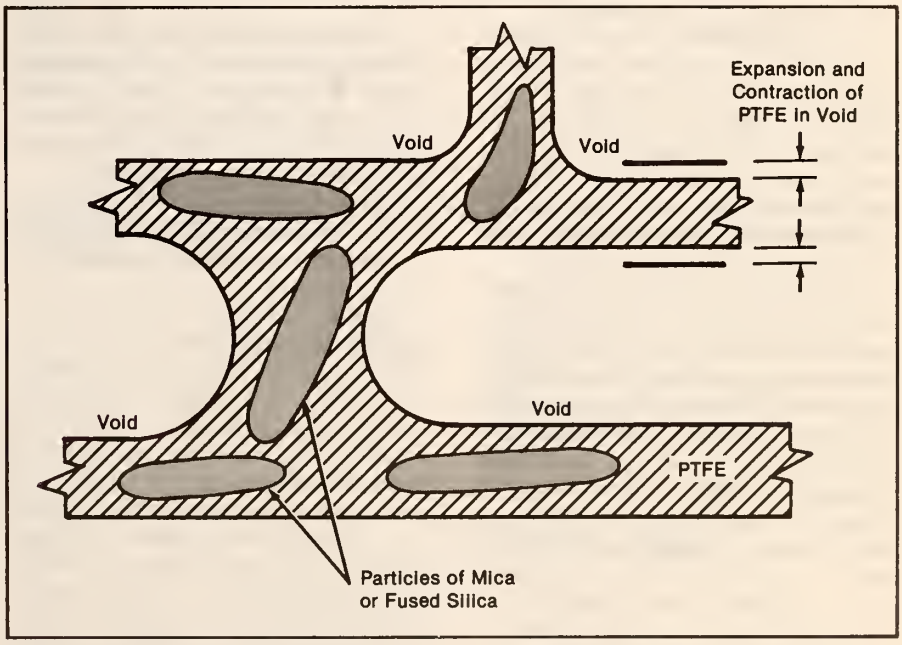

Particles and Voids embedded in the PTFE matrix function cooperatively. The particles take up compressive stress imposed by contracting PTFE, and the voids take up the expanding material. The particles increase the dielectric constant, while the voids reduce it.

This work was done by Sanford S. Shapiro of Hughes Aircraft Co. for **NASA's Jet Propulsion Laboratory**.

NPO-17189 /TN

FOR ADDITIONAL INFORMATION: *Contact: Director, Technology Transfer Division, P.O. Box 8757, BWI Airport, MD 21240; (301) 621-0100 Ext. 241*
REFER TO THE NUMBER LISTED AT THE END OF THIS ARTICLE

NASA Tech Brief
National Aeronautics and
Space Administration
Marshall Space Flight Center, Alabama

Multiple-Purpose Rigid Foam Insulation

Properties can be adapted to a variety of demanding applications.

A plastic foam promises to serve as a multiple-purpose thermal insulation. On the Space Shuttle (for which it was developed), the material can replace every insulating material on the external fuel tank, ranging from general surface insulation to ablative insulation on small areas subject to high aerodynamic heating. It can also be used on closeouts, ramps, and repairs. The material costs less than those currently used, but offers higher thermal resistance, greater strength, and lower weight.

The material is a rigid, closed-cell, thermally stable foam of urethane-modified isocyanate. It is made by reacting a polyol mixture with a polymeric diphenyl methane diisocyanate in the presence of a catalyst and a fluorocarbon blowing agent. Its properties can be customized for a particular application by adjusting the proportions of the ingredients in the polyol mixture.

The polyol mixture consists of a reactive flameproofing agent (15 to 30 percent by weight of the polyol mixture), a nonreactive flameproofing agent (10 to 40 percent), a nonhydrolyzable silicone copolymer (10 to 40 percent), and an amine-initiated polyether resin (3 to 16 percent). The catalyst consists of any two of the following compounds: a tertiary amine, an alkali metal salt organotin, or a quaternary ammonium salt.

The density of the cured insulation ranges from 2.4 to 3.5 lb/ft^3 (38 to 56 kg/m^3). Its flatwise tensile strength is 65 to 85 lb/in.^{2} (0.45 to 0.59 MPa) at room temperature. Its bond strength is 50 to 70 lb/in.^{2} (0.34 to 0.48 MPa). The material performed well in simulated ascent and reentry heating environments.

This work was done by Matthew T. Liu of Martin Marietta Corp. for **Marshall Space Flight Center**.

Title to this invention has been waived under the provisions of the National Aeronautics and Space Act [42 U.S.C 2457(f)], to the Martin Marietta Corp. Inquiries concerning licenses for its commercial development should be addressed to

Patrick M. Hogan
Assistant General Counsel Patents
Martin Marietta Denver Aerospace
P.O. Box 179
Denver, CO 80201

Refer to MFS-28264/TN

George C. Marshall Space Flight Center
Technology Utilization Officer: Ismail Akbay
Code AT01
Marshall Space Flight Center,
AL 35812
(205) 544-2223
Patent Counsel:
Leon D. Wofford, Jr.
Mail Code CC01
Marshall Space Flight Center,
AL 35812
(205) 544-0024

FOR ADDITIONAL INFORMATION: *Contact: Director, Technology Transfer Division, P.O. Box 8757, BWI Airport, MD 21240; (301) 621-0100 Ext. 241*
REFER TO THE NUMBER LISTED AT THE END OF THIS ARTICLE

NASA Tech Brief
National Aeronautics and Space Administration
Marshall Space Flight Center, Alabama

Licensing Opportunity

Polymer Coatings Reduce Electro-osmosis

Poly(ethylene glycol) film controls the ζ potential.

Electro-osmosis in quartz or glass chambers can be reduced or reversed by coating the inside surfaces of the chambers with monomacromolecular layers of poly(ethylene glycol). Because the new polymer coats are nontoxic, transparent, and neutral, they are advantageous for use in electrophoresis. The new coats are stable over long times. In contrast, methylcellulose, which is also effective in suppressing electro-osmosis on glass surfaces, desorbs during long storage periods.

The ζ potential (the electrostatic potential across the surface) of an untreated glass or plastic chamber used in electrophoresis is negative and attracts cations in an aqueous electrolyte. Because the cations are solvated, they entrain a flow of electrolyte as they migrate toward the cathode. This electro-osmotic flow interferes with the desired electrophoresis of particles suspended in the electrolyte.

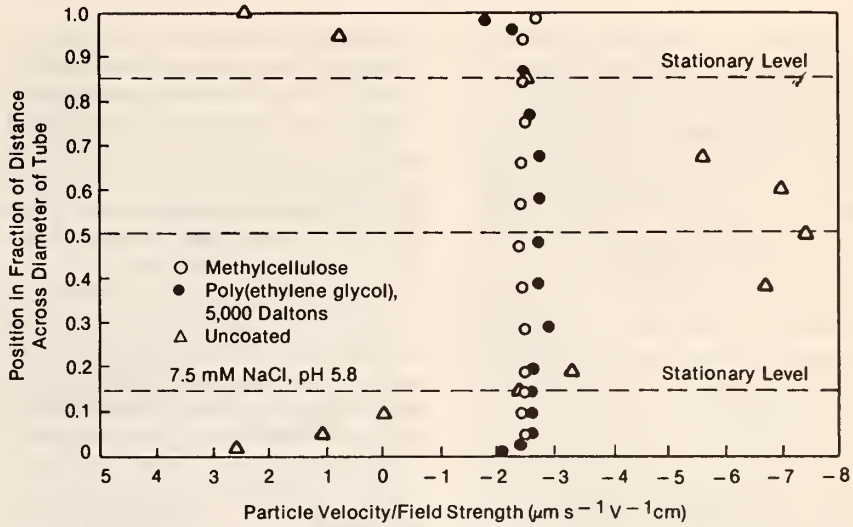

The **Degree of Electro-osmosis** in coated and uncoated capillary tubes is indicated by the approximately parabolic curvature in the plot of axial particle velocity versus position across the diameter of the tube.

The polymer coat is attached covalently to the surface. It suppresses electrophoresis by reducing, or eliminating, the ζ potential. The degree of change in the ζ potential depends on (and can presumably be controlled by varying) the composition, structure, molecular weight, and surface density of the bound molecules.

The effects of electro-osmosis and the suppression of electro-osmosis during electrophoresis are best observed in narrow quartz capillary tubes with closed electrode ends, containing charged polystyrene-latex particles suspended in a dilute salt solution. As the particles migrate at a characteristic velocity per unit applied electric field (defined as the particle electrophoretic mobility), the combination of electrophoresis, the electro-osmotic flow of liquid along the wall, and the compensating return flow of liquid along the center of the tube causes a parabolic distribution of particle velocities across the tube. Only at the stationary level, where the electro-osmotic flow is zero, is the apparent mobility of a particle due entirely to electrophoresis.

The figure shows the results of such experiments in quartz tubes with various interior-surface treatments. A coat of methylcellulose and one of poly(ethylene glycol) of molecular weight 5,000 daltons produced nearly-flat velocity profiles, indicating nearly total elimination of electro-osmosis. A similar result was obtained with a poly(ethylene glycol) coat of molecular weight 20,000 daltons (not shown).

The new poly(ethylene glycol) coats should be useful in controlling ζ potentials over a wide range of pH and making beads of varying electrophoretic mobility. Chambers of varying electro-osmosis could also be produced for use in continuous-flow electrophoresis where optimum results are achieved by balancing electro-osmotic and Poiseuille flows. The suppression of electro-osmosis would enhance isoelectric focusing and analytical particle microelectrophoresis.

This work was done by Blair J. Herren and Robert Snyder of **Marshall Space Flight Center** *and Steven G. Shafer and J. Milton Harris of the University of Alabama and James M. Van Alstine of the Universities Space Research Association.*

In accordance with Public Law 96-517, the contractor has elected to retain title to this invention. Inquiries concerning rights for its commercial use should be addressed to

The University of Alabama, Huntsville
Department of Chemistry
Huntsville, AL 35899
or
Universities Space Research Association
American City Building, Suite 311
Columbia, MD 21044

Refer to MFS-26050/TN

George C. Marshall Space Flight Center
Technology Utilization Officer: Ismail Akbay
Code AT01
Marshall Space Flight Center,
AL 35812
(205) 544-2223
Patent Counsel: Leon D. Wofford, Jr.
Mail Code CC01
Marshall Space Flight Center,
AL 35812
(205) 544-0024

FOR ADDITIONAL INFORMATION: *Contact: Director, Technology Transfer Division, P.O. Box 8757, BWI Airport, MD 21240; (301) 621-0100 Ext. 241*
REFER TO THE NUMBER LISTED AT THE END OF THIS ARTICLE

NASA Tech Brief
National Aeronautics and
Space Administration
Langley Research Center, Hampton, Virginia

Soluble Aromatic Polyimides for Film Coating

Films are nearly colorless and soluble and exhibit good mechanical properties.

Because of their toughness, flexibility, and remarkable thermal stability, linear all-aromatic polyimides are excellent candidate film and coating materials for advanced electronic circuitry and wires. However, the inherent insolubility of these polymers has somewhat limited their usefulness for electronic applications. A recent study determined the effects on solubility of changing isomeric points of attachment of phenoxy units in the diamine portions of several all-aromatic polyimides. Hexafluoropropane- and oxygen-containing dianhydrides (6FDA and ODPA) were used because of their known value in contributing to the stability of polyimides. The aromatic diamines used were varying isomers of oxydianiline (ODA) and bis(aminophenoxy)benzene.

Reactions of monomers yielded pale-yellow-to-colorless polyamic acid solutions. Tough, flexible, transparent films were produced by thermally converting the polyamic acids to polyimides at 300 °C in air. Films ranged in color from light yellow to essentially colorless, depending on thickness. The glass-transition temperatures (T_g) of films increased within each series of polymers as the linkages of the aromatic diamines were varied from all meta to all para. Polyimides prepared with 6FDA consistently displayed higher T_g than did ODPA dianhydride-containing polymers with the same diamines.

Polymers prepared with ODPA dianhydrides were less soluble overall than those prepared with 6FDA, which were exceedingly soluble in the solvents used. The solubility increased with the incorporation of meta isomerism or ortho isomerism, which serves to create more "kinks" and dissymmetry in the polymer chains. The same trend was observed to a lesser degree in films containing ODPA.

Ortho isomerism appeared to have a greater effect on the solubility of ODPA films than did meta isomerism. Polymers prepared with 3,3′-ODA and 2,4′-ODA were found to be readily soluble at greater than 30- to 40-percent solids at room temperature in amide solvents. These polyimides are also readily soluble in chlorinated solvents and other low-boiling-temperature solvents. They can therefore be spray-coated onto desired substrates in the fully imidized form, eliminating the need to heat the substrates.

These soluble, phenoxy-linked polyimides yield tough, flexible, colorless-to-pale-yellow transparent films from amide or chlorinated solvents. Their potential for electronic applications should be excellent.

This work was done by Anne K. St. Clair and Terry L. St. Clair of **Langley Research Center**. *Further information may be found in NASA TM-89016 Price Code: A02 [N87-16911/NSP], "Soluble Aromatic Polymides for Film Coating Applications."*

Copies may be purchased from the National Technical Information Service, Springfield, Virginia 22161, Telephone No. (703) 487-4650. Rush orders may be placed for an extra fee by calling (800) 336-4700. LAR-13700/TN

FOR ADDITIONAL INFORMATION: *Contact: Director, Technology Transfer Division, P.O. Box 8757, BWI Airport, MD 21240; (301) 621-0100 Ext. 241*
REFER TO THE NUMBER LISTED AT THE END OF THIS ARTICLE

NASA Tech Brief
National Aeronautics and Space Administration

Polymer Lubricants for Use in Vacuum

Both solid and film polyimides offer low friction and wear.

A report describes tests of the lubricating properties of 10 polymer-based materials — in particular, polyimides — in vacuum. Lubricant researchers previously noticed that the friction and wear of some polyimide films had dropped dramatically when the materials were heated in air. They postulated that the improvement was due to the thermal desorption of water vapor. Because water vapor would desorb in vacuum even at low temperature, polyimides might be good candidates for vacuum lubricants.

Commercially available materials, in the forms of solid bodies and films on metals, were tested on a pin-on-disk apparatus in a vacuum. Similar tests were also done in an air atmosphere at 50 percent relative humidity.

The following materials were evaluated:

1. A polyphenylene sulfide (PPS) disk reinforced with 40 percent of graphite fibers;
2. A poly(amide/imide) disk with polytetrafluoroethylene (PTFE) and graphite-powder additives;
3. A commercial polyimide with no additives;
4. A PMR-15 polyimide with 70 percent of PTFE powder added;
5. A polyimide made from the diamine 2,2-bis [4-(aminophenoxy)phenyl]-hexafluoropane (4-BDAF) and pyromellitic acid dianhydride (PMDA) (for short this polyimide is called "100 PMDA");
6. A copolyimide made from 4-BDAF and a combination of 80 mole percent of PMDA with 20 mole percent of benzophenonetetracarboxilic acid dianhydride (BTDA) (for short denoted as 80 PMDA/20 BTDA);
7. An 80 PMDA/20 BTDA polyimide reinforced with 50 percent of high-modulus graphite fibers;
8. A film of 100 PMDA polyimide;
9. A film of PI-4701 polyimide; and
10. A film of PI-4701 polyimide with 50 weight percent graphite fluoride, a solid lubricant.

All the polymer materials except the 80 PMDA/20 BTDA polyimide with 50 percent graphite fibers and the 100 PMDA solid and film produced lower coefficients of friction in vacuum than in air. Only the polyimides without solid-lubricant additives showed substantially-lower steady-state wear rates in vacuum than in air.

The best low-wear, low-friction material was the 80 PMDA/20 BTDA solid-body polyimide. The friction and wear properties of most of the polyimides were so good in vacuum that solid-lubricant additives were not necessary. In fact, powdered solid-lubricant additives tended to produce weak points where cracks and spallation could start under sliding contact.

Polymers containing graphite fibers did not wear well in vacuum. The fibers on the surface tended to crack and debond during sliding.

Although the 100 PMDA polyimide produced high friction in vacuum, its wear was low. It therefore may be suitable for traction drives in vacuums.

This work was done by Robert L. Fusaro of **Lewis Research Center**. *Further information may be found in NASA TM-88966 [N87-17906], Price Code A03 "Tribological Properties of Polymer Films and Solid Bodies in a Vacuum Environment."*

Copies may be purchased from the National Technical Information Service, Springfield, Virginia 22161, Telephone No. (703) 487-4650. Rush orders may be placed for an extra fee by calling (800) 336-4700. LEW-14661/TN

FOR ADDITIONAL INFORMATION: *Contact: Director, Technology Transfer Division, P.O. Box 8757, BWI Airport, MD 21240; (301) 621-0100 Ext. 241*

REFER TO THE NUMBER LISTED AT THE END OF THIS ARTICLE

NASA Tech Brief
National Aeronautics and
Space Administration
NASA's Jet Propulsion Laboratory, Pasadena, California

Measuring Fracture Times of Ceramics

Electrical measurements complement or replace fast cinematography.

A relatively simple electronic system measures the microsecond time intervals between the impacts of projectiles on ceramic tiles and the fracture of the tiles. The instrumentation is used in research on ceramics and ceramic-based composite materials such as armor. The hardness and low density of ceramics enable them to disintegrate projectiles more efficiently than metals can. However, the ceramics also disintegrate in the process, and research on ceramic armor depends on the accurate measurements of the intervals between impacts and disintegrations to ensure that the energies of the projectiles can be fully dissipated. High-speed cameras have been used to measure the intervals, but they are not precise or fast enough in the microsecond range.

The instrumentation includes a patterned resistive film on the ceramic specimen, a triggering switch, break-detection circuitry, and an oscilloscope (see figure). The triggering device detects the projectile at the instant of impact and signals the oscilloscope to start measuring time. As cracks propagate through the ceramic, they cut through the resistive film, increasing its resistance. The break-detection circuit senses the increase and increases the voltage to the oscilloscope proportionately. The oscilloscope thus generates a plot of the increasing resistance between impact and final disintegration during an interval of a few microseconds. The trace data are recorded on magnetic diskettes and on photographs of the oscilloscope traces.

The resistive film is formed by photolithography. First, an insulating layer of amorphous silicon 3,000 Å thick is deposited on the surface of the ceramic specimen. A layer of aluminum or titanium, also 3,000 Å thick, is deposited on the silicon by evaporation. A layer of photoresist is applied to the metal film and exposed to a pattern of concentric convoluted lines. The pattern is etched into the photoresist and into the metal film below it, leaving concentric convoluted arcs of metal on the ceramic. As the ceramic breaks after impact, the lines are cut progressively.

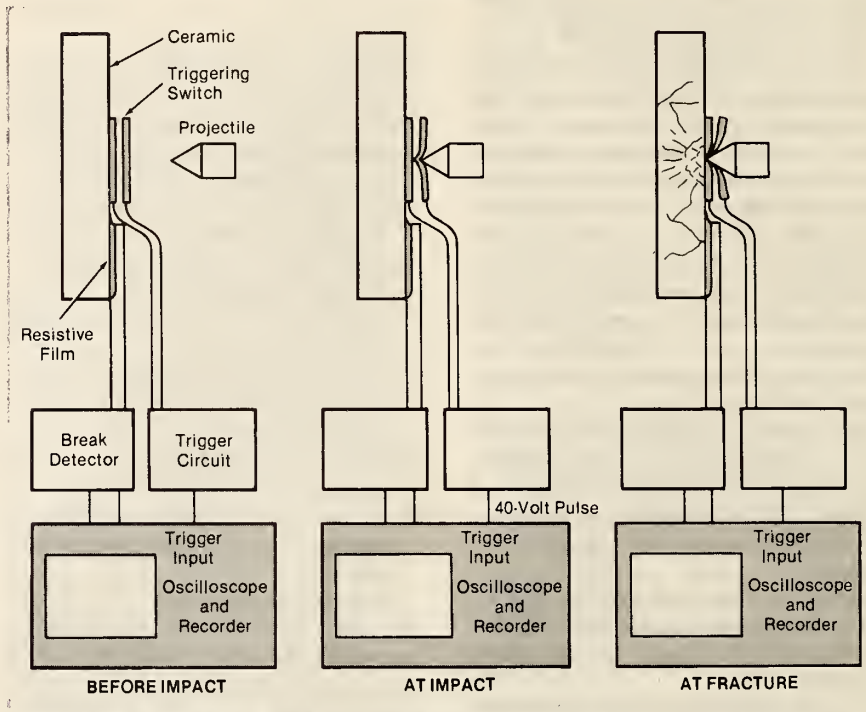

A **Projectile Approaches** a ceramic tile specimen (left). Penetrating the foil squares of a triggering device, it activates the display and recording instruments (center). As the ceramic and resistive film break, the oscilloscope plots the increase in the electrical resistance of the film (right).

Eight break-detection circuits monitor the integrity of segments of the metal lines. Each circuit generates a negative 5.6-V signal for the oscilloscope when its associated segment is broken.

The triggering switch consists of two squares of copper foil separated by an air-gap of 0.02 in. (0.5 mm). One square is bonded to the face of the specimen. When the projectile strikes the other square, it closes the gap, sending a 40-V pulse to the instrumentation to start the measurement of time.

This work was done by Paul J. Shlichta, Leo Bister, and Donald G. Bickler of Caltech for **NASA's Jet Propulsion Laboratory**. *NPO-16738 /TN*

FOR ADDITIONAL INFORMATION: *Contact: Director, Technology Transfer Division, P.O. Box 8757, BWI Airport, MD 21240; (301) 621-0100 Ext. 241*
REFER TO THE NUMBER LISTED AT THE END OF THIS ARTICLE

NASA Tech Brief
National Aeronautics and
Space Administration
Lewis Research Center, Cleveland, Ohio

Ultrasonic Detection of Transply Cracks in Composites

The densities and propagation of cracks are measured nondestructively.

A nondestructive testing technique measures the densities of transply cracks and can be used to monitor the propagation of such damage in advanced polymer-matrix composite materials. The development of this technique was motivated by the requirement, particularly in aerospace applications, for dimensional stability and the absence of cracks. Cracks reduce mechanical strength and expose fibers and interfaces to environmental (moisture and thermo-oxidative) effects.

Graphite/polyimide composites are now replacing metals in zones of moderately high temperatures (up to 316 °C) in jet engines. These types of applications will introduce thermal cycling in the composite structural materials. This, in turn, can produce transply cracks, the numbers of which can increase with time to significant levels. Because these transply cracks are undesirable, nondestructive testing techniques are needed to monitor structural parts to confirm the integrities of the structures during the expected operational lifetimes.

For a demonstration of the new technique, transply cracks were introduced into tensile specimens of cross-plied (0°/90°) unidirectional tape and fabric prepreg material. In both cases, the reinforcements were graphite fibers. The cracks were introduced by loading the specimens at various loads below the experimentally-determined failure load.

An acousto-ultrasonic measuring apparatus, shown in Figure 1, was used to measure stress-wave factors (SWF's) of undamaged specimens and specimens that contained various numbers of transply cracks. Time was partitioned into 5-ms intervals and frequency into 1.285-MHz bands. SWF measurements were taken at seven different crack densities. Figure 2 shows the results of linear least-squares fits to the data from both types of specimens. The acousto-ultrasonic technique is of value because it can be used to examine damage to the material from one surface only. Access to both sides of a structure is not necessary and is normally not easily obtained.

It was found that the SWF decreased with increasing density of cracks. The woven fabric is less attenuating than is the cross-plied, unidirectional, reinforced material, and, at high crack densities, the attenuation is about the same in the two materials. From the data that were examined, it was concluded that not only can the acousto-ultrasonic technique be employed to assess changes in the densities of transply cracks during the lifetimes of composite structures but also that the SWF has potential utility as a measure of the number of transply cracks in a damaged structure.

This work was done by Kenneth J. Bowles, Harold Kautz, John H. Hemann, and Paul Cavano of **Lewis Research Center**. *Further information may be found in NASA TM-100224 [N88-11758], Price Code: A02 "Transply Crack Density Detection by Acousto-Ultrasonics."*

Copies may be purchased from the National Technical Information Service, Springfield, Virginia 22161, Telephone No. (703) 487-4650. Rush orders may be placed for an extra fee by calling (800) 336-4700. *LEW-14700/TN*

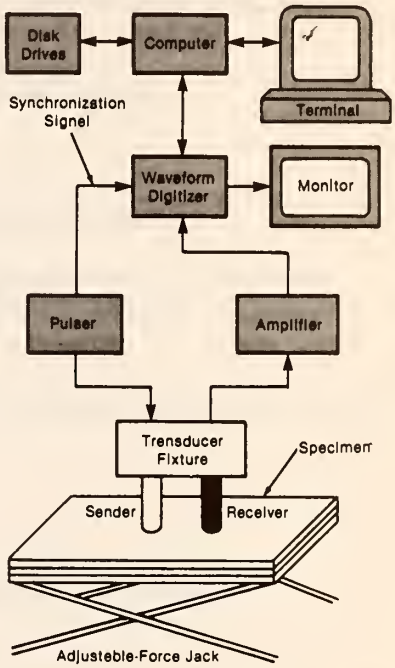

Figure 1. An **Acousto-Ultrasonic Apparatus** operates under the control of a computer, which interprets the ultrasonic measurements in terms of the density of transply cracks in a specimen.

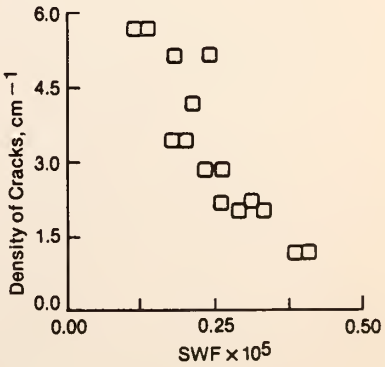

Figure 2. This **Linear Least-Squares Fit** to data from measurements at various crack densities shows that the stress-wave factor is related to the density of cracks.

FOR ADDITIONAL INFORMATION: *Contact: Director, Technology Transfer Division, P.O. Box 8757, BWI Airport, MD 21240; (301) 621-0100 Ext. 241*
REFER TO THE NUMBER LISTED AT THE END OF THIS ARTICLE

Medicine & Biology

0685 Method Developed for Locating a Small Magnetic Object in the Human Body

0686 Clues Found to Infectivity of Herpes Simplex Virus

0687 Naval Dental Research Institute Studies Potential Etiologic Agents of Periodontitis

0688 Laboratory Animal Resource for Biomedical Research

0689 Navy Develops New Wound Dressing

0690 Mouse Model Resource for Human Inherited Diseases

0691 Mandrels for Microtextured Small-Vessel Implants—A surface-relief pattern should encourage growth of a healthy neointima. (Licensing Opportunity)

0692 Multimembrane Bioreactor—Metabolizing cells are well nourished while inhabiting products are removed.

Other Items of Interest

0619 Bacterium Produces a Sugar Never Before Found in Nature

Method Developed for Locating a Small Magnetic Object in the Human Body

A piece of a thin acupuncture needle lodged under the right scapula of a patient could not be found in surgical procedures accompanied by studies of 30 standard X-ray images. To locate it, we mapped the magnetic field component normal to a plane lying above the object, using a superconducting quantim interference device (SQUID). Assuming that the needle could be modelled as a magnetic dipole, we were able to infer its lateral position, depth, orientation, and magnetic moment. With this information, directed CT scans, high-resolution X-ray films, and the subsequent surgical removal of the needle proved that it could be located in the body with an accuracy of about three millimeters.

A technique to detect and locate with millimeter precision magnetic objects in the human body has been developed. This procedure may be advantageous for applications as localizing magnetic objects causing discomfort, with the prospect of subsequent surgical removal, and for detecting magnetic objects prior to exposure to strong magnetic fields as when recording data for MR images. The object in the study was a portion of an acupuncture needle, lodged under the right scapula of a patient. The technique has general applicability to objects in other locations, so long as the magnetic field they produce is sufficiently strong. The technique mans the magnetic field normal to a plane above the object and from the measured field pattern deduces the lateral position, depth, orientation, and magnetic moment of the equivalent magnetic dipole.

The instrument having the highest sensitivity for low-frequency measurements of magnetic field is the SQUID (Superconducting QUantum Interference Device), commonly used for studies of the weak magnetic fields associated with the human body. The superconducting sensing elements of the SQUID magnetometer must be maintained in a vacuum-insulated container, or dewar, that contains liquid helium for low-temperature operation. The magnetic field is sensed by a detection coil that is part of a closed superconducting loop, which has the property that when a field is applied to the detection coil an electrical current is set up in the loop. A part of this loop is coupled magnetically to the SQUID. The SQUID's response is registered as an output voltage from room temperature electronics. The inherent sensitivity of such a field sensor is about 20×10^{-15} tesla for a 1-hertz bandwidth. By comparison, the earth's steady magnetic field is about 70×10^{-6} tesla. However, the sensitivity of the method for measurements of stead fields is limited by low-frequency

variations of the ambient field. The detection coil of our sensor had the geometry of a second-order gradiometer to reduce its sensitivity to ambient noise fields, which are comparatively uniform in space.

Analysis of the data was carried out by two methods. The first depended upon identifying the positions of the positive and negative field extrema, as well as determining the values of the field at these extrema. This information is sufficient to determine the three position coordinates of the dipole, the two angles specifying its orientation, and the moment specifying its strength. A second method was based on using a computer routine to determine the least-squares fit to the field pattern. The deduced positions of the dipole determined by the two methods agreed to better than 3 mm, with the least-squares method being more accurate. If the position is determined relative to reference points marked on the skin, a much greater error can be introduced from movement of the skin relative to underlying tissue. In such cases, either method of determining the source may be satisfactory.

FOR ADDITIONAL INFORMATION: A copy of this report is available from NTIS, Springfield, VA 22161; (703) 487-4600.
NTIS order number: AD-A193361/NAC
Price code: A02

NIH
Research & Technology
U.S. Department of Health and Human Services Public Health Service National Institutes of Health

Clues Found to Infectivity of Herpes Simplex Virus

Glycoprotein D (gD), which is found on the surface of herpes simplex virus type 1 (HSV-1), appears to play a role in virus entry and infection of cells, according to researchers at the University of Michigan Medical School in Ann Arbor. This protein is one of at least seven virus-encoded surface glycoproteins—proteins linked with carbohydrates—that may be important for HSV infection and immunity, they say.

Herpes simplex virus infections range from relatively harmless infections of skin, lips, and genitals to more serious cases of neonatal herpes and rare cases of encephalitis, or brain infection. Determining how glycoprotein-specific antibodies interfere with virus replication may lead to an understanding of the structure and biology of HSV and ultimately help prevent herpesvirus infections, according to Dr. Joseph C. Glorioso, assistant dean for research and graduate studies and professor of microbiology and immunology at the University of Michigan at Ann Arbor.

"This molecule has received considerable attention because it is thought to play a role in virus penetration of the plasma membrane that surrounds a cell and in its subsequent replication. It also is a primary target for neutralizing antibodies," he says.

Working in the department of microbiology and immunology and the unit for laboratory animal medicine, Dr. Glorioso, research associate Dr. Steven L. Highlander, and graduate student Philip J. Gage use gD-specific monoclonal antibodies to define the glycoprotein's antigenic structure and determine how structural areas called epitopes contribute to virus infectivity. An antigen is any substance that stimulates an immune response such as production of antibodies or activation of certain types of lymphocytes. Monoclonal antibodies are especially suited to studying immune responses because of their high specificity and uniformity. All molecules of a particular monoclonal antibody are identical because they are all derived from one immune cell.

The HSV particle is composed of an outer lipoprotein envelope enclosing DNA and proteins. Infection starts when HSV attaches to the surface of susceptible cells. Following attachment the viral envelope appears to fuse with the cellular plasma membrane and the uncoated virus enters the cytoplasm of the cell. In the cytoplasm viral proteins and DNA separate, and the DNA enters the cell nucleus to initiate production of new viral DNA and virus particles.

The Michigan researchers produced a series of monoclonal antibodies against gD and studied how the antibodies interfered with virus infection of

Dr. Joseph C. Glorioso, professor of microbiology and immunology at the University of Michigan, Ann Arbor, is studying how herpes simplex virus type 1 infects cells. By immunochemical and genetic engineering techniques he maps sites on the viral protein glycoprotein D that are important for viral entry into cells.

cultured cells. Four of the antibodies were able to neutralize the virus—prevent its replication—both before and after HSV had attached itself to the cell surface, suggesting that they might interfere with viral penetration of the plasma membrane. In support of this conclusion, Dr. Glorioso and his colleagues also found that the antibodies slowed the rate of viral entry into the cells.

To study which parts of the gD molecule the antibodies recognized, or bound to, Dr. Glorioso and his colleagues generated HSV mutants called "mar" (*m*onoclonal *a*ntibody *r*esistant) mutants that were no longer neutralized by the antibodies. As some of the monoclonal antibodies were directed against different epitopes and others against identical ones, the investigators could distinguish the epitopes on the gD molecule that are critical for viral infectivity by comparing the patterns of each antibody's inhibition of the mar mutants and the wild-type virus.

The researchers generated the individual mutants by propagating the HSV in cultured cells in the presence of each of the antibodies. "If a particular neutralizing monoclonal antibody is placed in culture with HSV, the wild-type virus is inactivated and surviving virus is necessarily neutralization-resistant because it is mutant in the antibody recognition site or epitope. By determining the different recognition patterns of all the mar mutants with each of the antibodies, antibodies with similar reactivity patterns or epitope specificities can be identified and their corresponding epitopes can be grouped to define epitope clusters referred to as antigenic sites," Dr. Glorioso explains.

Epitopes are composed of particular amino acids that interact with the monoclonal antibody's binding site. In a mar mutant glycoprotein D, a critical amino acid required for the antibody to recognize and bind to the gD antigen has been changed. Consequently it is unable to neutralize the virus.

On the basis of these findings, the investigators concluded that the gD molecule contains at least four antigenic sites that are important for virus penetration of the plasma membrane. When they blocked penetration, other manifestations of virus infection such as cell lysis, measured by a procedure called plaque formation, were not seen. "The ability of the antibody to neutralize virus comes about by blocking initial infectivity. In stopping penetration you are also stopping plaque formation and cell to cell infection," explains Dr. Highlander. "Recent data suggest that gD may interact with 'something cellular,' perhaps a receptor, for successful penetration," Dr. Glorioso adds.

Experiments are now under way to locate the antigenic sites on the gD molecule. Dr. Glorioso suspects that the major neutralizing site for antibodies is near the middle of the molecule, but a complete immunochemical and structural analysis is required before an assignment can be made.

In these studies the Michigan investigators are using genetic engineering methods to shorten the viral gene that encodes gD. By producing HSV mutants containing gD molecules of different lengths and monitoring how well they interact with particular monoclonal antibodies, the researchers identify which part of the molecule is important for antibody recognition. "If we test the virus mutants and find that antibody reactivity is lost, we can pinpoint a place on the protein that is critical to antibody binding. Using smaller and smaller polypeptides we can thus locate antigenic sites involved in viral infection," Dr. Glorioso explains.

Additional reading:

1. Ligas, M. W. and Johnson, D. C., A herpes simplex virus mutant in which glycoprotein D sequences are replaced by B-galactosidase sequences binds to but is unable to penetrate into cells. *Journal of Virology* 62:1486–1494, 1988.

2. Campadelli-Fiume, G., Arsenakis, M., Farabegoli, F., and Roizman, B., Entry of herpes simplex virus 1 in BJ cells that constitutively express viral glycoprotein D is by endocytosis and results in degradation of the virus. *Journal of Virology* 62:159–167, 1988.

3. Highlander, S. L., Sutherland, S. L., Gage, P. J., Johnson, D. C., Levine, M., and Glorioso, J. C., Neutralizing monoclonal antibodies specific for herpes simplex virus glycoprotein D inhibit virus penetration. *Journal of Virology* 61:3356–3364, 1987.

4. Fuller, A. O. and Spear, P. C., Anti-gD antibodies that permit adsorption but block infection by herpes simplex virus 1 prevent virion fusion at the cell surface. *Proceedings of the National Academy of Sciences USA* 84:5454–5458, 1987.

5. Cohen, G. H., Isola, V. J., Kuhns, S. H., Berman, P. W., and leisenburg, R. J., Localization of discontinued epitopes of herpes simplex virus glycoprotein D: Use of a nondenaturation ("native" gel) system of polyacrylamide gel electrophoresis coupled with Western blotting. *Journal of Virology* 60:157–166, 1986.

For Additional Information:

To locate information or professional contacts on this effort, contact:

Research Resources Information Center
1601 Research Boulevard
Rockville, MD 20850
(301) 984-2870

Refer to Volume XIII, No. 5/TN

Naval Dental Research Institute Studies Potential Etiologic Agents of Periodontitis

Studies have shown that an increase in oral spirochete populations is correlated with increased periodontal disease severity. Researchers at the Naval Dental Research Institute, Great Lakes, Illinois, have recently developed and characterized murine monoclonal antibodies (MAbs) specific for a serogroup of Treponema denticola, an oral spirochete. Antibodies secreted by clone IAA11 were judged to be the most useful, since they were able to detect 8 of 15 Treponema denticola strains. This MAb consisted of an immunoglobulin G3 heavy chain and a kappa light chain. MAb IAA11 was found to react with an epitope target located on the outer sheath of the cell wall. This MAb should be of diagnostic and scientific value in the study of Treponema denticola populations in human periodontitis.

For Additional Information:

Backup material on this effort is available from:

Navy Domestic Technology Fact Sheet Reader Reply Service
Code E211
Naval Surface Weapons Center
Dahlgren, VA 22448-5000
(703) 663-8921

Refer to 131102/TN

NIH
Research & Technology
U.S. Department of Health and Human Services Public Health Service National Institutes of Health

Laboratory Animal Resource for Biomedical Research

Principal Investigator:
J. Russell Lindsey, D.V.M.
University of Alabama at Birmingham
University Station
Birmingham, Alabama 35294
(205) 934-2117

Resources Provided

- *Diagnostic Services:* This laboratory is staffed to provide broad competence in pathology, microbiology, parasitology, clinical chemistry, and hematology, and has special expertise in infectious diseases of rodents. Diagnostic resources are designed primarily to serve the grantee and affiliated institutions. However, with approval by the principal investigator, they are available for collaboration in investigating laboratory animal disease problems.
- *Other Services:* The investigation of new animal models of human diseases. The resource is interested in having potential new animal models referred for investigation or development.
- *Contact Person:* J. Russell Lindsey, D.V.M., (205) 934-2117.

Research Emphasis or Application

- *Basic Objectives:* To improve the quality of animal research at the University of Alabama at Birmingham through a sound professional program of clinical laboratory animal medicine/animal health evaluation/disease control. To identify and characterize animal diseases that are useful models of human disorders. To characterize spontaneous diseases of laboratory animals and improve methods to detect and control those diseases that complicate biomedical research. To provide educational and training programs in animal experimentation for veterinarians training in laboratory animal medicine/comparative pathology, graduate students in the biomedical sciences, veterinary students, and biomedical research technicians.
- *Current Research:* Elucidation of the pathogenesis of, and development of improved methods for diagnosis and control of, mycoplasmal and viral infections in rodents; host-parasite relationships in latent mycoplasmal infections of rodents; mechanisms by which bacterial and viral infections interfere with research; influence of Dichlorovos treatment of mite infestations on breeding efficiency in mice; animal model of esophageal achalasia; and discovery and characterization of other new animal models of diseases that occur in humans.

NAVY
Domestic Technology Transfer Fact Sheet

Navy Develops New Wound Dressing

Under joint sponsorship of the Naval Medical Research and Development Center, Bethesda, Maryland, and the Office of Naval Technology (ONT), Arlington, Virginia, researchers at the Oregon Health Sciences University, Portland, Oregon, have developed a pourable dressing for large wounds, which provides an antiseptic cover and a medium for the growth of new cells and blood vessels.

The main component of the dressing is collagen, a protein material that is the main constituent of connective tissues and bone. When the liquid dressing is poured into a wound and is warmed to body temperature, it solidifies into a strong, protective gel. Connective tissue-producing cells and blood capillaries necessary for wound repair migrate into this gel and start the process of rapid healing. The gel incorporates a bacterial agent based on iodine, which decontaminates the wound and prevents infection.

Preliminary clinical trials of the new dressing, treating leg ulcers, will begin in 1989.

For Additional Information:

Backup material on this effort is available from:

Navy Domestic Technology Fact Sheet Reader Reply Service
Code E211
Naval Surface Weapons Center
Dahlgren, VA 22448-5000
(703) 663-8921

Refer to 131206/TN

Mouse Model Resource for Human Inherited Diseases

Principal Investigator:
Philip A. Wood, D.V.M., Ph.D.
Assistant Professor
Institute for Molecular Genetics
Baylor College of Medicine
One Baylor Plaza
Houston, Texas 77030
(713) 799-4247

Resources Provided

- *Animals:* The resource is under development.
- *Other Services:* Services available include diagnosis and biochemical characterization of mice with inherited metabolic diseases, including lysosomal and other metabolic storage diseases, disorders of amino acid metabolism, and organic acidemias. Specific services include clinicopathological evaluation and biochemical analyses of enzymes, amino acids, organic acids, lipids, oligosaccharides, and DNA. Services are provided on a collaborative basis. Our primary interest is in studying mice with clinical signs suggestive of inherited metabolic diseases as found in humans. We are interested in collaborating with other investigators studying mutant mice. This could be of particular interest to those involved in chemical or insertional mutagenesis projects. Although our primary focus is on mice, we are prepared to study other species.
- *Contact Person:* Philip A. Wood, D.V.M., Ph.D., (713) 799-4247.

Research Emphasis or Application

- *Basic Objective:* To discover and characterize mouse models of human inherited diseases.
- *Current Research:* In a major collaboration with the Jackson Laboratory, we are studying several established mutant mice, as well as phenotypic deviant mice with relevant phenotypes.

NASA Tech Brief
National Aeronautics and Space Administration
NASA's Jet Propulsion Laboratory, Pasadena, California

Licensing Opportunity

Mandrels for Microtextured Small-Vessel Implants

A surface-relief pattern should encourage growth of a healthy neointima.

Research has shown that artificial blood-vessel and heart-valve implants might be made more compatible with their biological environments by the use of regularly microtextured surfaces. In an experimental manufacturing process, an ion beam etches a patterned array of small pillars on the mandrel used to mold a tubular plastic implant. The pillars create tiny, regularly spaced holes in the inner surface of the tube. The holes are expected to provide sites for attachment of a healthy lining.

The human body naturally tries to incorporate a vascular prosthesis by encapsulating it in living tissue — neointima — by the deposition of various components of the blood on the implant material. In conventional prostheses, the intima can become overdeveloped or become detached, causing obstructions of the implant or in small blood vessels downstream. The new microtextured implants should hold the neointima securely, without danger of detachment or overdevelopment, especially in vessels having internal diameters of only 6 mm or less, which are particularly vulnerable.

Polytetrafluoroethylene (PTFE) is used as the mandrel material because it can be etched by an ion beam. The PTFE is first coated with a film of gold so that a photoresist will adhere to it. The photoresist is applied, cured, and exposed with ultraviolet light through a mask containing a square array of hexagons 9 μm on a side, spaced at 100 μm. The photoresist is developed and rinsed, leaving a pattern of hexagons on the mandrel. An argon-ion beam directed at the mandrel removes PTFE only where it is not covered by photoresist. Hexagonal pillars are thus formed (see figure).

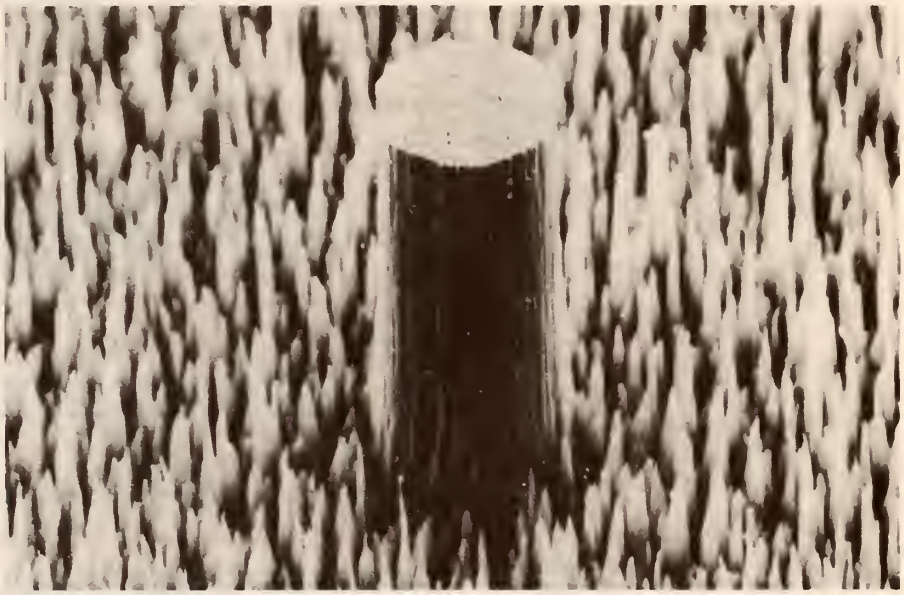

Microscopic Pillars are created on the surface of PTFE by impacts of argon ions through a photomask. Pillars about 30 μm high are produced in 15 minutes of etching.

In production, a tube of a biologically compatible polymer would be cast on a mandrel. The inner surface of the tube would be covered with an array of hexagonal holes corresponding to the pillars on the mandrel. Many tubes could be made from one mandrel.

This work was done by William D. Deininger and Stephen B. Gabriel of Caltech for **NASA's Jet Propulsion Laboratory**. *For further information, Circle 142 on the TSP Request Card.*

Title to this invention has been waived under the provisions of the National Aeronautics and Space Act [42 U.S.C 2457(f)], to the California Institute of Technology. Inquiries concerning licenses for its commercial development should be addressed to

Edward Ansell,
Director of Patents and Licensing
Mail Stop 301-6
California Institute of Technology
1207 East California Boulevard
Pasadena, CA 91125

Refer to NPO-16690, volume and number of this NASA Tech Briefs *issue, and the page number.*

Jet Propulsion Lab.
NASA Resident Office
Technology Utilization Officer: Gordon S. Chapman
Mail Stop 180-801
4800 Oak Grove Drive
Pasadena, CA 91109
(818) 354-4849
Patent Counsel: Paul F. McCaul
Mail Code 180-801
4800 Oak Grove Drive
Pasadena, CA 91109
(818) 354-2734

Technology Utilization Mgr. for JPL: Norman L. Chalfin
Mail Stop 156-211
4800 Oak Grove Drive
Pasadena, CA 91109
(818) 354-2240

FOR ADDITIONAL INFORMATION: *Contact: Director, Technology Transfer Division, P.O. Box 8757, BWI Airport, MD 21240; (301) 621-0100 Ext. 241*
REFER TO THE NUMBER LISTED AT THE END OF THIS ARTICLE

NASA Tech Brief
National Aeronautics and
Space Administration
NASA's Jet Propulsion Laboratory, Pasadena, California

Multimembrane Bioreactor

Metabolizing cells are well nourished while inhibiting products are removed.

A set of hydrophilic and hydrophobic membranes in a bioreactor allows the product of the reaction to be separated, while nutrients are fed to the reacting cells and byproducts are removed from them. The separation process requires no externally supplied energy; the free energy of the reaction is sufficient.

The membranes greatly increase the productivity of metabolizing cells by continuously removing the product and byproducts, which might otherwise inhibit the reaction, and by continuously adding oxygen and organic nutrients. The membranes also allow the use of product-extraction solvents that would otherwise kill the cells.

In production of ethanol by fermentation, for example, the membranes remove the CO_2 byproduct rapidly. If CO_2 were allowed to accumulate, it would displace the liquid around the cells in a few hours and stop the reaction. The membranes remove the ethanol product from the cells so that it cannot build up and inhibit cell metabolism. The ethanol is carried away by tri-normal-butyl phosphate (TBP), a solvent that would poison the yeast if it came in direct contact, but from which the product can be separated more simply and economically than from water.

A layer of yeast cells in water is sandwiched between a hydrophobic membrane and a hydrophilic membrane (see figure). Oxygen enters the cell layer through the upper hydrophobic membrane (which prevents water from leaving the cell layer). CO_2 leaves the layer through the upper hydrophobic membrane and is swept away by the gas stream that brought the oxygen.

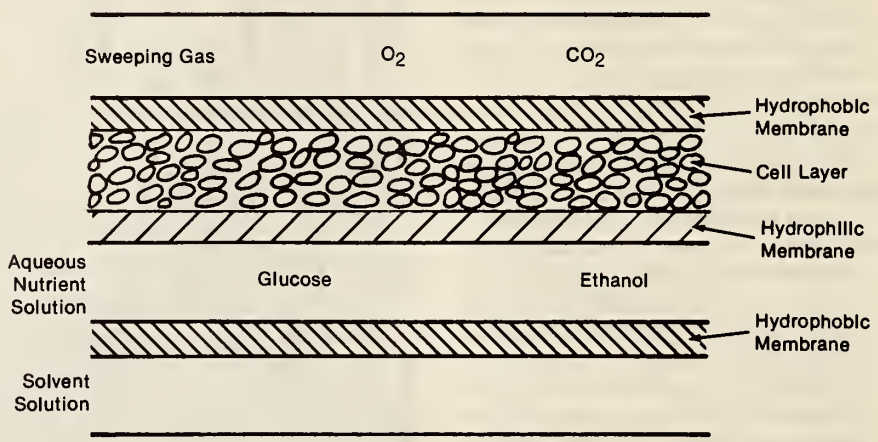

Three Membranes Perform Different Functions so that cells can metabolize efficiently. The membranes have been used to make ethanol, and the principle is adaptable to other biological reactions.

The hydrophilic membrane readily accepts the glucose nutrient in water solution for admission to the cell layer. The ethanol product leaves the cell layer through the hydrophilic membrane and continues through the water to the lower hydrophobic membrane, after which it is carried off by the flowing TBP solvent. The lower membrane does not allow the glucose solution to pass through to the TBP nor the TBP to pass through to the glucose solution, provided that the pressure of the aqueous solution is greater than that of the solvent solution but less than the critical pressure above which it would enter the membrane.

The membranes are made of microporous polypropylene film, each treated to give the special properties needed for its function. The upper hydrophobic membrane is Celgard 4410 (or equivalent), which is a gas-permeable, water-repellent film previously used to make vents in batteries. The middle (hydrophilic) membrane is a water-wettable film of Celgard 5511 (or equivalent) previously used in sterile packaging. The lower hydrophobic membrane is Celgard K-442 (or equivalent), a newly-developed water-repellent film sandwiched between two polypropylene webs that provide additional mechanical strength.

This work was done by Toohyon Cho and Michael L. Shuler of Cornell University for **NASA's Jet Propulsion Laboratory**.

NPO-17199/TN

FOR ADDITIONAL INFORMATION: *Contact: Director, Technology Transfer Division, P.O. Box 8757, BWI Airport, MD 21240; (301) 621-0100 Ext. 241*
REFER TO THE NUMBER LISTED AT THE END OF THIS ARTICLE

Natural Resources Technology & Engineering

Software

0693 DAMBREAK Flood Forecasting Model

0694 A Computer Program for Detecting or Predicting Fracture Zones

NOAA Technology Brief

National Oceanic and Atmospheric Administration

National Weather Service
Hydrologic Research Laboratory

Computer Software

DAMBREAK Flood Forecasting Model

NOAA's National Weather Service has developed a micro-computer program, DAMBRK, that predicts the extent and timing of flooding associated with a failed dam. The program is used extensively by the National Weather Service and by most Federal and state agencies concerned with dam safety and emergency evacuation planning in this country and in over 40 countries world-wide. Many state governments have made the use of this software mandatory in evaluating the safety of dams.

The mathematical model within DAMBRK consists of the one-dimensional equations of unsteady flow which are solved by an implicit finite difference technique. The model can be used in forecasting flooding due to dam failures, analyzing the hydraulics of rivers to aid design of river improvement facilities, scheduling of navigation, and hydro-power operation and development.

This work was performed by Dr. Danny Fread of the River Mechanics Section of the Hydrologic Research Laboratory.

Additional information is available from NOAA ORTA, Suitland Professional Center (SPC), Room 307, Suitland, Maryland 20233. Telephone: (301) 763-4240.

Technology News

From the Bureau of Mines, United States Department of the Interior

A Computer Program for Detecting or Predicting Fracture Zones

Objective

Develop a means for analyzing seismic crosshole data to predict and monitor the flow of leach solution during in situ mining.

Background

Improvements in predicting and monitoring in situ leach solution flow would aid in planning well field configurations. These improvements would also facilitate permit application by assuring regulatory agencies that leach solution would not escape from a well field undetected. Seismic tomography can detect fractured zones, which enables the prediction of probable flow paths, and it is a promising technique for monitoring leach solution injected above the water table. Tomographic analysis of crosshole seismic data provides a two-dimensional picture of the distribution of seismic velocities between the transmitter and receiver boreholes. The positions of fractured zones and of leach solution can then be inferred from the seismic velocities.

The Problem

To perform tomographic analysis, the area between the transmitter and receiver boreholes is mathematically divided into small elements called pixels. Tomography determines what distribution of seismic velocities among the pixels yields the best fit to travel times for the many paths crossing the area. Tomographic analysis of crosshole data without constraints does not yield a unique reconstruction, even with more measurements than pixels. Crosshole data can be fit equally well by many different reconstructions, so appropriate mathematical constraints must be applied to help select the correct one. A tomographic program providing a test for nonuniqueness and constraints to counteract nonuniqueness was needed. Commercially available programs did not provide such a test nor constraints appropri-

Examples of ray paths for crosshole seismic tomography.

ate for in situ mining applications.

Approach

The U.S. Bureau of Mines developed a tomographic computer program (BOMTOM--Bureau of Mines tomography) with a test for uniqueness and constraints to help obtain unique reconstructions. The program is easy to run on personal computers commonly used by mining companies and others. Options can be selected interactively. BOMTOM uses a simultaneous iterative reconstruction technique. It uses straight ray paths because the seismic velocity contrasts in an in situ mining operation are unlikely to be great enough to require curved ray analysis.

Tests and Constraints

BOMTOM allows the user to test uniqueness by varying the pattern of the initial velocity guesses used to start the iterative solution procedure. A unique reconstruction is independent of the initial velocity guesses.

BOMTOM provides the following options for constraints:

1. Maximum and minimum calculated velocities.

2. Known, fixed velocities in boreholes, such as from sonic logs.

3. Horizontal layers near the top and/or bottom of the investigated area in which seismic velocity does not vary with horizontal position.

4. Smoothing, in which the calculated velocity in a pixel is influenced by the velocities in neighboring pixels.

Other Applications

BOMTOM has been used for detecting zones of fractures in quarries by analyzing seismic refraction data. The velocity contrast in quarries is large enough to make curved ray analysis desirable. BOMTOM has also been used for examining building stone by analyzing seismic travel times for two pairs of faces to detect fractures that are not visible from the surface.

BOMTOM Features

- Test of uniqueness of reconstructions.
- Optional constraints to counteract nonuniqueness.
  - Maximum and minimum velocities.
  - Fixed velocity in boreholes.
  - Horizontal layers with uniform velocity.
  - Smoothing.
- Other options.
  - Comparisons with prior runs.
  - Generation of synthetic data.
- Ease of use.
  - Runs on personal computer.
  - Interactive setting of options.

For More Information

U.S. Bureau of Mines Report of Investigations (RI) 9159, by D.R. Tweeton, describes BOMTOM and results of testing the effectiveness of various combinations of constraints in obtaining unique reconstructions when simulating in situ mining. A free single copy of this report may be obtained by writing to the Bureau's Publication Distribution Section, P.O. Box 18070, Cochrans Mill Road, Pittsburgh, PA 15236.

The application to detection zones of fractures in quarries is described in "Application of Refraction Tomography to Map the Extent of Blast-Induced Fracturing," by C.L. Cumerlato, V.J. Stachura, and D.R. Tweeton, in "Key Questions in Rock Mechanics: Proceedings of the 29th U.S. Symposium (Minneapolis, MN, June 13-15, 1988). Balkema, 1988, pp. 691-698.

Source and executable codes in FORTRAN and QuickBasic on 5-1/4 and 3-1/2 inch IBM-compatible diskettes are available from D.R. Tweeton, U.S. Bureau of Mines, Twin Cities Research Center, 5629 Minnehaha Avenue South, Minneapolis, MN 55417 (612/725-4670).

Physical Sciences

0695 The Determination of pH by Flow Injection Analysis and by Fiber Optrode Analysis (Licensing Opportunity)

0696 Nonaggregating Microspheres Containing Aldehyde Groups—Aggregation is avoided by irradiating hydrophilic monomers in the presence of acrolein. (Licensing Opportunity)

Software

0697 Isothermal-Gas-Transfer Program—One or two tanks with or without venting or consumption can be simulated.

Testing & Instrumentation

0698 Fourier Transform Infrared Spectrometry of Ambient Aerosols

0699 Investigation 2,4-Dinitrophenylhydrazine Impregnated Adsorbent Tubes for the Collection of Airborne Aldehydes

0700 Acoustical Measurement of Furnace Temperatures—Simple probes withstand severe conditions, yet give spatially-resolved temperature readings. (Licensing Opportunity)

0701 Correlation Functions Aid Analyses of Spectra—Signals much weaker than noise are identified.

0702 Thermal-Wave Microscope—Images are produced by a modified computer-controlled scanning electron microscope.

0703 Phase-Modulation Gas-Correlation Spectroscopy—Features include high spectral discrimination and sensitivity.

Other Items of Interest

0646 Special Plug Lets Researchers 'See' Inside Auto Engines

0658 Densitometry by Acoustic Levitation—Detailed knowledge of the acoustic field is not necessary.

0663 Automated Chemical Analysis for Process Solutions

0672 Low Dislocation Density GaAs Crystals Grown Using Advanced Vertical Gradient Freeze Technique

0680 Polymer Coatings Reduce Electro-osmosis—Poly(ethylene glycol) film controls the electrostatic potential across the surface. (Licensing Opportunity)

Licensing Opportunity

United States Environmental Protection Agency

Environmental Monitoring Systems Laboratory Las Vegas NV 89193-3478

Research and Development

EPA

Project Summary

The Determination of pH by Flow Injection Analysis and by Fiber Optrode Analysis

Two new protocols for measuring pH have been developed. The first measures pH colorimetrically using an indicator dye mixture in a flow injection analysis (FIA) procedure. The second measures pH using a fiber optic chemical sensor (FOCS or optrode) specifically developed for pH determinations. The FOCS method measures pH by monitoring the fluorescence of fluorescein derivative bonded to the distal end of a fiber optic cable. The FIA method currently has a precision and accuracy of about ±0.2 pH units and can measure 100 samples/hour. The matrix may affect the precision and accuracy but has not been fully investigated. The FOCS method has a precision of ±0.05 to 0.20 pH units and an accuracy of ±0.1 to 0.6 pH units. The bias is largely due to inadequacy of the calibration model, which needs further development. About 10-60 samples can be analyzed. The response time is matrix dependent. It varied from 10 seconds to 7 minutes in the solutions studied, with slowest response in dilute, poorly buffered samples.

This Project Summary was developed by EPA's Environmental Monitoring Systems Laboratory, Las Vegas, NV, to announce key findings of the research project that is fully documented in a separate report of the same title (see Project Report ordering information at back).

Introduction

An important parameter determined for acid deposition characterization and monitoring is pH. It has been measured during all of the EPA's Aquatic Effects Research Program Surface Water Surveys in both the field (on-site) and analytical laboratories. Laboratory measurements with pH electrodes were generally precise and accurate (+0.05 pH units), but proved to be time consuming and labor intensive. When used in the field, electrodes and meters performed marginally (±0.5 to ±1 pH unit) Future surveys and long-term monitoring projects will require field pH measurements using either in-situ or closed-system techniques. This necessitates the development of new methods for determining pH in the field.

In an initial step to develop a field method, this study was undertaken to fully characterize two indicator-based pH methods and check their suitability for field use. The first involves the use of an indicator dye mixture with a pH dependent absorbance in a FIA method. The second method uses an optical fiber coated with fluorescein, the fluorescence of which at 530 nm is pH dependent.

Procedure

All chemicals were ACS analytical reagent grade or better. Solutions were prepared in ASTM Type II water and were stored in high density polyethylene bottles at 4 degrees centigrade. Real lake water samples were field audit samples from the Eastern Lake Survey. They were originally taken from Big Moose Lake and Bagley Lake and were homogenized and stabilized for use in the survey. The pH and other physical and chemical properties of these real samples were extensively characterized.

Table 1. Comparison of Analytical Figures of Merit of Electrode, FIA, and FOCS pH Methods

	pH Electrode	*FIA*	*FOCS*
Rate (samples/hr)	*4-20*	*100*	*10-60*
pH Range	*3-10*	*3.6-6.8*	*3.6-7.5*
Bias (pH Unit)	*±0.05*	*±0.01*	*±0.1 to ±0.6*
Precision (pH Unit)	*±0.05*	*±0.05 to ±0.20*	*±0.02 to ±0.2*

In the flow injection analysis method, a pH indicator reagent is mixed with sample and injected into a deionized water carrier stream. The absorbance of the effluent is monitored at 555 nm. The pH indicator reagent is a proprietary mixture of pH indicator dyes whose absorbance at 555 nm is proportional to pH.

A fiber optic chemical sensor (FOCS or optrode) for pH is constructed by immobilizing fluorescein to the distal end of a fiber optic. Fluorescein is a fluorescent compound which emits light at 530 nm when excited at 485 nm. The intensity of fluorescence at 530 nm is pH dependent. Sample pH is measured by dipping the probe into the sample and monitoring the fluorescence at 530 nm while exciting at 485 nm.

The following issues were addressed in evaluating the methods: calibration curves, precision, accuracy, sample analysis rate, matrix effects, and real sample analysis. The basic method analytical characteristics were determined using stable, well characterized pH buffers. The effects of several matrix variables (ionic strength and buffering capacity) on the analytical characteristics were studied using acetate, phosphate, and sulfuric acid solutions. Finally, the performance of the method was tested with two real lake water samples.

Results and Discussion

The analytical figures of merit of the three methods of pH determination are given in Table 1. The FIA method compares very well with the pH electrode for the routine determination of pH in natural surface waters. It has acceptable precision and bias and has a very high sampling rate. Improvement in both precision and accuracy are possible by improving the FIA hardware (more accurate and precise solution handling, using syringe pumps). Also the linearity and applicable pH range may be increased by modifying the indicator reagent mixture and/or monitoring more than one wavelength.

The results of the FOCS pH method were encouraging, but the technique needs more development than the FIA method. The optrodes investigated were prototypes and consequently the analytical characteristics varied from optrode to optrode. The bias was dependent upon the optrode sensitivity and varied from ±0.1 to ±0.6 pH unit. The bias is magnified by the inadequacy of the calibration model. The linear model chosen for the optrode does not explain all of the variation. A polynomial model will be tested when the software becomes available. Another optrode characteristic is a limited lifetime. Optrode sensitivity decreases from day to day. Finally, while the optrodes are generally faster than electrodes, the achievable sampling rate is affected by ionic strength and buffering capacity.

Conclusions and Recommendations

The FIA method appears to be the more promising of the two new techniques at this time. With further work, a method suitable for long-term, unattended monitoring of pH in surface waters could be developed. The FOCS pH optrode will require manufacturing changes and further characterizations in order for it to become analytically viable.

Potential interferences in the FIA method should be further investigated. For example, the bias for dilute acid standards was larger than anticipated. The bias appeared to be related to the pH or acid used rather than ionic strength. Also, interferences from potential organic components in surface waters should be studied. Finally, a larger set of real samples should be analyzed and compared to pH electrode data.

In the near future, the use of chemically sensitive field effect transistors (Chemfet) for pH measurement will be studied. Preliminary indications are that Chemfets will be an excellent tool for measuring pH directly or as a detector in a FIA method.

Stephen H. Pia, Donna P. Wallman, and Daniel C. Hillman are with Lockheed Engineering and Management Services Company, Inc., Las Vegas, NV 89109

Edward M. Heithmar is the EPA Project Officer (see below).

The complete report, entitled "The Determination of pH by Flow Injection Analysis and by Fiber Optrode Analysis," (Order No. PB 88-235 502/AS; Cost: $14.95, subject to change) will be available only from:

National Technical Information Service
5285 Port Royal Road
Springfield, VA 22161
Telephone: 703-487-4650

The EPA Project Officer can be contacted at:

Environmental Monitoring Systems Laboratory
U.S. Environmental Protection Agency
Las Vegas, NV 89193-3478

NASA Tech Brief
National Aeronautics and Space Administration
NASA's Jet Propulsion Laboratory, Pasadena, California

Licensing Opportunity

Nonaggregating Microspheres Containing Aldehyde Groups

Aggregation is avoided by irradiating hydrophilic monomers in the presence of acrolein.

Cobalt gamma irradiation of hydrophilic monomers in the presence of acrolein yields exceptionally-stable, nonaggregating microspheres. Previous microspheres containing aldehyde groups (such as polyglutaraldehyde microspheres) tended to aggregate during reaction with amines and proteins.

Mixtures of 2-hydroxyethyl methacrylate (HEMA) and acrolein form homogeneous solutions in distilled water containing 0.4 percent polyethylene oxide (PEO). After deaeration with nitrogen, the mixtures are irradiated at room temperature with gamma rays from a cobalt source; total exposure time is 4 hours, at a rate of 0.2 milliroentgen per hour. The reaction product is centrifuged three times for purification and is kept in distilled water.

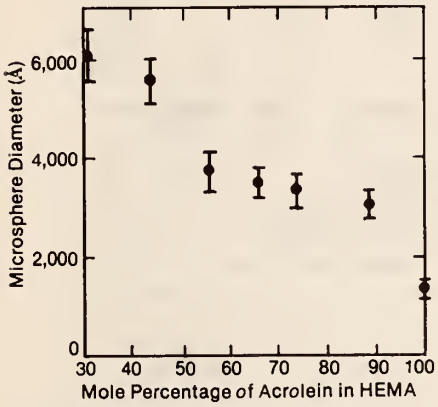

Microsphere Diameter is an inverse function of HEMA/acrolein ratio, but the variation is slight in the range from about 60 to 90 percent acrolein. Therefore microspheres can be prepared with similar size but different hydrophobicity.

The irradiation of pure acrolein in water containing PEO produces colloidal particles approximately 1,000 Å in diameter. Adding HEMA increases the diameter of the microspheres; but, as the figure shows, variation is slight in the middle range of monomer ratios. Therefore microspheres can be prepared with similar size but different degrees of hydrophobicity.

To produce cross-linked microspheres containing acid functions, N, N′-methylene-bis-acrylamide and methacrylic acid are added to the HEMA/acrolein polymerization mixture. The size characteristics of the cross-linked microspheres closely approximate those in the figure. Seven of these preparations were analyzed for the presence of aldehyde groups. The acrolein homopolymer was found to contain approximately 65 percent of the expected aldehyde groups.

This work was done by Alan Rembaum of Caltech for **NASA's Jet Propulsion Laboratory**.

Title to this invention, covered by U.S. Patent No. 4,413,070, has been waived under the provisions of the National Aeronautics and Space Act [42 U.S.C. 2457(f)]. Inquiries concerning licenses for its commercial development should be addressed to

Edward Ansell
Director of Patents and Licensing
Mail Stop 301-6
California Institute of Technology
1207 East California Boulevard
Pasadena, CA 91125
Refer to NPO-15459/TN

Jet Propulsion Lab.
NASA Resident Office
Technology Utilization Officer: Gordon S. Chapman
Mail Stop 180-801
4800 Oak Grove Drive
Pasadena, CA 91109
(818) 354-4849
Patent Counsel: Paul F. McCaul
Mail Code 180-801
4800 Oak Grove Drive
Pasadena, CA 91109
(818) 354-2734
Technology Utilization Mgr. for JPL: Norman L. Chalfin
Mail Stop 156-211
4800 Oak Grove Drive
Pasadena, CA 91109
(818) 354-2240

FOR ADDITIONAL INFORMATION: *Contact: Director, Technology Transfer Division, P.O. Box 8757, BWI Airport, MD 21240; (301) 621-0100 Ext. 241*
REFER TO THE NUMBER LISTED AT THE END OF THIS ARTICLE

Isothermal-Gas-Transfer Program

One or two tanks with or without venting or consumption can be simulated.

The Isothermal Gas Transfer program (GASXFER) solves a variety of problems in which a gas or gas mixture is transferred between two containers. The model is general in nature, consisting of an upstream tank and a downstream tank. As many as three different feed gases may be combined in the upstream tank. Downstream flow may be defined either as constant, dependent on the size of the orifice, or variable in such a way that constant pressure is maintained in the upstream tank. The program assumes isothermal flow and isothermal conditions within the tank.

The program can simulate a single tank by setting the volume of the downstream tank either to zero (no vent flow) or to infinite volume, which simulates venting into an environment of constant pressure or a vacuum. In addition to adjusting the volume of the containers, the user may also adjust the feed. For example, the feed gases can be used to simulate a purge of the upstream tank. In another combination, the feed gases may be used to simulate a life-support system in the cabin of a spacecraft. The three feed gases in this case would then consist of oxygen, nitrogen, and either carbon dioxide or water vapor, where the negative value of oxygen feed simulates consumption by the crew.

Special features of the program include its ease of entering data and ease of obtaining output. The program displays, prints, or graphs a complete pressure history of each gas as a function of time.

GASXFER was written in the Lotus Symphony macrolanguage as implemented on the IBM PC-series computers. It requires a fixed disk and at least 384K of random-access memory and Lotus Symphony 1.0 or greater. The program was released in 1988.

This program was written by Don I. Levine of Rockwell International Corp. for **Johnson Space Center**.

MSC-21400/TN

FOR ADDITIONAL INFORMATION

CONTACT:

COSMIC®
112 Barrow Hall
University of Georgia
Athens, GA 30602
(404) 542-3265

United States
Environmental Protection
Agency

Environmental Monitoring
Systems Laboratory
Research Triangle Park, NC 27711

Research and Development

EPA

Project Summary

Fourier Transform Infrared Spectrometry of Ambient Aerosols

Introduction

The collection and analysis of ambient aerosols is an important means of studying the chemistry of the troposphere. The major constituents of the fine fraction (< 2.5 μm diameter) of the particulate matter in the atmosphere are ammonium sulfate, ammonium nitrate, and elemental and organic carbonaceous particles. Knowledge of the origins, interaction, and deposition of these compounds is important in the study of visibility degradation, atmospheric chemistry, acid deposition, and the effects of these particles on human health and terrestrial ecology.

Ambient aerosols are typically collected with dichotomous air samplers which collect particles in two size fractions. The fine fraction particles are < 2.5 μm in diameter and the coarse fraction particles are in the 2.5 - 15 μm diameter size range. The size fractions correspond to the bimodal distribution of particles sizes found in the atmosphere. The particles are collected on various filter media including Teflon, Nylon, quartz, and paper filters. The choice of filter media depends, among other things, upon the compounds to be measured, on the analysis technique to be used, and the cost of the filters.

There are a number of chemical analysis techniques available to measure the concentrations of elements and compounds collected on air filters. Sulfate and nitrate ions collected on the filters are typically measured using ion chromatography. Ion chromatography is a very sensitive but destructive analytical technique for the determination of sulfate, nitrate, and a number of other ions. The method requires liquid extraction, followed by separate analysis of cations and anions, and provides no direct information concerning compound speciation of the ions. In addition, the extraction procedure can alter the species found on the filter.

Another method for determining sulfate collected on filters is x-ray fluorescence (XRF) analysis. This nondestructive method of analysis has been used in an automated system to determine elemental sulfur, as well as other elements, deposited on Teflon filters. Sulfate concentrations can be inferred by assuming that all of the sulfur is in the form of sulfate. Ion chromatography analysis for sulfate has been compared to XRF analysis for sulfur on Teflon air filters and the two methods have been shown to provide equivalent results for sulfate. X-ray fluorescence provides no information concerning nitrate deposition due to the low energy of the characteristic nitrogen x-ray emission.

X-ray diffraction is a nondestructive technique that can provide for compound identification. It is difficult to obtain quantitative results using x-ray diffraction for two reasons: (1) The sensitivity of this technique is relatively low. Consequently, high particle loadings are required to obtain adequate measurements for accurate compound identification. High particle loadings introduce the possibility of chemical reactions between particles concentrated on the filter. (2) Water in the sampled air can promote recrystallization of particles on the filter. This introduces a preferred orientation in the sample which will change the peak ratios in the diffraction signals causing difficulties in calibration.

Recently, another method for particle analysis on Teflon filters has been reported by other researchers who have shown that ammonium and sulfate can be measured directly on Teflon filters using FTIR transmission spectrometry. Their results showed the equivalence of XRF and FTIR spectroscopy for the quantitative determination of sulfate. They also reported quantitative measurements of the ammonium cation. In addition to the discrete absorption bands associated with the vibrational modes of specific molecular species, the mid-infrared spectrum of these ambient aerosols shows continuous absorption across the entire spectrum which is characteristic of carbonaceous particles. To the extent that a relationship between this absorption and the elemental carbon

content can be established, a method for nondestructive automated analysis of carbon particle concentration simultaneously with that for sulfate, ammonium, and nitrate particles could result. Finally, this technique is appealing because it makes use of a common filter media, Teflon, is nondestructive, requires no sample preparation, is amenable to automation, and can provide simultaneous analysis of compounds that typically require different types of analysis on different filter media.

This report describes an experimental program intended to build on previous work reported in the literature, where a number of suggestions are proposed to improve lower limits of detection for sulfate. This study has implemented and tested those suggestions. Experiments to test analytical methods to quantitatively determine sulfate, nitrate, ammonium, and elemental carbon on laboratory-generated samples and ambient samples are also described.

An FTIR spectrometer was modified with the addition of an automatic sample changing compartment. The FTIR instrument and sample changing compartment will be described; however, a detailed description of the FTIR system can be found in the operating manual accompanying the instrument.

Conclusions

Automated FTIR analysis of aerosol samples using a Nicolet model 5DXB* Fourier transform infrared spectrometer has been realized with the design and construction of a specialized sample handling system. The sample compartment directly accepts the sample carousel from a commercial air sampler produced by Sierra/Andersen Inc. thereby minimizing sample handling. Software was developed and added to the existing data collection and analysis programs in the Nicolet FTIR to allow complete control of the position of any filter. Software was also written to analyze ambient air samples by automatically providing an optimal background subtraction and integration of absorption bands of interest of the collected particles. This instrument provides automated nondestructive sulfate analysis of up to 40 Teflon air filters with minimal sample handling and operator intervention.

Quantitative spectral analysis methods were developed to analyze sulfate in aerosols collected on Teflon filters. Laboratory experiments showed that detection limits are eight times lower for analysis using the sulfate absorption band at 1117 cm^{-1} than for the band at 620 cm^{-1}. However, spectral interferences found in ambient samples prevented use of this former band for routine sulfate analysis. Analysis of air samples collected in Los Angeles during the California Air Resources Board CARB study showed good correlation of the FTIR method of analysis for sulfate with ion chromatography (IC) analysis of the same sample filters.

Small improvements in the detection limit for sulfate using the 620 cm^{-1} band were realized by using 2 µm pore size Teflon filters, saving reference spectra of each blank filter prior to air sampling for use during background subtraction, and maintaining the physical orientation of the filters during infrared spectral measurements. All of these practices contribute to more accurate background subtraction which leads to a more accurate measurement for sulfate. The lower limit of detection for sulfate in ambient aerosols using the 620 cm^{-1} absorption band was measured to be 5.8 $\mu g/cm^2$ during the CARB study in which the filter orientation was not maintained throughout the analysis. If filter orientation is maintained, then the lower limit of detection is estimated to be 1 - 2 $\mu g/cm^2$ for ambient sulfate.

Spectral analysis methods were developed to quantitatively measure ammonium nitrate in the presence of interferences due to ammonium sulfate. Ammonium nitrate measurements were accurate to within 3 - 5% after ammonium sulfate spectral interferences were removed on laboratory-prepared aerosol samples. The lower limit of detection for the measurement of ammonium nitrate was found to be 1.32 $\mu g/cm^2$ for laboratory-generated samples.

A high degree of correlation was found between elemental carbon measurements on infrared spectra of ambient samples collected on Teflon filters and elemental carbon measured by thermal methods on samples collected on quartz filters. However, attempts to develop a direct elemental carbon calibration standard on Teflon filters using laboratory generated soot particles was unsuccessful. It was concluded that calibrations must be made with co-collected air samples on quartz filters analyzed by thermal methods.

Martin Pollard and Joseph Jaklevic are with Lawrence Berkeley Laboratory, University of California, Berkeley, CA 94720.
William A. McClenny is the EPA Project Officer (see below).
The complete report, entitled "Fourier Transform Infrared Spectrometry of Ambient Aerosols," (Order No. PB 88-213 236/AS; Cost: $14.95, subject to change) will be available only from:
National Technical Information Service
5285 Port Royal Road
Springfield, VA 22161
Telephone: 703-487-4650
The EPA Project Officer can be contacted at:
Environmental Monitoring Systems Laboratory
U.S. Environmental Protection Agency
Research Triangle Park, NC 27711

United States
Environmental Protection
Agency

Environmental Monitoring
Systems Laboratory
Research Triangle Park NC 27711

Research and Development

EPA

Project Summary

Investigation 2,4-Dinitrophenylhydrazine Impregnated Adsorbent Tubes for the Collection of Airborne Aldehydes

Introduction

The determination of aldehydes and other carbonyl compounds in the atmosphere is of interest because of their importance as precursors in the production of photochemical smog, as photochemical reaction products and as a major source of free radicals in polluted environments. Additionally, short-term exposures to aldehydes such as formaldehyde, acetaldehyde, acrolein and crotonaldehyde are known to result in irritation of the eyes, skin and mucous membrane of the upper respiratory tract.

These carbonyl species are emitted into the atmosphere either directly from certain industrial processes or as secondary products from combustion sources. In rural areas, concentrations of 0.6 to 1.3 ppb formaldehyde have been reported. In urban environments, formaldehyde levels range from several ppb to over 50 ppb depending upon location and meteorological conditions. Acetaldehyde levels 20 to 50 percent of formaldehyde concentrations are generally found. Very little ambient air data exist, however, for the other carbonyl species.

The limited amount of speciated aldehyde data is largely due to the lack of a simple, sensitive, and selective analytical method. Derivatization techniques utilizing 2,4-dinitrophenylhydrazine (DNPH) reagent are currently being evaluated and will likely replace the earlier analytical methods—chromatropic acid, pararosaniline, and direct analysis via gas chromatography. With the DNPH technique, a derivative is formed by the reaction of DNPH with the carbonyl compound in the presence of acid to form the corresponding hydrazone derivative. Initially, the DNPH derivatives were separated and identified using packed column gas chromatographic techniques. More recently, high performance liquid chromatography (HPLC) has been employed by researchers to more easily separate and elute the DNPH derivatives. Quantitation of the hydrazone derivatives using HPLC is accomplished with a UV detector.

Sampling for carbonyl species is generally accomplished with either impinger or solid adsorbent techniques. With impinger methods, aqueous or organic solvents (or mixtures of both) have been used to prepare the DNPH absorbing solution. The use of DNPH/acetonitrile solutions permit the direct analysis of the adsorbing solution using reversed phase HPLC. The DNPH/acetonitrile impinger technique has simplified sampling efforts, but it is not ideally suited for extended sampling periods (solvent evaporation) nor for field use when samples are to be stored and shipped to a central laboratory for analysis. The use of adsorbent traps coated with DNPH circumvents some of the short-comings of the impinger technique. Adsorbents that have been impregnated with DNPH include XAD-2, silica gel, glass beads, commercially packaged plastic cartridges (e.g., Sep-Pak C_{18}), and glass fiber filters.

The objective of this study was to further investigate the use of DNPH impregnated adsorbent for sampling airborne aldehydes. Specific areas that were examined include:

- determination of collection and recovery efficiency of adsorbent tubes versus impingers
- design of leak-tight sample storage devices/improvement of adsorbent tube design
- improvement of sampling/analysis accuracy and precision for ambient aldehydes
- investigation of alternative detection schemes.

Conclusions and Recommendations

Based on the results of this work, it is concluded that the DNPH-coated Sep-Pak cartridges provide the researcher with a simple yet accurate means for sampling airborne aldehydes. Furthermore the analysis of the hydrazone derivatives is facilitated by the use of high performance liquid chromatographic methodology. Specific conclusions and recommendations are given below:

1. Experimental results using a 17 m^3 environmental chamber and various spiked amounts of aldehyde material showed that the DNPH-coated Sep-Pak cartridge and the DNPH/acetonitrile impinger methods gave equivalent results. Cartridge/impinger ratios of $\geq$ 0.85 were obtained for most of the tested aldehydes (acrolein ratio = 0.74). Based on the calculated chamber concentrations, both sampling methods showed absolute recoveries greater than 80 percent for formaldehyde, acetaldehyde, butyraldehyde and benzaldehyde. Considering the generated concentration levels and the adsorptive nature of these compounds, the above absolute recovery is quite acceptable. However for acrolein, recoveries ranged from 28 to 44 percent. For crotonaldehyde, recoveries of 127 to 159 percent were found. Both compounds are olefinic aldehydes and it is likely that these species undergo additional chemical reactions during the sampling and analysis process. We do not recommend using the cartridge sampling approach for these two carbonyl species.

2. Blank levels of the DNPH coated Sep-Pak cartridges were investigated as a function of storage time using various containers and temperature conditions. Canisters pressurized with nitrogen provided the best storage device. Storage in a refrigerator or freezer also resulted in lower blank levels than storage at room temperature. Coated cartridges showed no detectable amount of the aldehyde derivatives when analyzed within several hours of preparation. However, we found measurable levels after six days of storage. Blank levels did not appear to increase significantly after the sixth day. During these tests, several different batches of the Sep-Pak cartridges were housed within the same storage device. We observed an eight-fold difference in blank levels. This batch-to-batch difference may significantly affect the quality of data collected during a monitoring study. To assure that quality data will be obtained, cartridges should be grouped according to batch number and blank levels should be determined prior to any field monitoring effort. We recommend that the blank cartridge level be an order of magnitude lower than the sample cartridge level (i.e., adjust sampled volume accordingly).
3. High performance liquid chromatography was shown to be a sensitive and stable analytical method for the hydrazone derivatives. Very good precision was obtained from the analyses of an eight component standard (2 ng/μl) over a two month period. Although gas chromatography methods were also examined and gave better sensitivity, a considerable number of extraneous peaks prohibited acceptable identification and quantitation of the aldehyde derivatives.
4. Good interlaboratory agreement was obtained from the analysis of an eight component standard (2 ng/μl). These results demonstrate that the hydrazone derivatives can be prepared accurately at the lower ng/μl level and are stable in solution for at least four months.
5. Aldehyde samples collected at a suburban location showed good analytical precision and low blank levels. These results demonstrate that low ppb levels of airborne aldehydes can be determined with the sampling and analysis methodology discussed in this report.
6. A continuous monitoring analyzer was evaluated and exhibited good sensitivity and selectivity for formaldehyde. The unit was able to detect $\geq$ 8 ppb formaldehyde and was nonresponsive to ppb levels of other aldehydes.

M. W. Holdren, D. L. Smith and N. K. Russel are with Battelle's Columbus Division, Columbus, OH 43201-2693.
W. A. McClenny and J. D. Mulik are the EPA Project Officers (see below).
The complete report, entitled "Investigation of 2,4-Dinitrophenylhydrazine Impregnated Adsorbent Tubes for the Collection of Airborne Aldehydes," (Order No. PB 88-220 223/AS, Cost, $14.95, subject to change) will be available only from:
National Technical Information Service
5285 Port Royal Road
Springfield, VA 22161
Telephone: 703-487-4650
The EPA Project Officers can be contacted at
Environmental Monitoring Systems Laboratory
U.S. Environmental Protection Agency
Research Triangle Park, NC 27711

NASA Tech Brief
National Aeronautics and Space Administration

Licensing Opportunity

NASA's Jet Propulsion Laboratory, Pasadena, California

Acoustical Measurement of Furnace Temperatures

Simple probes withstand severe conditions, yet give spatially-resolved temperature readings.

A prototype acoustical system has been developed to measure temperatures from ambient to 1,800 °F (1,000 °C) in such structures as large industrial lime kilns and recovery-boiler furnaces. The acoustical temperature probes are simple, rugged

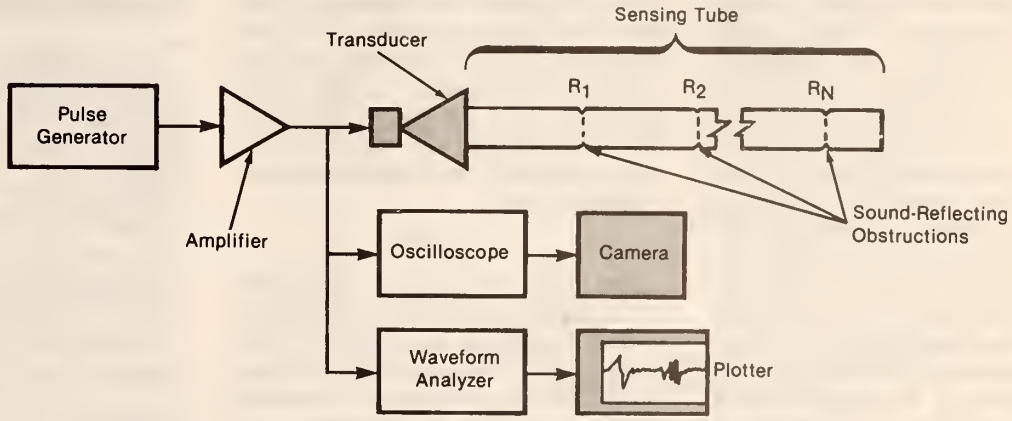

TEMPERATURE-MEASURING SYSTEM

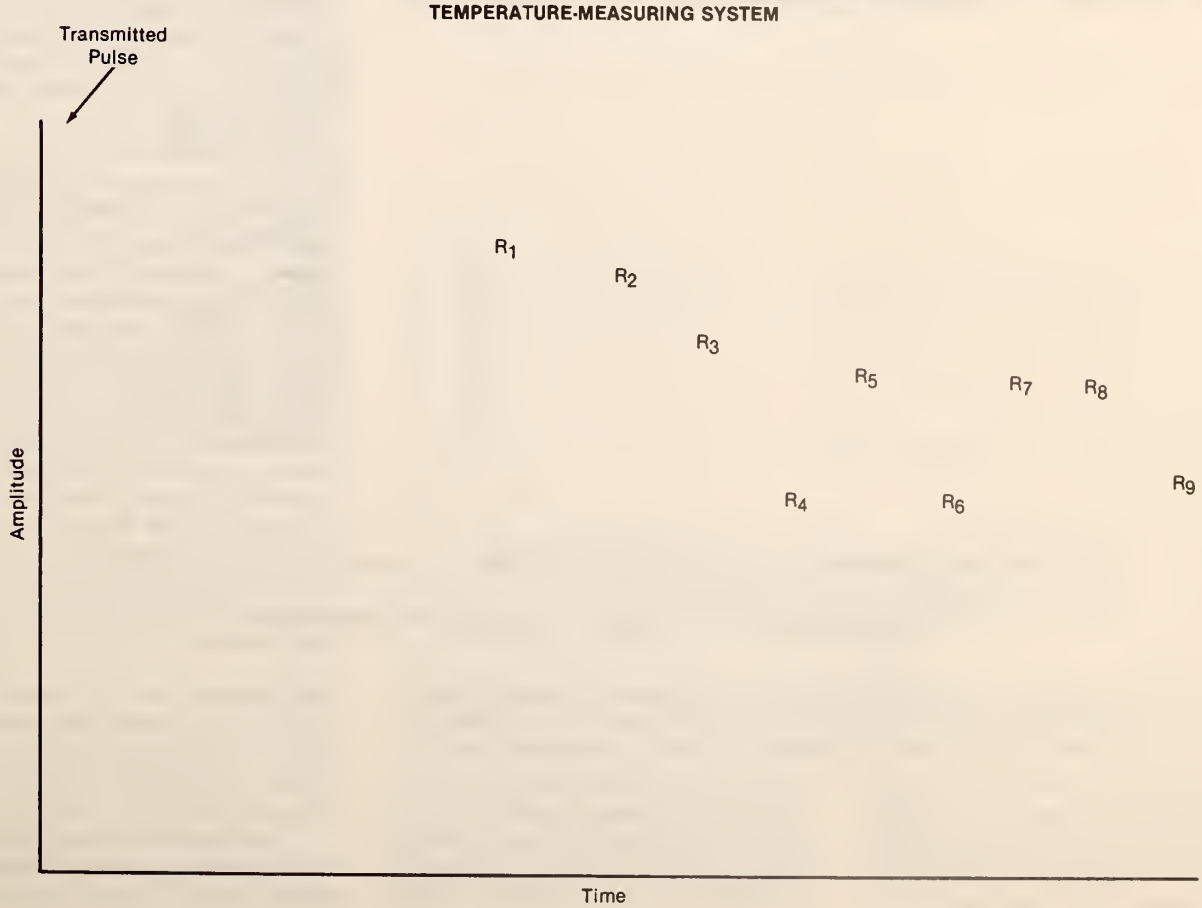

Pulses of Sound are reflected from obstructions in the sensing tube. The speed of sound and the temperature in each segment are deduced from the travel times of the pulses.

tubes of stainless steel, ceramic, or other suitable materials. The acoustical system gives spatially resolved measurements of temperature and replaces thermocouples, which are attacked by the corrosive atmospheres of the kilns and furnaces. Although pyrometers could be used in place of thermocouples, they cannot resolve spatial variations of temperature within their fields of view.

The system (see figure) is based on measurement of the travel times of pulses of sound. A loudspeaker or other suitable transducer at one end of the sensing tube acts as the transmitter and receiver. Signals from a pulse generator are converted by the transducer to pulses of sound, which travel along the sensing tube. Holes, diametrical rods, or other obstructions are placed at intervals along the tube to reflect sound back to the transducer.

The transducer converts the reflected pulses of sound back into electrical signals, which are displayed on an oscilloscope or fed to a digital waveform analyzer. The oscillogram or the analyzer output gives the time between the transmitted pulse and each of the received pulses. The speed of sound C_n in the segment of the tube between the $n-1$st and nth reflectors is given by

$$C_n = 2l_n/(t_n - t_{n-1})$$

where l_n is the distance along the tube between the two reflectors and t_n and t_{n-1} are the times of receipt of the nth and $n-1$st pulses, respectively.

The transducer end of the sensing tube can be left open to the atmosphere or, if the tube is sealed along its length, can be connected to a supply of a suitable gas at a known regulated pressure. In either case, the temperature T_n in the nth segment of the tube is deduced from the simple relationship between the temperature and the speed of sound:

$$T_n = C_n^2/\gamma R$$

where γ is the ratio of specific heats and R is the gas constant for the gas in the tube.

The dimensions and material of the sensing tube are chosen so that the transfer of heat along the tube by conduction and convection is much weaker than the radial transfer of heat through the wall of the tube. Thus, at a given location along the tube, temperature of the gas inside the tube is nearly the same as that of the gas just outside the tube, and the travel times of the pulses give good indications of the local temperatures in the gas just outside the segments of the tube.

This work was done by Shakkottai Parthasarathy and Shakkottai P. Venkateshan of Caltech for **NASA's Jet Propulsion Laboratory**.

In accordance with Public Law 96-517, the contractor has elected to retain title to this invention. Inquiries concerning rights for its commercial use should be addressed to

Edward Ansell,
Director of Patents and Licensing
Mail Stop 301-6
California Institute of Technology
1207 East California Boulevard
Pasadena, CA 91125

Refer to NPO-17007/TN

Jet Propulsion Lab.
NASA Resident Office
Technology Utilization Officer: Gordon S. Chapman
Mail Stop 180-801
4800 Oak Grove Drive
Pasadena, CA 91109
(818) 354-4849
Patent Counsel: Paul F. McCaul
Mail Code 180-801
4800 Oak Grove Drive
Pasadena, CA 91109
(818) 354-2734
Technology Utilization Mgr. for JPL: Norman L. Chalfin
Mail Stop 156-211
4800 Oak Grove Drive
Pasadena, CA 91109
(818) 354-2240

FOR ADDITIONAL INFORMATION: *Contact: Director, Technology Transfer Division, P.O. Box 8757, BWI Airport, MD 21240; (301) 621-0100 Ext. 241*
REFER TO THE NUMBER LISTED AT THE END OF THIS ARTICLE

NASA Tech Brief
National Aeronautics and Space Administration
NASA's Jet Propulsion Laboratory, Pasadena, California

Correlation Functions Aid Analyses of Spectra

Signals much weaker than noise are identified.

New uses have been found for correlation functions in analyses of spectra. In an approach that combines elements of both pattern-recognition and traditional spectral-analysis techniques, spectral lines can be identified in data that appear useless at first glance because they are dominated by noise. The new approach should be particularly useful in the measurement of concentrations of rare species of molecules in the atmosphere.

The cross-correlation function, $C(x)$, of two functions $f_1(x)$ and $f_2(x)$ is defined by

$$C(x) = \int_{-\infty}^{\infty} f_1(x'+x)\, f_2(x')dx'$$

Depending on its sign, x is called the "lead" or "lag." If f_1 and f_2 are identical, then $C(x)$ becomes the autocorrelation function $A(x)$. A new quantity called the "heteromorphic coefficient" (H) is defined to express the degree to which f_1 and f_2 match each other:

$$H = [A_1(0) - A_2(0)]/C_{max}$$

where C_{max} = the peak value of $C(x)$, usually (but not always) found at $x = 0$. H is 0 if f_1 and f_2 are identical and diverges toward infinity if f_1 and f_2 are uncorrelated.

Suppose that $f_1(x)$ represents an especially-noisy spectral intensity as a function of the reciprocal of wavelength and $f_2(x)$ represents a synthetic, laboratory, or theoretical spectrum for which one is searching in the noisy data. $C(x)$ is computed, and, if a correlation peak is found (see figure), then f_2 is adjusted in amplitude and wavelength until it gives the best fit as indicated by the approach of H to 0. Because of noise in the autocorrelation functions, H cannot necessarily reach precisely 0; and one can compute a limiting value of H toward which to strive, to avoid overfitting of data.

The lead or lag in the correlation peak also yields useful information. In the example of the figure, the lag of 0.049 cm $^{-1}$ indicates a Doppler shift caused by a relative velocity of about 6.3 km/s between the spectrometer and the atmosphere.

Correlation analysis is much more effective than traditional spectral-analysis techniques in the extraction of weak signals that appear to be hopelessly "buried" in noise. Both visual inspection and least-squares analysis are point-by-point-comparison techniques that fail to identify signals lower than about 1 standard deviation of the noise. On the other hand, cross-correlation exerts a powerful averaging effect that suppresses the effect of noise because it considers an entire spectral inter-

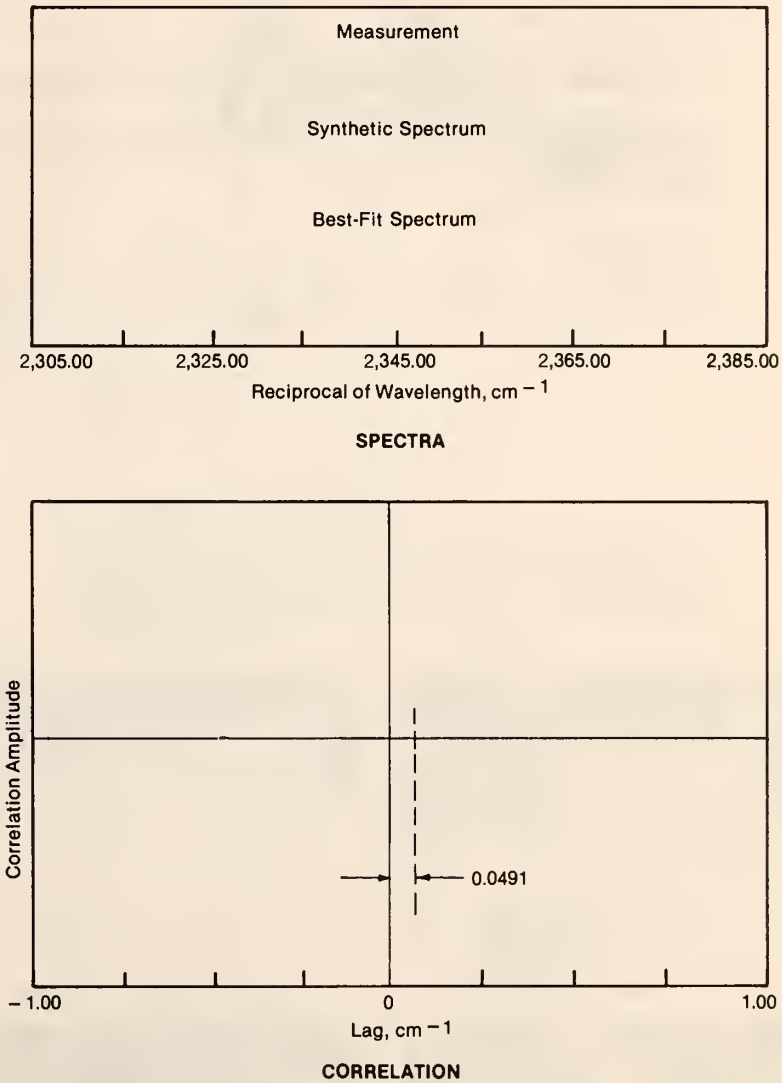

A **Noisy Spectrum** was measured in the upper atmosphere in the search for the characteristic lines of CO_2. A correlation peak was found between a synthetic CO_2 spectrum and the noisy data, leading to a "best-fit" CO_2 spectrum extracted from the measurements.

val instead of the small interval around an individual spectral line.

Correlation analysis works best over large spectral intervals containing highly structured spectra with many lines. It is not expected to be useful in the search for broad, shallow spectral continua. When spectral lines of more than one molecule are sought, all have to be fitted concurrently to make H converge properly: the technique to do this will require further research. When a Doppler shift is present, the spectral interval must be restricted somewhat so that the dependence of the shift on frequency does not, itself, result in decorrelation. (However, a correction for this dependence could presumably be made in the synthetic spectrum.)

This work was done by Reinhard Beer and Robert H. Norton, Jr., of Caltech for **NASA's Jet Propulsion Laboratory**.

NPO-17306/TN

FOR ADDITIONAL INFORMATION: *Contact: Director, Technology Transfer Division, P.O. Box 8757, BWI Airport, MD 21240; (301) 621-0100 Ext. 241*

REFER TO THE NUMBER LISTED AT THE END OF THIS ARTICLE

NASA Tech Brief
National Aeronautics and Space Administration
Lewis Research Center, Cleveland, Ohio

Thermal-Wave Microscope

Images are produced by a modified computer-controlled scanning electron microscope.

A computer-controlled thermal-wave microscope has been developed to investigate III-V compound semiconductor devices and materials. Thermal-wave microscopy is a nondestructive technique that can provide information on subsurface thermal features of solid samples. Furthermore, because this is a subsurface technique, three-dimensional imaging is also possible.

Thermal-wave imaging is performed with a modified scanning electron microscope (see Figure 1). An intensity-modulated electron beam generates thermal waves in the specimen. The modulation frequency is typically in the range of 0.1 to 10 MHz.

The thermal waves generated by the electron beam are critically damped, but they interact with thermal features in the specimen. The thermal waves are not detected directly. Instead, the acoustic waves generated by the thermal waves are detected by an acoustic transducer glued to the sample. The transducer signal is amplified and fed to a lock-in amplifier before undergoing analog-to-digital conversion. The image is built up point by point as the electron beam is indexed through a raster of points under the control of the computer. The software that controls the scanning electron microscope and handles the image data was written in FORTRAN 77.

Thermal-wave microscopy is limited by low signal levels, extremes in signal contrast, and poor edge definition. However, once the image data are in the computer, various digital techniques can be applied to enhance features of interest in the image. The resulting images can be fed back to the scanning electron microscope for display or can be stored on a magnetic disk.

Thermal-wave images of a stainless-steel specimen from a single image scan and from averages over 16 and 100 scans show the effectiveness of image averaging in reducing noise (see Figure 2). These images show a granular structure, whereas an ordinary secondary electron image of the same sample shows only the surface texture of the sample.

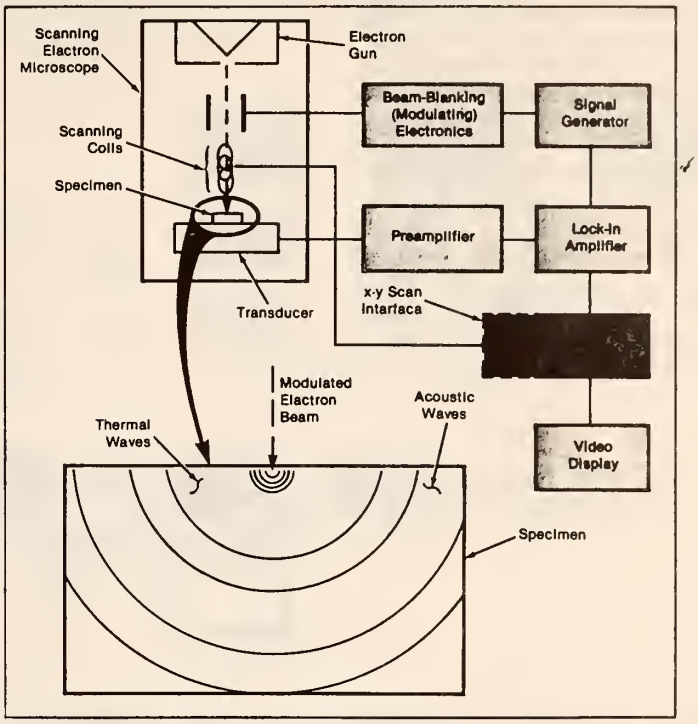

Figure 1. The **Thermal-Wave Microscope** uses an intensity-modulated electron beam of a modified scanning electron microscope to generate thermal waves in a sample. Acoustic waves generated by the thermal waves are received by a transducer and processed in a computer to form images that can be displayed on the video display of the microscope or recorded on a magnetic disk.

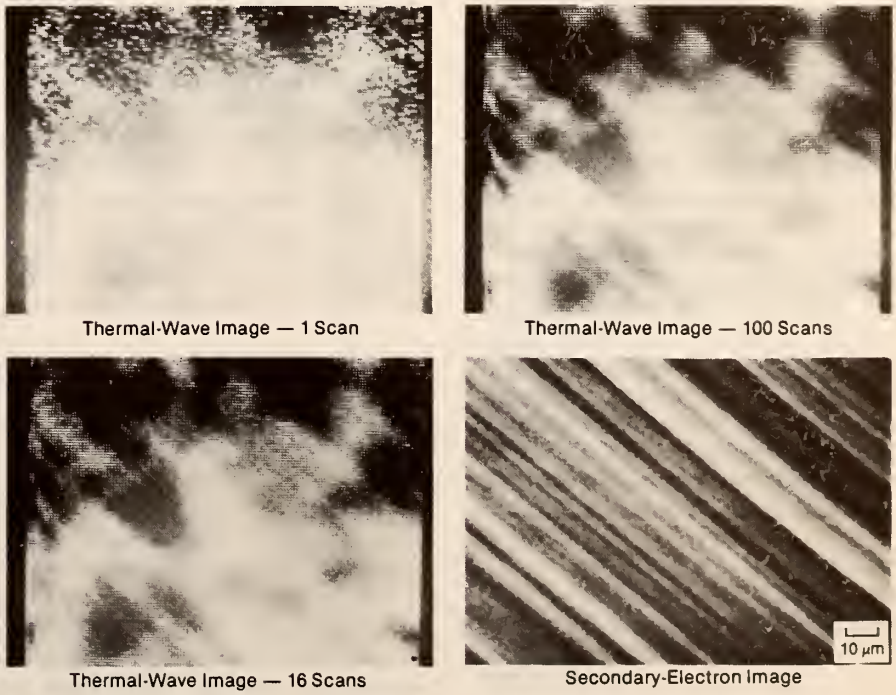

Figure 2. The **Noise in a Thermal-Wave Image** of subsurface grain structure of stainless steel is reduced by averaging over a number of scans. Also shown for comparison is a scanning electron micrograph, which shows the surface texture of the specimen but not the subsurface grain structure.

This work was done by Robert E. Jones, Ihor Kramarchuk, Wallace D. Williams, and John J. Pouch of **Lewis Research Center** *and Percy Gilbert of Purdue University. Further information may be found in NASA TM-100157 [N87-26278], Price Code: A02 "Computer Control of a Scanning Electron Microscope for Digital Image Processing of Thermal-Wave Images."*

Copies may be purchased from the National Technical Information Service, Springfield, Virginia 22161, Telephone No. (703) 487-4650. Rush orders may be placed for an extra fee by calling (800) 336-4700. The report is also available on microfiche at no charge. LEW-14740/TN

FOR ADDITIONAL INFORMATION: *Contact: Director, Technology Transfer Division, P.O. Box 8757, BWI Airport, MD 21240; (301) 621-0100 Ext. 241*

REFER TO THE NUMBER LISTED AT THE END OF THIS ARTICLE

NASA Tech Brief
National Aeronautics and Space Administration
NASA's Jet Propulsion Laboratory, Pasadena, California

Phase-Modulation Gas-Correlation Spectroscopy

Features include high spectral discrimination and sensitivity.

Electro-optic phase-modulation gas-correlation spectroscopy has been demonstrated in laboratory tests to be a promising candidate technique for remote sensing of gases, temperatures, and wind velocities in the atmosphere. In this technique radiation emitted by the sample atmosphere is passed through an electro-optic phase modulator, and the modulated and unmodulated versions of the spectrum are alternately passed through a reference absorption cell containing the gas to be detected. The radiation emerging from the reference cell is band-pass filtered and detected. The correlation signal is the difference in intensity between the phase-modulated and unmodulated detected signals.

The phase modulation redistributes the emission spectrum into upper and lower sidebands displaced from the original spectral lines by integral multiples of the modulating frequency. Emission or absorption lines in the modulated sample spectrum that correlate with absorption spectral lines of the gas in the reference cell alter the power transmitted to the detector. Thus, the measurement is most sensitive to the spectrum in the input radiation corresponding to the species contained in the reference cell.

The laboratory prototype system shown in Figure 1 has been used to measure part of the infrared spectrum of N_2O. Blackbody radiation from a glow bar at a temperature of 1,000 K is chopped mechanically at a rate of 500 Hz and passes through a 1-cm-thick cell containing the N_2O sample gas. The radiation, which now contains an N_2O absorption spectrum, passes through an electro-optic phase modulator and through a 1-cm-thick reference cell containing N_2O.

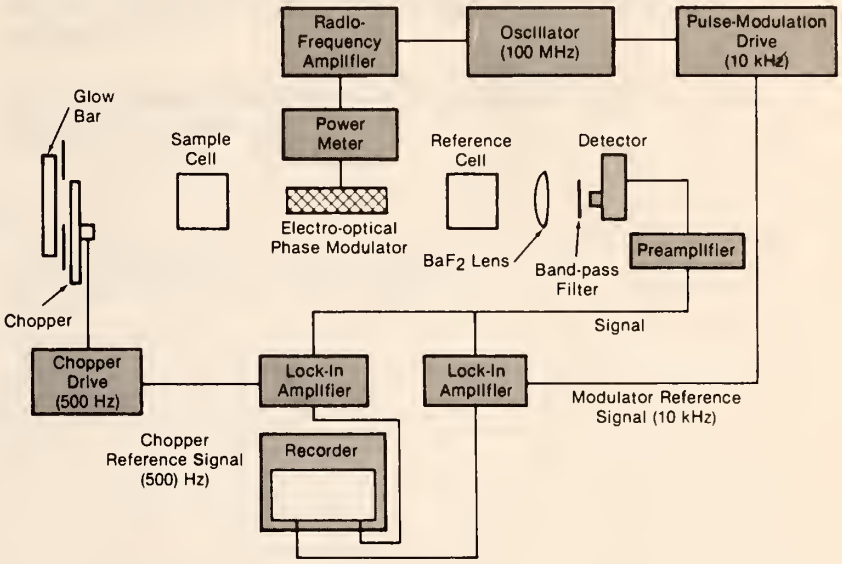

Figure 1. This **Laboratory Prototype System** was used to demonstrate electro-optical phase-modulation gas-correlation spectroscopy.

The modulator, a crystal of CdTe, is activated and deactivated by turning a 15-W, 100-MHz modulating signal on and off at a repetition rate of 10 kHz. A lock-in amplifier synchronized to the 10-kHz signal processes the detector output to obtain the correlation signal. Another lock-in amplifier synchronized to the mechanical chopper processes the detector output to obtain a measure of the total radiant energy transmitted through the system.

The system was tested at various pressures of N_2O in the sample and reference cells from 0 to 10 torr (0 to 1.3 kPa). The measurements showed that as the pressure in the sample cell rises (at a given fixed pressure in the reference cell), the correlation signal first increases, then levels off to a maximum, then decreases. The experimental and theoretical correlation curves were in excellent agreement (see Figure 2).

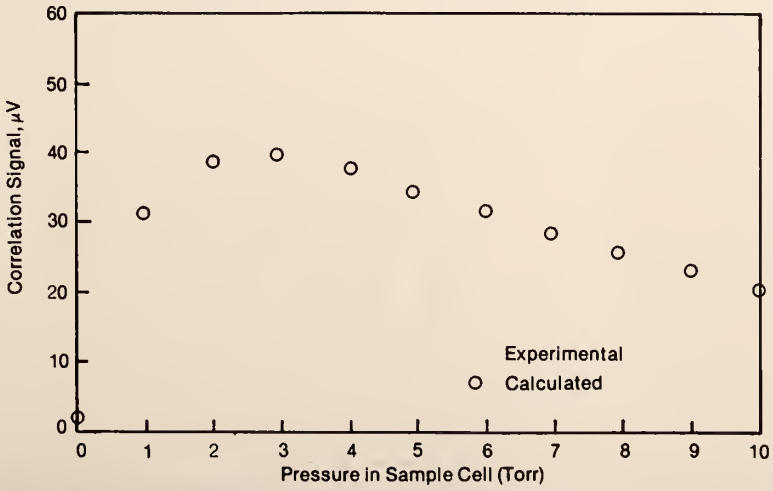

Figure 2. The **Correlation Signal** was measured and calculated as a function of the pressure of the N_2O gas in the sample cell of the system of Figure 1. For this set of data, the pressure in the reference cell was 1 torr (130 Pa).

This work was done by David M. Rider, John T. Schofield, Jack S. Margolis, and Daniel J. McCleese of Caltech for **NASA's Jet Propulsion Laboratory**.

NPO-17013/TN

FOR ADDITIONAL INFORMATION: *Contact: Director, Technology Transfer Division, P.O. Box 8757, BWI Airport, MD 21240; (301) 621-0100 Ext. 241*

REFER TO THE NUMBER LISTED AT THE END OF THIS ARTICLE

Transportation & Components

0704 Injected Water Augments Cooling in Turboshaft Engine—Additional cooling enables operation at higher than usual power.

0705 Study of Flow About a Helicopter Rotor—A noninvasive instrument verifies a computer program that predicts velocities (Licensing Opportunity)

0706 Vibration-Testing Facility for Aircraft—Equipment, methods, and experience are described.

Software

0707 Software Helps Select Patrol Vehicles

NASA Tech Brief
National Aeronautics and
Space Administration

Injected Water Augments Cooling in Turboshaft Engine

Additional cooling enables operation at higher than usual power.

A report describes experiments in which water was injected into the compressor-bleed cooling air of an aircraft turboshaft engine. The injection of water had previously been suggested as a way to provide the additional cooling needed to sustain operation at power levels higher than usual. Such operation involves turbine-inlet temperatures high enough to shorten the lives of the first-stage high-pressure turbine blades. The latent heat of vaporization of the injected water serves as an additional heat sink to maintain the blades at their design operating temperatures during high-power operation.

The engine was modified by addition of the water-injecting apparatus to the cooling-air accelerator, and the usual complement of instrumentation was retained. Additional instrumentation was installed to measure the pressures of the cooling air upstream and downstream of the cooling-air accelerator. Thermocouples were added to measure the temperatures of the inflowing water and of the steam/air mixture upstream and downstream of the accelerator. An optical pyrometer measured the temperatures of the leading edges of the first-stage turbine blades.

By itself, the injection of water both lowered the temperatures of the blades and caused the engine to run slower. This result was anticipated because the cooling air becomes denser as water is added; and as more compressor air is diverted for cooling, less is available to drive the turbine. Furthermore, the cooling shortens the turbine blades by thermal contraction, causing an increase in the clearance of the tips of the blades and a consequent decrease in efficiency.

In another test, the cooling water was turned on and the flow of fuel then increased until the engine reached the normal operating speed for dry cooling. In this condition, the temperature at the leading edges of the blades was near the normal value, but the output power was higher than it was without water. The increase in power was about 3.5 percent for a water/cooling-air flow ratio of 6 to 7 percent, and the corresponding increase in the inlet temperature was 60 °F (33 °C).

The injection of water at flow ratios beyond 7 percent did not provide an additional decrease in the temperature of the leading edges of the blades, apparently on account of peculiarities of the apparatus. Concern for other unprotected components in the hot section of the engine prohibited tests at higher powers. However, projections from design studies and the tests thus far indicate that if these limitations can be overcome and the inlet temperature raised by 300 °F (167 °C), then the power could be increased by 17 percent without affecting the normal blade temperature.

This work was done by Thomas J. Biesiadny of **Lewis Research Center** *and Brett Berger, Gary A. Klann and David A. Clark of the U.S. Army Aviation Research and Technology Activity. Further information may be found in NASA TM-89817 [N87-20280], Price Code: A02 "Contingency Power for Small Turboshaft Engines Using Water Injection into Turbine Cooling Air."*

Copies may be purchased from the National Technical Information Service, Springfield, Virginia 22161, Telephone No. (703) 487-4650. Rush orders may be placed for an extra fee by calling (800) 336-4700. LEW-14706/TN

FOR ADDITIONAL INFORMATION: *Contact: Director, Technology Transfer Division, P.O. Box 8757, BWI Airport, MD 21240; (301) 621-0100 Ext. 241*
REFER TO THE NUMBER LISTED AT THE END OF THIS ARTICLE

NASA Tech Brief
National Aeronautics and
Space Administration

Licensing Opportunity

Study of Flow About a Helicopter Rotor

A noninvasive instrument verifies a computer program that predicts velocities.

Laser velocimeter measurements confirm predictions of the transonic flow field around the tip of a helicopter-rotor blade, according to a report. The report discusses the measurements, which yielded high-resolution orthogonal velocity components of the flow field at rotor-tip Mach numbers from 0.85 to 0.95, and the use of the measurements in verifying the ability of the computer program ROT22 to predict the transonic flow field, including the occurrences, strengths, and locations of shock waves that cause high drag and noise.

A fringe-mode, forward-scatter laser velocimeter system using the 4,880- and 5145-Å lines of an argon ion laser was designed for the measurements. Because the velocimeter looks along the rotor blade toward the hub as the tip of the blade sweeps by, one spectral line can be used to measure the induced chordwise component of velocity, while the other is used to measure the induced vertical component of velocity. The transmitting and receiving optics could also be moved along the walls of the test chamber to obtain a view along a line perpendicular to the edge of the approaching or retreating blade so that the radial and vertical components of the induced velocity could be determined.

The ROT22 code calculates the flow about a lifting rotor blade in forward flight. Although the full-potential equation is solved, the formulation is quasi-steady in that the derivatives of the perturbation potentials with respect to time are neglected to speed up the computation greatly. However, regardless of the simplifying approximation, the computation is exact for the hovering flight simulated in the experiments. With the code, the flow field over the entire blade was calculated for the tip Mach numbers of the experiment.

The angle of incidence in the tip region was small and had little effect on the flow beyond the tip. Therefore the good agreement between the calculated and measured velocities indicates that the ROT22 code can be used with confidence to predict the important flow field in the tip region.

This work was done by Michael E. Tauber of **Ames Research Center** *and F. Kevin Owen of Complere, Inc. Further information may be found in Paper 85-1558 of AIAA 18th Fluid Dynamics and Plasmadynamics and Lasers Conference.*

Copies may be purchased from AIAA Technical Information Service Library, 555 West 57th Street, New York, New York 10019, Telephone No. (212) 247-6500.

Inquiries concerning rights for the commercial use of this invention should be addressed to the Patent Counsel, Ames Research Center Refer to ARC-11790/TN

Ames Research Ctr.
Technology Utilization Officer: Laurance Milov
Mail Code 223-3
Moffett Field, CA 94035
(415) 694-4044
Patent Counsel:
Darrell G. Brekke
Mail Code 200-11
Moffett Field, CA 94035
(415) 694-5104

FOR ADDITIONAL INFORMATION: *Contact: Director, Technology Transfer Division, P.O. Box 8757, BWI Airport, MD 21240; (301) 621-0100 Ext. 241*
REFER TO THE NUMBER LISTED AT THE END OF THIS ARTICLE

NASA Tech Brief
National Aeronautics and
Space Administration

Vibration-Testing Facility for Aircraft

Equipment, methods, and experience are described.

A report describes equipment and techniques used in the vibration testing of aircraft on the ground at the Dryden Flight Research Facility. It includes discussions of the role of ground vibration testing in the qualification of new and modified aircraft for flight and of the experience gained from various applications.

Ground vibration tests are performed to identify structural vibrational modes and the associated natural frequencies and dampings. Data from such tests are correlated with the predictions of finite-element mathematical models of the aircraft dynamics. Data from ground vibration tests performed before and after modifications of research vehicles can be compared to assess the significance of those modifications. Vibration-test data can also help to resolve anomalies observed in flight.

A ground vibration test may involve a complete airplane mounted on soft supports like air bags to permit free vibrations, a complete airplane resting on its landing gear, specific parts on a complete airplane, or single components of an airplane tested in isolation. A test is conducted by the sine-dwell excitation method, the single- or multiple-input random-excitation method, or the impact-excitation method; some equipment is unique to each method, while some is common to all. For example, electrodynamic shakers with force ratings of 10, 50, and 150 lb (45, 222, and 667 N, respectively) are used in all methods except impact excitation.

In the sine-dwell method, two or more shakers excite the vibrations in the airplane as the frequency is swept through the range of interest. The vibrational response as a function of frequency is measured by accelerometers at several locations. After the initial frequency sweeps, each vibrational mode of interest is analyzed in detail by measurement of coincident and quadrature components of force and acceleration. Once a mode is thus finely tuned, a modal survey is performed by roving accelerometers.

In the random-excitation method, the shakers are driven by a random forcing function of bandwidth and amplitude specified by the user. Vibrational-response data from accelerometers are processed by a structural-analysis minicomputer system to obtain transfer and coherence functions with sufficient bandwidth to include the vibrational modes of interest. Once data are acquired for the entire airplane, modal parameters are found from calculations in the time domain.

The impact-excitation method is used primarily to test components. The specimen is struck by an instrumented hammer. The decaying vibrational-response signal is multiplied by an exponential window function to reduce leakage. The data are analyzed in the same manner as in the random-excitation method.

Each combination of equipment and technique has its advantages and disadvantages, and none is relied upon solely for all testing. Examples of tests that have been performed include the following:

- Sine-dwell tests of the highly maneuverable aircraft technology (HiMAT) airplane,
- Sine-dwell tests of the flaperon system of the X-29A forward-swept-wing airplane,
- Sine-dwell and random tests of the Jet Star laminar-flow-control airplane,
- Impact tests of a landing-gear door of the rotor systems research aircraft (RSRA), and
- Impact tests of an aileron of the F-15 supersonic airplane.

This work was done by Michael W. Kehoe of **Ames Research Center**. *Further information may be found in NASA TM-88272 [N87-27655/NSP], Price Code: A02 "Aircraft Ground Vibration Testing at NASA Ames-Dryden Flight Research Facility."*

Copies may be purchased from the National Technical Information Service, Springfield, Virginia 22161, Telephone No. (703) 487-4650. Rush orders may be placed for an extra fee by calling (800) 336-4700.

Inquiries concerning rights for the commercial use of this invention should be addressed to the Patent Counsel, Ames Research Center. Refer to ARC-12141/TN

FOR ADDITIONAL INFORMATION: *Contact: Director, Technology Transfer Division, P.O. Box 8757, BWI Airport, MD 21240; (301) 621-0100 Ext. 241*

REFER TO THE NUMBER LISTED AT THE END OF THIS ARTICLE

National Institute of Standards & Technology
(Formerly the National Bureau of Standards)
U.S. Department of Commerce, Gaithersburg, MD 20899

Software Helps Select Patrol Vehicles

A computer software program that police fleet managers can use to select patrol vehicles best suited to their needs has been written by an economist in the NIST Center for Computing and Applied Mathmatics. The program, called AutoBid, was sponsored by the institute's Law Enforcement Standards Laboratory through funding from the National Institute of Justice (NIJ). AutoBid is based on Michigan State Police patrol vehicle performance test data and runs on an MS - DOS(tm) - based personal computer with at least 384K bytes of RAM. AutoBid offers users two methods of assessing vehicles: performance or value. Performance is based on vehicle test scores alone, ranking vehicles independently of cost. The value method is based on both vehicle cost and test scores.

FOR ADDITIONAL INFORMATION: The AutoBid program is available to law enforcement agencies from the NIJ's Technology Assessment Program Information Center, Box 6000, Rockville, MD 20850. To discuss these efforts furthur, contact Dr. Stephen F. Weber, Admin. Building, Room A415, National Institute of Standards & Technology, Gaithersburg, MD 20899, (301) 975-6137.

U.S. DEPARTMENT OF COMMERCE
National Technical Information Service
Springfield, VA 22161

NTIS ORDER FORM

Use this form ONLY to order reports designated as available from NTIS.

TELEPHONE ORDERS (703) 487-4650 FAX (Telecopier) (703) 321-8547 TELEX 89-9405

For Subscription Questions
(703) 487-4630

For Tracing an Order
(703) 487-4660

Editorial Questions
(703) 487-4805

Postage:
NTIS uses First Class Delivery, or equivalent service, on all shipping. For information about one day RUSH ordering, call (800) 336-4700 or (703) 487-4700.

NTIS PRICE SCHEDULE *

This schedule converts into actual prices the price codes cited in those Tech Notes having a report available from NTIS.

Microfiche	
A01	$6.95
Paper copy	
A02	10.95
A03	13.95
A04 through A05	15.95
A06 through A09	21.95
A10 through A13	28.95
A14 through A17	36.95
A18 through A21	42.95
A22 through A25	49.95
A99	Call for price

These prices are for customers in United States, Canada, and Mexico. Other addresses should write for the price listing, number PR-360-4.

Prices effective January 1, 1989

† Billing Service: There is a $7.50 charge for this service. It is restricted to customers in the United States, Canada, and Mexico. A late payment charge will be applied to all billings more than 30 days overdue.

If your address lable on this Tech Notes is NOT correct, call the NTIS Subscriptions Department on (703) 487-4630.

1 ADDRESS INFORMATION

Last Name .....

Title .....

Company/Organization .....

Address .....

.....

City/State/ZIP .....

Telephone Number .....

2 METHOD OF PAYMENT

☐ Charge my NTIS Deposit Account .... – .....

☐ Check/Money order enclosed payable to NTIS for $ .....

☐ Please bill **ADD $7.50 per order** (see below for restrictions)†

Purchase order number .....

Charge my ☐ American Express ☐ VISA ☐ MasterCard

Account Number..... Exp. .....

Signature .....
(Required to validate order)

3 ORDER SELECTION (Use only for reports stated as available from NTIS)

NTIS Order Number	*Price**	*Quantity*	*Total Price*
..... /NAC	.....	.....	.....
..... /NAC	.....	.....	.....
..... /NAC	.....	.....	.....
..... /NAC	.....	.....	.....
..... /NAC	.....	.....	.....
		Handling fee	$3.00
		Total	.....

- Agriculture & Food
- Computers
- Electrotechnology
- Energy
- Engineering
- Environmental Science & Technology
- Manufacturing, Machinery, & Tools
- Materials
- Medicine & Biology
- Natural Resources Technology & Engineering
- Physical Sciences
- Transportation & Components

Route To:

PENN STATE UNIVERSITY LIBRARIES
A000072010112

DEPARTMENT OF COMMERCE
onal Technical Information Service
gfield, Va. 22161

IAL BUSINESS
ty for Private Use, $300

AN EQUAL OPPORTUNITY EMPLOYER

BULK RATE
POSTAGE & FEES PAID
NTIS
Permit No. G-292